EFFECT OF CLAY TYPE AND CLAY CONTENT ON MOISTURE CONTENT AND BULK SOIL ELECTRICAL CONDUCTIVITY AS MEASURED USING TIME DOMAIN REFLECTOMETRY

by

Abdolmajid Liaghat

A thesis submitted to the Faculty of Graduate Studies and Research, in partial fulfilment of the requirments for the degree of Master of Science

Department of Agricultural Engineering
Macdonald Campus of McGill University
Ste-Anne de Bellevue, Quebec, Canada
September 1993

Name [illegible]

Dissertation Abstracts International is arranged by broad, general subject categories. Please select the one subject which most nearly describes the content of your dissertation. Enter the corresponding four-digit code in the spaces provided.

[illegible] | 0537 | U·M·I

SUBJECT TERM | SUBJECT CODE

Subject Categories

THE HUMANITIES AND SOCIAL SCIENCES

COMMUNICATIONS AND THE ARTS
- Architecture 0729
- Art History 0377
- Cinema 0900
- Dance 0378
- Fine Arts 0357
- Information Science 0723
- Journalism 0391
- Library Science 0399
- Mass Communications 0708
- Music 0413
- Speech Communication 0459
- Theater 0465

EDUCATION
- General 0515
- Administration 0514
- Adult and Continuing 0516
- Agricultural 0517
- Art 0273
- Bilingual and Multicultural 0282
- Business 0688
- Community College 0275
- Curriculum and Instruction 0727
- Early Childhood 0518
- Elementary 0524
- Finance 0277
- Guidance and Counseling 0519
- Health 0680
- Higher 0745
- History of 0520
- Home Economics 0278
- Industrial 0521
- Language and Literature 0279
- Mathematics 0280
- Music 0522
- Philosophy of 0998
- Physical 0523
- Psychology 0525
- Reading 0535
- Religious 0527
- Sciences 0714
- Secondary 0533
- Social Sciences 0534
- Sociology of 0340
- Special 0529
- Teacher Training 0530
- Technology 0710
- Tests and Measurements 0288
- Vocational 0747

LANGUAGE, LITERATURE AND LINGUISTICS
- Language
  - General 0679
  - Ancient 0289
  - Linguistics 0290
  - Modern 0291
- Literature
  - General 0401
  - Classical 0294
  - Comparative 0295
  - Medieval 0297
  - Modern 0298
  - African 0316
  - American 0591
  - Asian 0305
  - Canadian (English) 0352
  - Canadian (French) 0355
  - English 0593
  - Germanic 0311
  - Latin American 0312
  - Middle Eastern 0315
  - Romance 0313
  - Slavic and East European 0314

PHILOSOPHY, RELIGION AND THEOLOGY
- Philosophy 0422
- Religion
  - General 0318
  - Biblical Studies 0321
  - Clergy 0319
  - History of 0320
  - Philosophy of 0322
- Theology 0469

SOCIAL SCIENCES
- American Studies 0323
- Anthropology
  - Archaeology 0324
  - Cultural 0326
  - Physical 0327
- Business Administration
  - General 0310
  - Accounting 0272
  - Banking 0770
  - Management 0454
  - Marketing 0338
- Canadian Studies 0385
- Economics
  - General 0501
  - Agricultural 0503
  - Commerce Business 0505
  - Finance 0508
  - History 0509
  - Labor 0510
  - Theory 0511
- Folklore 0358
- Geography 0366
- Gerontology 0351
- History
  - General 0578
  - Ancient 0579
  - Medieval 0581
  - Modern 0582
  - Black 0328
  - African 0331
  - Asia, Australia and Oceania 0332
  - Canadian 0334
  - European 0335
  - Latin American 0336
  - Middle Eastern 0333
  - United States 0337
- History of Science 0585
- Law 0398
- Political Science
  - General 0615
  - International Law and Relations 0616
  - Public Administration 0617
- Recreation 0814
- Social Work 0452
- Sociology
  - General 0626
  - Criminology and Penology 0627
  - Demography 0938
  - Ethnic and Racial Studies 0631
  - Individual and Family Studies 0628
  - Industrial and Labor Relations 0629
  - Public and Social Welfare 0630
  - Social Structure and Development 0700
  - Theory and Methods 0344
- Transportation 0709
- Urban and Regional Planning 0999
- Women's Studies 0453

THE SCIENCES AND ENGINEERING

BIOLOGICAL SCIENCES
- Agriculture
  - General 0473
  - Agronomy 0285
  - Animal Culture and Nutrition 0475
  - Animal Pathology 0476
  - Food Science and Technology 0359
  - Forestry and Wildlife 0478
  - Plant Culture 0479
  - Plant Pathology 0480
  - Plant Physiology 0817
  - Range Management 0777
  - Wood Technology 0746
- Biology
  - General 0306
  - Anatomy 0287
  - Biostatistics 0308
  - Botany 0309
  - Cell 0379
  - Ecology 0329
  - Entomology 0353
  - Genetics 0369
  - Limnology 0793
  - Microbiology 0410
  - Molecular 0307
  - Neuroscience 0317
  - Oceanography 0416
  - Physiology 0433
  - Radiation 0821
  - Veterinary Science 0778
  - Zoology 0472
- Biophysics
  - General 0786
  - Medical 0760

EARTH SCIENCES
- Biogeochemistry 0425
- Geochemistry 0996
- Geodesy 0370
- Geology 0372
- Geophysics 0373
- Hydrology 0388
- Mineralogy 0411
- Paleobotany 0345
- Paleoecology 0426
- Paleontology 0418
- Paleozoology 0985
- Palynology 0427
- Physical Geography 0368
- Physical Oceanography 0415

HEALTH AND ENVIRONMENTAL SCIENCES
- Environmental Sciences 0768
- Health Sciences
  - General 0566
  - Audiology 0300
  - Chemotherapy 0992
  - Dentistry 0567
  - Education 0350
  - Hospital Management 0769
  - Human Development 0758
  - Immunology 0982
  - Medicine and Surgery 0564
  - Mental Health 0347
  - Nursing 0569
  - Nutrition 0570
  - Obstetrics and Gynecology 0380
  - Occupational Health and Therapy 0354
  - Ophthalmology 0381
  - Pathology 0571
  - Pharmacology 0419
  - Pharmacy 0572
  - Physical Therapy 0382
  - Public Health 0573
  - Radiology 0574
  - Recreation 0575
  - Speech Pathology 0460
  - Toxicology 0383
- Home Economics 0386

PHYSICAL SCIENCES

Pure Sciences
- Chemistry
  - General 0485
  - Agricultural 0749
  - Analytical 0486
  - Biochemistry 0487
  - Inorganic 0488
  - Nuclear 0738
  - Organic 0490
  - Pharmaceutical 0491
  - Physical 0494
  - Polymer 0495
  - Radiation 0754
- Mathematics 0405
- Physics
  - General 0605
  - Acoustics 0986
  - Astronomy and Astrophysics 0606
  - Atmospheric Science 0608
  - Atomic 0748
  - Electronics and Electricity 0607
  - Elementary Particles and High Energy 0798
  - Fluid and Plasma 0759
  - Molecular 0609
  - Nuclear 0610
  - Optics 0752
  - Radiation 0756
  - Solid State 0611
- Statistics 0463

Applied Sciences
- Applied Mechanics 0346
- Computer Science 0984
- Engineering
  - General 0537
  - Aerospace 0538
  - Agricultural 0539
  - Automotive 0540
  - Biomedical 0541
  - Chemical 0542
  - Civil 0543
  - Electronics and Electrical 0544
  - Heat and Thermodynamics 0348
  - Hydraulic 0545
  - Industrial 0546
  - Marine 0547
  - Materials Science 0794
  - Mechanical 0548
  - Metallurgy 0743
  - Mining 0551
  - Nuclear 0552
  - Packaging 0549
  - Petroleum 0765
  - Sanitary and Municipal 0554
  - System Science 0790
- Geotechnology 0428
- Operations Research 0796
- Plastics Technology 0795
- Textile Technology 0994

PSYCHOLOGY
- General 0621
- Behavioral 0384
- Clinical 0622
- Developmental 0620
- Experimental 0623
- Industrial 0624
- Personality 0625
- Physiological 0989
- Psychobiology 0349
- Psychometrics 0632
- Social 0451

Title of thesis: Effect of clay soils on Time Domain Reflectometry Readings

ABSTRACT

Time domain reflectometry (TDR) is becoming a widely used method to determine volumetric soil water content (θ) and bulk soil electrical conductivity (EC_a). It has been found that the θ and EC_a values obtained by this method, on certain soils, require calibration. The purpose of this study was to monitor the effects of soil texture (most particularly the clay mineralogy and clay content) on θ and EC_a estimated by TDR.

Water contents were measured, gravimetrically and by TDR, on packed columns of nine soil mixtures composed of three clay types (Hydrite, Bentonite, and Ste. Rosalie clay) and coarse sand at three levels (8, 16, and 30% by weight) of these clay materials. Three replicates of each mixture (a total of 27 columns) were made to statistically establish the effect of the clay type and the clay content on θ and EC_a readings by TDR. It was found that the TDR overestimated θ for the Hydrite and Ste. Rosalie (Natural) materials but accurately predicted for the Bentonite materials, compared to gravimetric determinations.

Bulk soil electrical conductivity was simultaneously measured by two independent techniques, TDR and 4-probe, on the same soils. It was found that the clay types and clay contents have almost equal effects on the EC_a as measured by TDR and 4-probe techniques. It was found that the estimated EC_a values obtained by TDR and 4-probe methods for the fine-textured Bentonite materials were lower than those for the Hydrite and Ste. Rosalie materials at equal θ and EC_w (electrical conductivity of soil water).

RESUME

La réflectométrie temporelle (TDR) est de plus en plus utilisée pour déterminer la teneur en eau volumétrique du sol (θ) et de la conductivité électrique apparente du sol (EC_a). Il a été démontré que dans certains sols les valeurs de θ et EC_a obtenues par cette méthode requièrent une calibration. L'objectif de cette étude était de déterminer les effets de la texture du sol (plus particulièrement du type et du pourcentage d'argile) sur θ et EC_a estimées par la réflectométrie temporelle.

La teneur en eau du sol a été mesurée par gravimétrie et avec le TDR sur des colonnes contenant 9 mélanges de sol composés de 3 types d'argile (hydrite, bentonite et argile Ste-Rosalie) répartis selon 3 pourcentages (8, 16 et 30%). Trois répétitions de chaque combinaison (un total de 27 colonnes) ont permis d'établir statistiquement l'effet du type et du pourcentage d'argile sur θ et EC_a sur les lectures de TDR. Il est apparu que le TDR, en comparaison de la méthode gravimétrique, surestimait θ pour l'hydrite et l'argile Ste-Rosalie mais donnait de bons résultats avec la bentonite.

La conductivité électrique apparente a été mesurée simultanément par deux techniques indépendantes: le TDR et "les quatre sondes" (4-probe), sur les mêmes sols. Les résultats ont montré qu'il n'y avait pas de différence entre la conductivité électrique apparente mesurée avec le TDR et la technique des "quatre sondes", quelque soit le type d'argile ou son pourcentage. On a également trouvé que les valeurs de EC_a estimées pour la bentonite, à texture fine, étaient plus faibles que celles de l'hydrite et de l'argile Ste-Rosalie, la teneur en eau et la conductivité électrique de l'eau du sol étant égale.

ACKNOWLEDGEMENTS

The author cheerfully expresses his sincere appreciation to his supervisor, Dr. Robert S. Broughton, for his helpful suggestions during the two years of study.

The author would like to express a very great appreciation to his co-supervisor, Dr. Robert Boyd Bonnell, for his encouragement in completing this study, for his patience in editing the many versions of the manuscripts and for his generous help that the author has received during this study.

The author would like to thank Boyd Fuller for his helpful suggestions in some parts of this thesis.

The author is happy to acknowledge his sponsor, Ministry of Culture and Higher Education of the Islamic Republic of IRAN, for their financial support (scholarship) during these two years of study.

The author would like to thank his parents for their encouragement, moral support and kindness.

Finally the author wishes to thank his wife and oldest son for their assistance during the preparation of soil samples and recording of data for this study and he dedicates this thesis to his wife, Mitra, and his three sons, Mehdi, Rasoul and Amin.

TABLE OF CONTENTS

List of Tables

List of Figures

LIST OF SYMBOLS

a	attenuation coefficient of a TEM
c	propagation velocity of an TEM in free space ($3 * 10^8$ m/s)
D.C.	direct current (amps)
EC_a	bulk soil electrical conductivity (dS/m)
EC_S	soil particle surface conductance (dS/m)
EC_{TDR}	bulk soil electrical conductivity as determined by TDR method (dS/m)
EC_W	electrical conductivity of a solution (dS/m)
EC_{4P}	bulk soil electrical conductivity as determined with the 4-probe electrical resistivity meter (dS/m)
EC_{25}	electrical conductivity of a solution at 25^0C
EMP	electromagnetic pulse
f	wave frequency(s^{-1})
f_t	temperature factor
H_Z	hertz $(s)^{-1}$
k	cell factor
K_d	dielectric constant
ε_r	real part of K_d
ε_i	imaginary part of K_d
L	probe lengths (mm)
ln	natural log function
n	number of reflections
PVC	polyvinylchloride
r	reflection coefficient
r_0	reflection coefficient measured at X_{co}
R	resistance (ohm)
R_t	resistance at temperature t

T	tortuosity coefficient
TDR	time domain reflectometry
TDR-EC_a	same as EC_{TDR} (dS/m)
TEM	transverse electromagnetic wave
TM	transverse magnetic (field)
t	time of travel of the TEM wave along the probes (ns)
v	signal propagation velocity (m/sec)
V	voltage (volts)
V_R	ratio of transmitted to reflected wave voltage along probe length
V_T	ratio of transmitted to reflected wave voltage just past end of probes
V_n	reflection coefficient measured at "n" number of reflections
V_1	magnitude of the voltage pulse along the wave guide
V_2	magnitude of the signal reflected at the end of the probes
V_f	attenuation fraction
V_p	velocity of propagation of a wave
ω	angular velocity (radians per second)
X_{co}	x axis distance with probe in the air
X_c	x axis distance with probe in the soil
x	distance along probes as displayed by the TDR unit (mm)
Z_L	load impedance (ohms)
Z_o	source environment impedance (ohms)
α	wave attenuation
θ	volumetric soil moisture content (mm^3/mm^3)
θ_{TDR}	volumetric soil moisture as measured by the TDR (cm^3/cm^3)
π	mathematical constant 3.1416
σ	conductivity (dS/m)
σ_{dc}	direct current conductivity (dS/m)
μ	magnetic permittivity (henrys/m)
μ_o	μ of free space $(4\pi(10)^{-7}$ henrys/m)

μ_R	relative magnetic permeability
ω_o	electric permittivity of free space ($10^{-9}/36\pi$ farads/m)
ω_r	real part of ω

CHAPTER I

1.1 INTRODUCTION

Information on the soil moisture and the bulk soil electrical conductivity status of a soil is of considerable value to many disciplines, including hydrology, agriculture and various aspects of civil engineering. Thus the need for an accurate, quick, non-destructive means of measuring volumetric soil moisture (θ) and bulk soil electrical conductivity (EC_a) at the same time is obvious. Curently, a few methods exist for measuring water content and salinity in a non-destructive fashion, these include; small tensiometers, pressure transducers and gamma ray techniques for determining soil moisture and, neutron scattering method, 4-probe method, "porous ceramic" salinity sensors and porous ceramic extraction caps for estimating bulk soil electrical conductivity. The first method of measuring water content is tedious, problematic and limited in range; the second is expensive and the third requires highly specialized equipment. For measuring bulk soil electrical conductivity (which leads to estimates of bulk soil salinity) an often used approach is the four-electrode or 4-probe wenner array technique, as defined by Rhoades et al. (1977). But this technique requires concurrent knowledge of soil moisture. There are some limitations to all these methods and a related problem is that water content and soil salinity determinations can not be obtained simultaneously with one approach.

Recent studies have shown that time domain reflectometry (TDR) can be used for measuring both θ and EC_a simultaneously and in a non-destructive manner (Dalton et al., 1984, Dalton and Van Genuchten; 1986, Dasberg and Dalton; 1985, Topp et al., 1988, and Nadler et al., 1991). Measurement of θ and EC_a by TDR is based upon the velocity of propagation (to obtain the dielectric constant of the soil, K_d,) and the magnitude of signal

reflection of an electromagnetic pulse (EMP) guided along metal probes placed in the soil. The dielectric constant of a soil can be defined as the ratio of the electric permittivity of the soil to that of free space. The soil surrounding the metal probes acts as a dielectric causing some impedance and attenuation of the EMP. The dielectric constant of the soil is used to determine soil water content (Topp et al., 1980) and signal attenuation is used to determine EC_a (Dalton et al., 1984).

In recent years TDR has become an accepted means of measuring soil moisture (Hoyhoe et al., 1983; Patterson and Smith, 1981; Stein and Kane, 1983; Topp and Davis, 1982; and Topp and Davis, 1985) which has many advantages over other methods: it can provide excellent spatial resolution, is able to measure close to the soil surface, and is inherently conducive to multiplexing and automation for most mineral soils. For θ determinations it also appears to be essentially independent of soil type, salinity, soil density and soil temperature (Topp et al., 1980). Yet in some instances calibration may be required. Although the application of TDR has been successfully reported upon in many studies, questions still arise with regard to the measurement of the dielectric constant and EC_a determinations of some soil types (peat soils and clay soils). For example, the calibration data of the soils with very high clay fractions or an unusual clay component, have been shown to deviate significantly from the θ calibration curve of Topp et al. (1980) (Dasberg et al., 1992), and soils high in organic matter have been shown to exibit different dielectric characteristics, than those for mineral soils (Herkelrath et al., 1991). Herkelrath et al. (1991) attributed lower dielectric values to the presence of soil organic material, as previously postulated by Topp et al. (1980). Moreover, several investigators working in the microwave range of frequency (1-20 GHz) found a dependence of dielectric constant (K_d) on soil texture (Newton, 1977; Wang and Schmugge, 1980; and Dobson et al., 1985). Unfortunately most researchers do not state at which frequency their measurements have been recorded. Fine textured soils were

found to have lower dielectric values than coarse-textured soils at the same water content, a difference that increased with water content (Dasberg and Hopmans 1992). Bonnell et al. (1991) in determining EC_a, found different calibration curve slopes for different types of soils (sand, silt loam, and clay loam). They suggest that the type and amount of clay present in a soil may have some effect on soil EC_a as determined using TDR.

From reading the above discussion it is evident that a more detailed look at how soil texture (most particularly the clay component) affect θ and EC_a as determined by TDR. Thus, this research project was undertaken to monitor the effect of clay type and clay content on bulk soil electrical conductivity using TDR.

1.2 OBJECTIVES

The objectives of this research are:

i) to record TDR measurements of EC_a and θ for clay soils;

ii) to establish the extent to which clay content effects the dielectric constant and reflection coefficient of the EMP.

iii) to obtain TDR calibration curves for both moisture content and EC_a determinations for the various soils used.

CHAPTER II

2.1 LITERATURE REVIEW

2.1.1 Background

Time domain reflectometry is a technique involving an electromagnetic wave propagation, which can be used to measure the high-frequency electrical properties of materials. In soils applications TDR is used to measure the dielectric constant and signal attenuation to attain an estimate of θ and EC_a respectively. In the TDR technique a step voltage pulse or signal is propagated along a transmission line. The signal's propagation velocity and the amplitude and the polarity of the reflected signal are dependent upon the electrical properties of the materials of which the transmission line is composed.

Every material is characterized by a dielectric permittivity that, in general, is complex and a function of signal frequency. As given by Campbell (1990):

$$\varepsilon = K_d \varepsilon_0 , \quad K_d = \varepsilon_r - i\varepsilon_i \qquad \text{.....} \qquad (2.1)$$

Where the electric permittivity (ε) of a material is proportional to the dielectric constant (K_d) for that material and the electric permittivity of free space ($\varepsilon_0 = 8.85 \times 10^{-12}$ farads/m). The K_d can be divided into real and imaginary dielectric components (ε_r) and (ε_i) respectively. The imaginary dielectric constant which is related to a purely real conductivity (σ) is interrelated by:

$$\varepsilon_i = \sigma / \omega \varepsilon_0 \qquad \text{.....} \qquad (2.2)$$

where ω is the angular frequency of the propagating signal.

Since the dielectric constant of common soil mineralogical materials range from about 2 to 14 while the dielectric constant of water is approximately 80, the dielectric constant of soil is a potentially sensitive indicator of soil moisture. The dielectric constant for a dry soil is approximately 3, while for a saturated soil it is about 25.

The first measurements of the dielectric constant of organic solutions using time domain reflectometry were made by Fellner-Feldegg (1969). Since that time TDR has been applied to the measurement of dielectric properties of many materials including soils. A discussion of TDR applications to soils can be found in Davis and Chudobiak (1975) and Davis (1980). The strong dependence of the dielectric constant on volumetric water content of a soil was found by Topp et al. (1980), and by Topp and Davis (1985) for a number of mineral soils with varying textures. They concluded that the high-frequency dielectric constant is only weakly dependent on soil type, soil density, soil temperature, and pore water conductivity. Thus the volumetric water content of the soil, θ, can be calculated from the empirical equation given by Topp et al. (1980) with an accuracy of + 0.02 m^3/m^3 and a precision or repeatability of + 0.01 m^3/m^3.

$$\theta = -0.053 + 0.029\, K_d - 5.5 \times 10^{-4}\, K_d^2 + 4.3 \times 10^{-6}\, K_d^3 \quad \text{..... (2.3)}$$

where K_d is the dielectric constant (electric transmissivity) of a soil matrix and is determined from the travel time, t, of an electromagnetic pulse passing through a soil by

$$K_d = (ct/2L)^2 \quad \text{..... (2.4)}$$

where c = velocity of light in free space (3×10^8 m/sec) and L = actual length of the probe inserted in the soil. In the commercial TDR instrument used (a Tektronix 1502B),

the term ct/2 is reduced to X_w resulting in

$$K=(X_w/L)^2 \quad \text{.....} \quad (2.5)$$

where X_w is the apparent length of the soil-embeded transmission lines (soil probe) as seen by the TDR unit.

Pepin et al. (1991) established an empirical relationship between the volumetric water content and the apparent dielectric constant, measured in the laboratory, for peat blocks with bulk densities ranging from 0.06 to 0.25 $Mg.m^{-3}$. It is:

$$\theta = 0.85 \times 10^{-1} + 1.92 \times 10^{-2} K_d - 0.95 \times 10^{-4} K_d^2 \quad \text{.....} \quad (2.6)$$

This relationship can be used to estimate volumetric water content between 0.21 and 0.95 cm^3/cm^3 with a standard deviation of 0.03 cm^3/cm^3. They conclude that the calibration curve obtained for peat soil is similar to the one derived by Topp et al. (1980) for an organic soil within the 0.21-0.55 cm^3/cm^3 water content range (**Fig. 2.1**). Also, the results of the experiment, obtained in the 100-200 MHz and within the 75-100% moisture content range for peat, by Toikka and Hallikainen (1989) agreed well with the curve presented by Pepin et al. (1991).

Recent advances in the application of TDR for soil moisture measurements (Dalton and Van Genuchten 1986; Dasberg and Dalton 1985; Malicki 1990; Malicki and Skierucha 1989; Topp and Davis 1985) make it possible to measure water content with an array of TDR probes and to monitor unsaturated water flow phenomena in undisturbed soil cores using standard sampling cylinders.

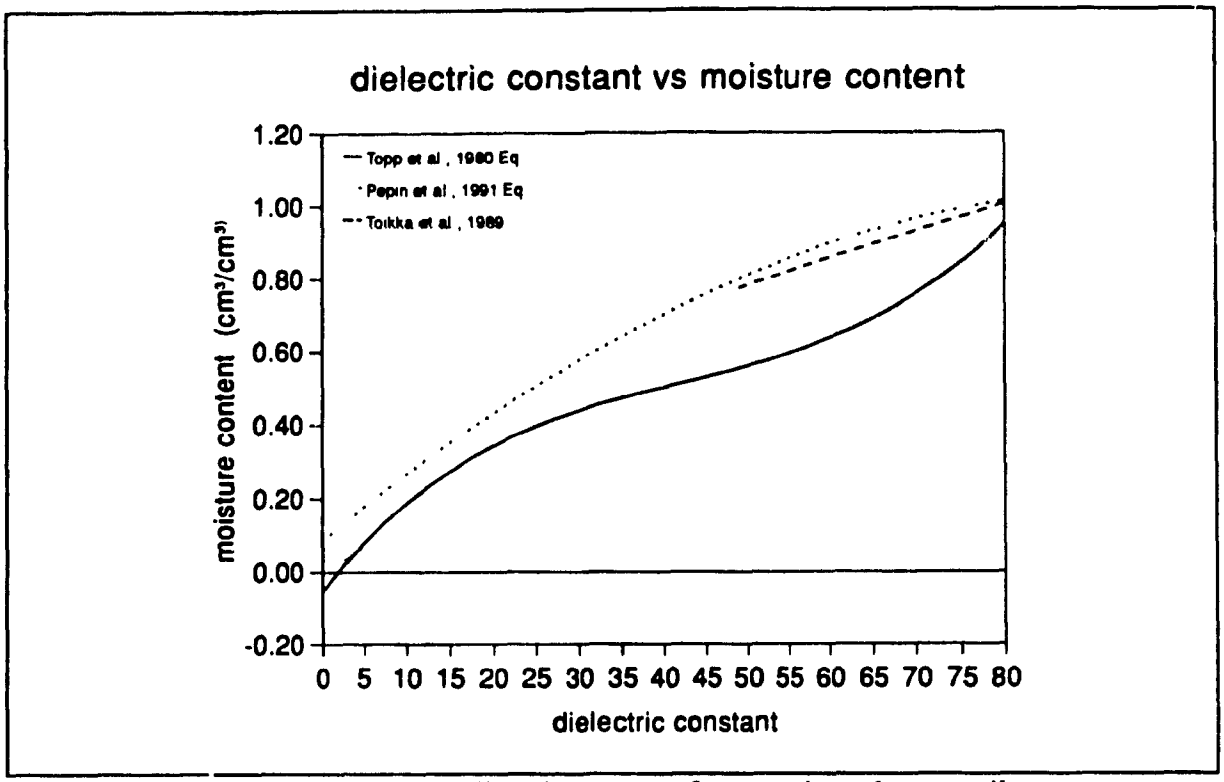

Figure 2.1: Comparison of TDR calibration curves for organic and peat soils.

2.1.2 The evolution of TDR for soil salinity

Fellner-Feldegg (1969) proposed that the shape of the reflected TDR signal could be analyzed to give the low-frequency electrical counductivity of the soil; however Van Gemert (1971) found that Fellner-Feldegg's (1969) approach did not have enough resolution to be practical. Bucci et al. (1972) proposed fitting the TDR response curve asymptotically to a function of the inverse of the square root of time. The coefficient providing a fit to the function was related to the electrical conductivity. A review by Clarkson et al. (1977), following the approach of Giese and Tiemann (1975), includes electrical conductivity in the equation for the reflection coefficient of the dielectric interface at the beginning of the sample as shown:

$$EC_{GT} = (\varepsilon_o c / L)(Z_o / Z_u) [(2V_o / V_f) - 1] \quad \text{.....} \quad (2.7)$$

where $EC_{GT} = EC_a$ as determined by Giese and Tiemann (1975)

ε_o = electric permittivity of free space, 8.85 X 10^{-12} farads/m

c = velocity of electromagnetic waves in free space, 3 x 10^8 m/s

Z_0 = impedance of the transmission line

Z_u = output impedance of the TDR system

V_o = magnitude of signal coming from the TDR

V_f = attenuation fraction

Dalton et al. (1984) and Davis (1980) have demonstrated the feasibility of TDR for measuring soil salinity. It has been noted that there exists a relationship between bulk soil salinity and TDR signal attenuation (Dalton et al., 1984; Topp et al., 1988; and Zegelin et al., 1989).

For a conducting medium such as a saline soil, the launched pulse voltage is attenuated by a number of factors including conduction and dielectric losses into the medium. The amplitude of the reflected pulse voltage is thus diminished in proportion to the electrical conductivity of the transmitting medium. **Fig. 2.2** shows a schematic of a TDR system with a typical TDR output trace on an oscilloscope screen. Point A corresponds to the point where the probe enters the soil and point C corresponds to the probe ends, the point of the first reflection of interest. V_0 represents the output of the pulse generator, V_1 is the magnitude of the voltage pulse that enters the parallel-rod wave guide, and V_2 is the magnitude of the signal reflected at the end of the probes (Fellner-Feldegg, 1969). For an ideal lossless medium, V_2 will be equal to V_1.

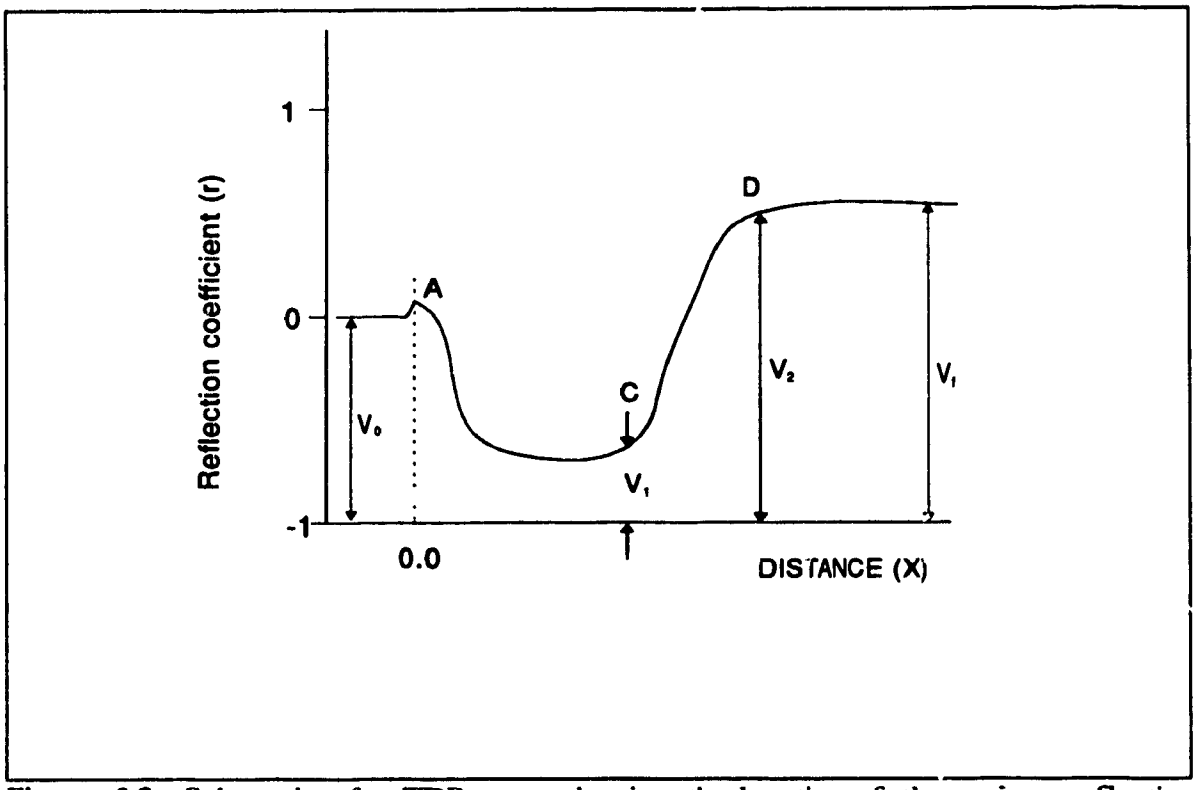

Figure 2.2: Schematic of a TDR trace showing the location of the various reflection coefficients measured.

In the laboratory, Dalton et al. (1984) followed by Dasberg and Dalton (1985) in the field, estimate that the applied voltage pulse, V_1, is attenuated according to

$$V_2 = V_1 + V_1 \exp(-2 \alpha L) \quad \ldots\ldots\ldots\ldots \quad (2.8)$$

where α is an attenuation coefficient which is approximated by

$$\alpha = (EC_a / 2)(\mu_R \mu_o / \varepsilon_r \varepsilon_o)^{1/2} \quad \ldots\ldots\ldots\ldots \quad (2.9)$$

In Eq. 2.9 EC_a is the electrical conductivity of the medium (in siemens per meter); ε_r is the relative dielectric constant of the medium; ε_o is the electric permittivity of free space; μ_o is the magnetic permeability of free space ($4\pi(10^{-7})$ N/m); and μ_R is the relative

magnetic permeability of the medium. For soils low in magnetic material, $\mu_R = 1$ and Eq. 2.9 becomes

$$\alpha = 60\ \pi\ EC_a\ /\ K^{1/2} \qquad \text{.....} \qquad (2.10)$$

combining Eq. 8 and 10 yields the medium electrical conductivity, EC_a (EC_D is EC_a as defined by Dalton et al., 1984), as

$$EC_D = (K^{1/2}/120\pi L)\ln[V_1/(V_2-V_1)] \qquad \text{.....} \qquad (2.11)$$

Topp et al. (1988) state that the nonuniform frequency dependence of any outstanding impedance mismatches must be taken into account. They deal with this problem by attributing the difference in electrical conductivity to the contribution of the imaginary part of the dielectric constant of the soil. They have found that measuring solution conductivity by TDR using both a one round-trip of the TDR signal for analysis and the thin sample approach of Giese and Tiemann (1975) agreed well with the 4-probe conductivity method of Rhoades et al. (1976) and concluded that the imaginary component of the dielectric constant was therefore negligible for solutions. But for soils only the thin sample approach of Giese and Tiemann (1975) produced valid results. Since the one round trip of the TDR signal approach did not work, they concluded that for soils, the imaginary component of the dielectric component is not negligible. They proposed that further investigation of the frequency dependence of the dielectric constant and attenuation was necessary to identify the relative contributions of the real and imaginary parts of the dielectric constant.

Topp et al. (1988) suggested a direct consideration of the reflected pulse after one round tripe so as to avoid any problems with multiple reflections (parameter explained in

the next page) and obtained an approximation of electrical conductivity (EC_T) of the medium, as shown by Zegelin et al. (1989), in

$$EC_T = (K_d^{1/2}/120\pi L)\ln\{[V_1(2V_0 - V_1)]/[V_0(V_2 - V_1)]\} \quad \ldots\ldots\ldots\ldots \quad (2.12)$$

According to the above method, the magnitude of the reflected pulse (V_2) can be defined as:

$$V_2 = V_1 + (V_2 - V_1)^{-2\alpha L} \quad \ldots\ldots\ldots\ldots\ldots\ldots \quad (2.13)$$

where the attenuation coefficient (α) is:

$$\alpha = 60\,\pi\,(\omega\,\varepsilon_o\,\varepsilon_i + \sigma_{dc})\,/\,\varepsilon_r^{1/2} \quad \ldots\ldots\ldots\ldots\ldots\ldots \quad (2.14)$$

In equation (2.14) ε_r and ε_i are the real and imaginary parts, respectively, of the complex dielectric constant, ω is the angular frequency of the propagating signal and σ_{dc} is the static or direct current conductivity.

The analysis used by Dalton et al. (1984), Dalton and Van Genuchten (1986), and Dasberg and Dalton (1985) ignores the effect of multiple reflections of the signal within the soil transmission line. Topp et al. (1988) point out that frequency-dependent attenuation makes V_2 a somewhat arbitrary measure. To overcome this, Yanuka et al. (1988) introduced a multiple reflection model and used the amplitude of the signal, V_f, after all reflections within the cell had taken place (see Fig. 2.2). In this model all interfaces cause partial reflection and partial transmission of the wave energy travelling away from and back to the TDR recorder. Thus a portion of the wave energy which is reflected back to the recorder from the ends of the probes is again reflected back to the

probe ends at the soil surface interface. This phenomena leads to multiple reflections occurring at all interfaces. The curve beyond point D (Fig. 2.2) represents the accumulation of the energy of these multiple reflections. Yanuka et al. (1988), using a more rigorous theoretical approach, and correcting for multiple reflections as applied by Zegelin et al. (1989) obtained an approximation of EC_a by:

$$EC_Y = (K_d^{1/2} / 120\pi L) \ln\{[V_1 V_f - V_0(V_1 + V_f)]/[V_0(V_1 - V_f)]\} \quad \ldots\ldots\ldots \quad (2.15)$$

The results from the thin sample analysis of Giese and Tiemann (1975) which, although being theoretically valid for samples only a few millimetres thick, was found by Topp et al. (1988) to work well in coaxial cells. Zegelin et al. (1989), following the results from Topp et al. (1988), adapted the thin-sample analysis of Giese and Tiemann (1975) and concluded that this approach was an improvement over the method employed by Dalton et al. (1984) provided that the measured probe characteristic impedances are used. Yet estimates of electrical conductivity were only within 10% of values determined using a control method, provided EC_a was greater than 10 mS/m. Zegelin et al. (1989) used the following equation to estimate EC_a:

$$EC_z = (K_d^{1/2} / 120\pi L) (V_1/V_f)[(2V_0 - V_f)/(2V_0 - V_1)] \quad \ldots\ldots\ldots\ldots \quad (2.16)$$

Van Loon et al. (1990), recognizing that signal reflection is not only influenced by the soil medium but also by the measuring system itself, corrected for measuring system influence by comparing a soil reflection measurement with a reference measurement performed with the probe in air. The air reference measurement was assumed to be characteristic of the system itself and any change in the signal, when the probe was inserted into the soil, was attributed to the soil itself. Their results were comparable to those of Dalton (1987), Heimovaara et al. (1988) and Topp et al. (1988). They assumed

that the attenuation due to the measuring device itself was constant and contrary to Topp et al. (1988) assumed that the influence of the imaginary part of the dielectric constant can be neglected and the use of superposition to correct for the influences of measurement system itself was valid.

According to the above assumptions the attenuation coefficient (α) can be written as (Van Loon et al., 1990):

$$\alpha = (1 / 2L) \ln (r_0 / r) \quad \ldots\ldots\ldots\ldots \quad (2.17)$$

Equation 2.17 is independent of multiple reflections. This approach avoids the necessity of accounting for cable and probe impedance mismatches by calibrating the probe in air and comparing these results with those obtained with the probes in the soil. The bulk electrical conductivity is then:

$$EC_V = [K_d^{1/2} / (120 \pi L)] \ln(r_0 / r) \quad \ldots\ldots\ldots\ldots \quad (2.18)$$

where the recording of r_o (the magnitude of the reflection coefficient) is taken at X_{c0} and that of r is taken at X_c, with the probe in air and in the soil respectively. X_{c0} and X_c are the x-axis distances as read on the oscilloscope with the probe in air and in the soil respectively (**Fig. 2.3**). It should be noted that (r_0) is a constant for any particular probe configuration and has to be determined only once. The choice of X_{c0} at which to measure r_0 is arbitrary, but to obtain the best resolution it should be measured near the maximum of the curve at a point beyond the probe ends, ie. in the region of point D of Fig.2.3. The magnitude of r and r_0 is composed of the addition of 1.0 plus the vertical distance of the curve above (+ve) or below (-ve) the horizontal zero line as shown in Fig. 2.3. Note that r and r_0 have an absolute value of 1.0 when measured from the x-axis up to the horizontal

zero line of Fig. 2.3.

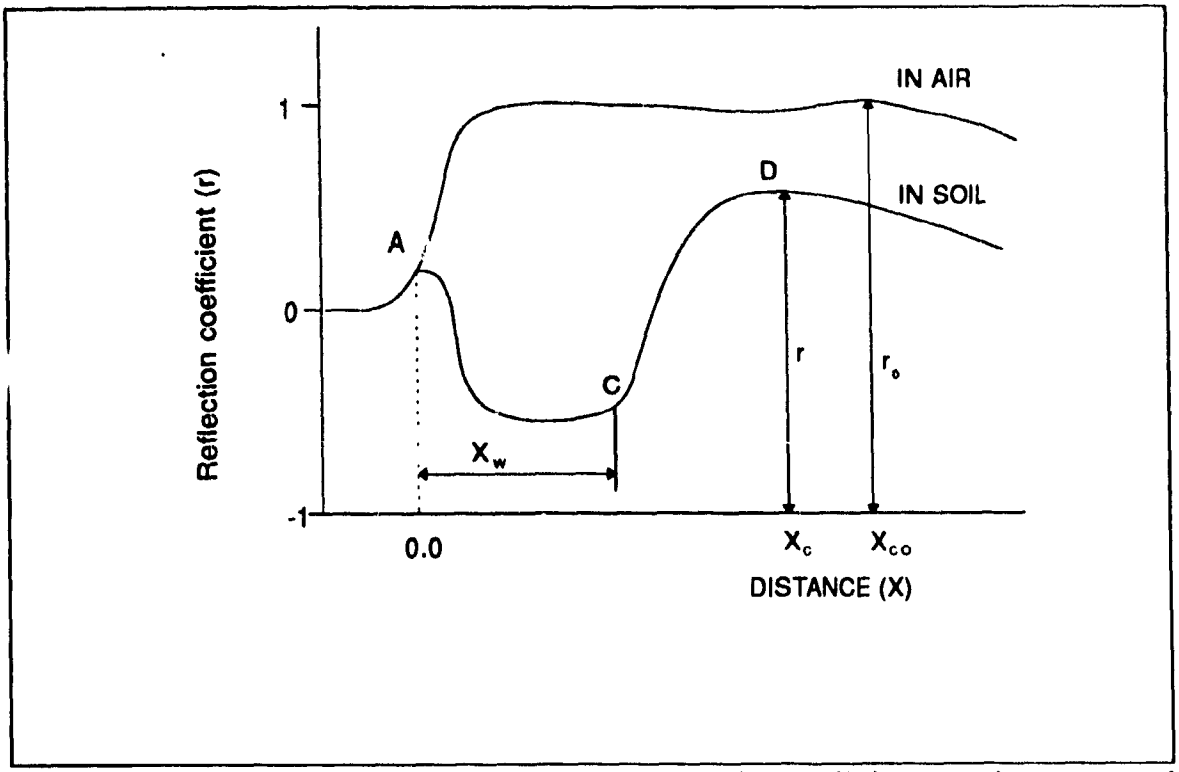

Figure 2.3: A TDR trace in air and soil showing reflection coefficient, r and r_0, measured at x_c and x_{co} respectively.

As explained by Bonnell et al., 1991, "In the method of Van Loon et al. (1990) the basic premise is to measure the reflection of the signal from the probe in the air (r_0) at a chosen location or number of reflections (n) beyond point D. If for example, the point of 10 reflection is required, then from the definition of K above, $X_{c0} = nLK_d^{1/2} = 10 LK_d^{1/2}$. In air, K_d is essentially equal to 1.0. Next, the probe is inserted into the soil and r is measured at X_c. The change in magnitude of the reflection coefficient from r_0 to r is attributed to the effect on EMP attenuation by the soil. Since EMP travel time is longer in the soil than in air, the distance X_c must be smaller than X_{c0} to correspond to a point representing the same number of reflections. Thus, the soil measurement of r must be made at a different position on the X-axis to correspond to the same time frame. The

determination of X_c at which to measure r is given by $X_c = 10LK_d^{1/2}$ (the 10 corresponds to 10 reflections and once in the soil, K_d is a function of X_w)."

Nadler et al. (1991) used an approach similar to that of Van Loon et al. (1990) to overcome multiple reflection interferences caused by impedance mismatches and also to simplify EC_a measurement by reducing the number of parameters required for the calculation. They assume that at very long distances along the trace, all the reflections are suppressed and the signal approaches a constant value (V_f), which they assume is the result of impedance of the direct current only. They found that V_f is independent of the probe configuration, transfer efficiency of pulse energy or multiple reflections. Nadler et al. (1991) used the voltage reflection coefficient (r) to determine the impedance of the transmission line according to

$$r = (Z_L - Z_0) / (Z_L + Z_0) \quad \text{.....} \quad (2.19)$$

where Z_0 is the characteristic impedance of the cable and Z_L is the load of the transmission line embedded in the medium under investigation. Therefore, measuring the amplitude of the signal at a long distance gives r values, which can be read directly from the instrument screen, from which the load of the transmission line (Z_L) can be calculated, and converted to EC_a by using the probe's geometric constant.

The geometric constant (K_c) can be experimentally determined by immersing the transmission line in a solution of known salinity (EC_a), measuring the resistance R_L by TDR, and using an equation identical to Rhoades and Van Schilfgaarde (1976) as:

$$K_c = EC_{ref}(25^0)\ R_L / f_t \quad \text{.....} \quad (2.20)$$

where $EC_{ref}(25°)$ is a solution of known electrical conductivity at 25 °C, and f_t is a temperature-correction coefficient. The author cautions against using such an approach because of the differing results obtained by Topp et al., (1988) and Bonnell et al., (1991) when measuring EC of solutions and that of moist soils. In conclusion, Nadler et al. (1991) found that their approach and the calculation procedures of Dalton et al. (1984) are the most suitable for calculating EC_a. They found the method of Topp et al. (1988), Yanuka et al. (1988) and Zegelin et al. (1989) not to correlate as well as their own approach. Yet Bonnell et al. (1991) found that the equation given by Dalton and Van Genuchten (1986) for determination of absolute EC_a values is not valid for all conditions, but is valid for measuring aqueous salinity levels.

In another work, Bonnell et al. (1991) obtained different slope values of calibration curves for different soil types. They hypothesized that these differences may be attributed to the transmission coefficient, [T] (as defined by Rhoades et al., 1976), of the soils and clay type which in turn is a function of soil texture and structure with respect to continuity of the soil pores. Rhoades et al. (1989) found a soil structure dependency of EC_a to EC_w, where EC_w is EC of the soil water, sufficiently important to make field calibrations necessary and used undisturbed soil for evaluating volumetric soil water content in fine pores. However, Nadler (1991) reports a minimal effect of structure disruption on bulk soil electrical conductivity, determined by electromagnetic induction. The reason is based on an electromagnetic pulse signal interacting with the electric field of ions in the soil solution and not on direct contact (Nadler, 1991).

Current research in field applications of TDR technology is also looking into improved probe design. Zegelin et al. (1989) propose the use of simulated coaxial transmission lines, i.e. three- or four-rod probes, to avoid the necessity of using an impedance matching transformer (balun) at the coaxial wire to soil probe connection.

Malicki and Skierucha (1989) have developed an in series probe design whereby several probes can be monitored without switching. Hook et al. (1992) have developed a transmission line (3-rod probe) combined with a remote shorting diode to provide maximal amplitude reflections defining the point at which the transmission line enters the soil and of points within the soil. This has the advantage of eliminating extraneous reflections and allows easy and reliable waveform interpretation by unskilled operators or by automated system software.

TDR has also been successfully used to monitor the travel time density function of a conserving tracer added as a pulse under conditions of a constant surface water flux density (Kachanoski et al., 1992).

Recent innovations that allow several wave guides to be automated and continuously monitored by one unattended TDR unit (Baker and Allmares, 1990; and Wraith et al., 1991) have made TDR a potentially powerful tool for studying root water uptake.

It is clear that the use of TDR for determination of EC_a has not been clearly established and requires a better understanding of the complexities of the dielectric behaviour of a soil matrix and of the electromagnetic phenomena which affect wave attenuation and velocity of propagation (Bonnell et al., 1991). Bonnell (1993) in his thesis presented a detailed discussion of electromagnetic wave propagation theory and a number of caveat factors related to the TDR technique. He presented a number of unanswered questions related to the EM problems in the use of the TDR equipment for soil measurements. "The number of possible unknowns is still so large that a rigorous causal relationship is still elusive and the need of an empirical calibration approach is necessary" (Bonnell, 1993).

CHAPTER III

3.1 MATERIALS AND METHODS

3.1.1 SOILS AND SALT SOLUTION

Two artificial clay materials (Hydrite R Kaolin and Korthix-H Bentonite) and a natural clay soil (Ste. Rosalie) were used in the experiment. Note that the Hydrite and Bentonite materials are 100% clay mineral, but they have 80% and 90% clay size respectively. Some characteristics of the Hydrite, Bentonite and Ste. Rosalie clay soil are given in **Table 3.1** (Typical particle size distributions and detailed properties are presented in **Appendix A**). The natural clay soil was air-dried and passed through a 2 mm sieve. Each of these materials (Hydrite, Bentonite and Ste. Rosalie) was mixed with a sand soil (Ste. Sophie) at three different levels; 8%, 16% and 30% by weight (resulting in nine different mixtures). In order to maximize homogeneity, the clay material and sand were

Table 3.1: Physical/Chemical properties of Hydrite R, Korthix-H Bentonite and Ste. Rosalie clay.

	Type of clay		
Property	**Hydrite R**	**Bentonite**	**Rosalie**
Colour	White	White	Dark brown
Form	Fine powder	Fine Powder	Granular
pH	4.2 - 5.2	9-10	5.2 - 7.8
% clay size	80	90	43.5
Specific surface (m^2 /g)	5 - 20	700-800	Unknown
Swelling capacity	Low	High	Low
Cation exchange capacity (meq/100 g)	3 - 15	80 - 100	5 -20

Table 3.2: Physical/Chemical properties of different mixture soils.

Type of mixture	Property		
	Clay content %	Specific surface (m^2/g)	Cation exchange capacity (meq/100g)
H-8%	6.40	0.4-1.6	0.24-1.2
H-16%	12.80	0.8-3.2	0.48-2.4
H-30%	24.00	1.5-6.0	0.9-4.5
B-8%	7.20	5.6-6.4	6.4-8.0
B-16%	14.40	11.2-12.8	12.8-16.0
B-30%	27.00	21.0-24.0	24.0-30.0
N-8%	3.48	Unknown	0.4-1.6
N-16%	6.96	Unknown	0.8-3.2
N-30%	13.05	Unknown	1.5-6.0

H-8% : 8% Hydrite clay material mixed with 92% coarse sand by weight.
H-16% : 16% Hydrite clay material mixed with 84% coarse sand by weight.
H-30% : 30% Hydrite clay material mixed with 70% coarse sand by weight.
B-8% : 8% Bentonite clay material mixed with 92% coarse sand by weight.
B-16% : 16% Bentonite clay material mixed with 84% coarse sand by weight.
B-30% : 30% Bentonite clay material mixed with 70% coarse sand by weight.
N-8% : 8% natural (Ste. Rosalie) clay soil mixed with 92% coarse sand by weight.
N-16% : 16% natural (Ste. Rosalie) clay soil mixed with 84% coarse sand by weight.
N-30% : 30% natural (Ste. Rosalie) clay soil mixed with 70% coarse sand by weight.

thoroughly mixed by hand. Some properties of these mixtures are presented in **Table 3.2**. Texture and particle-size analyses of the Ste. Rosalie caly soil and sand were determined using the hydrometer and seive methods respectively (**Appendix A**). Three replicates of each mixture were packed into PVC cylinders (150 mm diameter and 200 mm in length)

to a depth of 150 mm from the bottom with a bulk density of 1.66 Mg/m^3. Thus there was a total of 27 cylinders. The cylinders were open on top and a wooden base with an entrance hole at the centre was glued on the bottom. Tap water was mixed with potassium chloride (KCl) salt to obtain a soaking solution of 10 dS/m. The solution conductivity was measured using a standard conductivity meter. The salt solution was introduced into the soil columns via the bottom entrance hole. A small positive head was maintained and the samples were allowed to saturate by capillary rise until the soil surface glistened. Readings of bulk electrical conductivity (EC_a) of the soils (method described below) were recorded every four or five days as the soils dried by evaporation. To obtain more data points, the samples were resaturated and readings were again recorded over a period of 70 days. Values of θ were determined by recording changes in the weight of each core at the same time as each EC_a reading was performed. At the finish of the EC_a readings, the cores were oven dried to determine a final θ from which all previous moisture contents were determined by back-calculation, using the changes in weight previously recorded.

3.1.2 EC_a MEASUREMENT

Two completely independent, electrical techniques for measuring EC_a were used: (i) In the TDR technique, the data were recorded using a Tektronix 1502B cable Tester connected via a 50 ohm coaxial cable to a wave guide made of three parallel stainless steel rods (Zegelin et al., 1989), spaced 3 cm, 6 cm long and 2 mm in diameter (**Fig. 3.1**). As shown in **Fig. 3.1** the central probe is isolated from the metal shield by a plastic dielectric and passes through the centre part of this shield and is connected to the centre conductor of the coaxial cable. The two outer probes are screwed into the metal shield. Inturn the outer wire shield of the coaxial cable is split in two and connected to the metal shield. For calculating EC_a from transmitted and reflected pulse voltages, the Van Loon

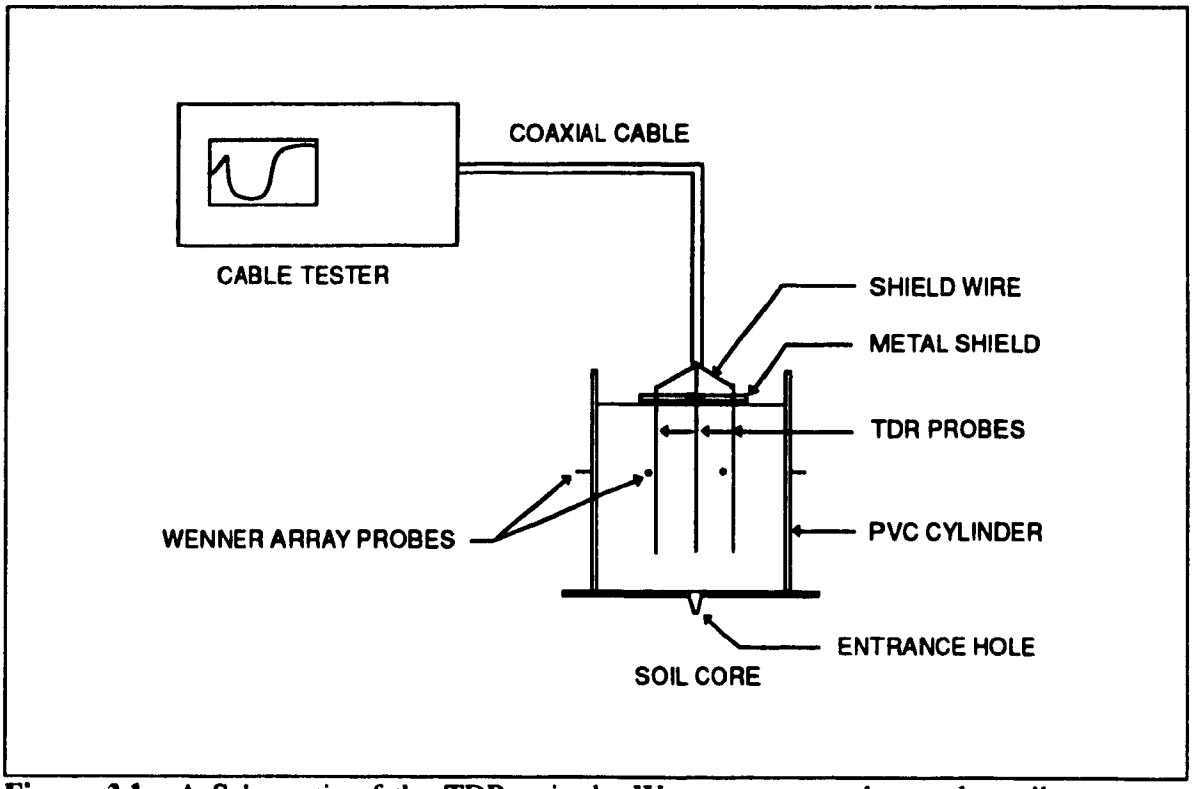

Figure 3.1: A Schematic of the TDR unit, the Wenner array probes and a soil core.

procedure (eq. 2.18 in literature review) was used and the following measurements were taken by eye directly from the screen for each combination of the packed soils.

X_w - the travel distance of the pulse through the soil (or apparent length).

r - the magnitude of the reflected signal at X_c with 10 reflection.

(ii) In the four-probe technique, the readings were performed using a Meggar ET3 Earth Tester connected to four electrodes of stainless steel (40 mm long by 1 mm in diameter). Eight electrodes were inserted horizontally through the sides of each PVC column to a depth of 10 mm into the soil. The holes through which the electrodes protruded were sealed with an epoxy glue. The electrodes were inserted at 45° intervals around the column circumference and stationed at 85 mm from the bottom of each column (**Fig. 3.1**).

These electrodes were used to measure bulk soil electrical conductivity (EC_a) via the four-electrode technique as outlined by Rhoades et al. (1977). Any four neighbouring electrodes can be regarded as a Wenner array, the outer two are used as current electrodes and the inner two as potential electrodes. By rotating the connections, four independent measurements were obtained for any sample and the averaged value was used to calculate EC_{4p} (EC_{4p} is EC_a as measured by 4-probe method, dS/m) as:

$$EC_{4p} = K f_t / R_t \quad \text{.....} \quad (3.1)$$

where f_t is the appropriate temperature factor for correcting resistance and conductivity data (presented in **Appendix B**). The cell factor (K) determined for a cylinder by filling it with a solution of known electrical conductivity at 25°C (EC_{25}) and measuring the resistance at temperature t (R_t ohms), and then calculating K as:

$$K = EC_{25} \cdot R_t \cdot 1/f_t \quad \text{.....} \quad (3.2)$$

The temperature of the soil for each reading was determined using a metal thermometer. This temperature value was then used to determine the f_t factor for correcting EC_a.

3.1.3 Surface conductance (EC_a) and transmission factor [T] determination

Bulk soil electrical conductivity (EC_a) is known to be influenced by the properties of the soil liquid and the solid phases of a soil matrix. Rhoades et al. (1976) have advocated the following equations to describe this functional relation:

$$EC_a = EC_w \, \theta \, T + EC_s \quad \text{.....} \quad (3.3)$$

$$[T] = a + b \, \theta \quad \text{.....} \quad (3.4)$$

where [T] is a transmission coefficient (pore geometry factor) linearly dependent on θ with a and b being empirical parameters which are dependent on the tortuosity of the current path as a consequence of soil texture and structure, EC_w is the electrical conductivity of the soil solution and EC_s is soil particle surface conductance.

The equations above show that EC_a is a function of a number of parameters. In an effort to isolate the effects of some of these parameters, such as surface conductance, EC_S, and transmission coefficient, [T], the same cylinders were used and refilled with the same soil mixture types, in the same method described above. Salt solutions of 2.5, 26 and 54.2 dS/m were used to saturate the soils from the entrance hole in the bottom. Readings of bulk electrical conductivity of the soils, using the 4-probe method, were recorded every 5 days as the soils dried out by evaporation. The values of θ were determined by recording changes in weight of each core in the same manner (back-calculation) as mentioned above. Then the procedure as outlined by Rhoades et al. (1976) was used to determined [T] and EC_s. The ranges of water content and salinities used in this study are shown in **Table 3.3.**

Table 3.3: Range of volumetric water content, θ (cm^3/cm^3), and liquid phase electrical conductivity, EC_w (dS/m), used in this experiment.

Soil	θ	EC_w	Soil	θ	EC_w	Soil	θ	EC_w
H-8%	0.05-0.25	2.5-54.2	B-8%	0.05-0.20	2.5-54.2	N-8%	0.05-0.30	2.5-54.2
H-16%	0.05-0.25	2.5-54.2	B-16%	0.10-0.25	2.5-54.2	N-16%	0.05-0.30	2.5-54.2
H-30%	0.10-0.40	2.5-54.2	B-30%	0.15-0.30	2.5-54.2	N-30%	0.10-0.30	2.5-54.2

As water evaporates from the cores, the salt concentration of the remaining soil water increases proportionally. It has been found that because of this inverse proportional relationship between EC_w and θ, the product (EC_w θ) will not change appreciably as θ

decreases (Halvorson and Rhoades, 1974 and; Rhoades et al., 1976). EC_a is affected by changes in θ due to the influence of θ on [T]. As θ decreases, the effect of [T] increases linearly (Rhoades and Halvorson, 1977). Therefore, as the initially wetted soil cores dry by evaporation, a linear decrease in EC_a can be expected.

CHAPTER IV

4.0 RESULTS AND DISCUSSION

4.1 Soil salinity parameters

Bulk soil electrical conductivity (EC_a), described by Rhoades et al. (1976), is known to be influenced by a number of parameters such as surface conductance, EC_S, and transmission coefficient, [T], which are dependent on soil texture and structure. The following equations show this functional relation:

$$EC_a = EC_w\ \theta\ T + EC_S \quad \text{.....} \quad (4.1)$$

$$[T] = a + b\ \theta \quad \text{.....} \quad (4.2)$$

The following describes how EC_S and [T] were determined for different mixtures.

Values of EC_a (measured by 4-Probe method) / EC_w for various combinations of water content and EC_w are shown in **Fig. 4.1** for the B-8% material (results for all other materials are presented in **Appendix C**). Note that from equation (4.1) EC_S (at any value of θ) will equal EC_a if EC_w equals zero. With this in mind, Fig. 4.2 was constructed from Fig. 4.1 by reading values of EC_a and EC_w for set values of θ at the intersections of the vertical lines and curves in Fig. 4.1. The value of EC_S was then obtained by extrapolating the curves in Fig. 4.2 to $EC_w = 0$ and equals 0.165 dS/m for the B-8% material. Note that the value of EC_S is essentially independent of the water content. This value of EC_S was used to replot the data points given in Fig. 4.1 in the form of $(EC_a - EC_S)/EC_w$ versus θ, as shown in Fig. 4.3. Fig. 4.3 illustrates that, after this correction for

surface conductance, the data points for all three values of EC_w tend to fall on one curve (R-square = 0.91). According to Eq. 4.1, the ratio $(EC_a - EC_s)/EC_w$ is equal to θ T. The vertical axis of Figure 4.4 is of $(EC_a - EC_s)/EC_w\ \theta = T = a + b\ \theta$. Figure 4.4 shows R-square equal to 0.99 when a = -0.065 and b = 1.59. This procedure for determining EC_s and a and b values was repeated for each of the soil materials used. The related graphs are presented in **appendix C** and the overall data is presented in **Table 4.1**.

The surface conductivities found range from 0.035 dS/m for the N-8% soil to 0.511 dS/m for the B-30% material. EC_s recorded in Table 4.1 and plotted in **Figure 4.5** (for all the nine soil mixes) become progressively larger as the fine fraction of the soil texture increases. This is as expected, because an increase in the clay fraction increases the electrically active portion of the soil matrix surface area (surface charge density). Figure 4.5 shows quite clearly the gradual increase in EC_s with increase in clay material content for the Hydrite and natural clay soils. There is a much greater increase in EC_s for increasing amounts of Bentonite clay material. This figure also, illustrates the much larger EC_s values for the Bentonite material compared to the Hydrite and natural materials. This is also expected, because the surface charge density, related to the cation exchange capacity (CEC), of the Bentonite clay material is larger than the Hydrite and natural clay materials. The ranges of CEC are 80-100 meq/100g for the Bentonite clay material, 3-15 meq/100g for the Hydrite clay material and 5-20 meq/100g of soil for the natural (Ste Rosalie)clay soil.

Transmission coefficient, [T], is a pore geometry factor linearly dependent on θ with a and b being empirical parameters appropriate for the particular soil. Table 4.1 shows the values of a and b for all the soil materials used in this study. The b (slope) values (illustrated in Figure 4.6) for the Bentonite material is larger compared to the other clay type materials. This can be attributed to the total pore space and size of these pores. Sandy soils show a range of from 35 to 50 percent pore space, whereas medium- to fine-

textured soils vary from 40 to 60 percent or even more in the case of marked granulation (Brady, 1974). In a sandy soil, in spite of the low total porosity, the movement of electrons (electrical current) in the liquid phase is surprisingly rapid because of the dominance of the macrospaces. Fine-textured soils allow relatively slow movement despite the unusually large amount of total pore space.

It has been found (Rhoades et al., 1976) that if θ is smaller than a threshold water content, θ_t defined as - a/b, the conductivity due to EC_w will be zero. As shown in Table 4.2, the threshold water content, θ_t, ranged from 0.012 for N-16% soil to 0.14 for B-30% soil. The dash mark (-) for θ_t in Table 4.2 represent that some soils do not show any limitation to the moisture content. Thus, the conductivity due to EC_w can not be zero for them even with a very small moisture content.

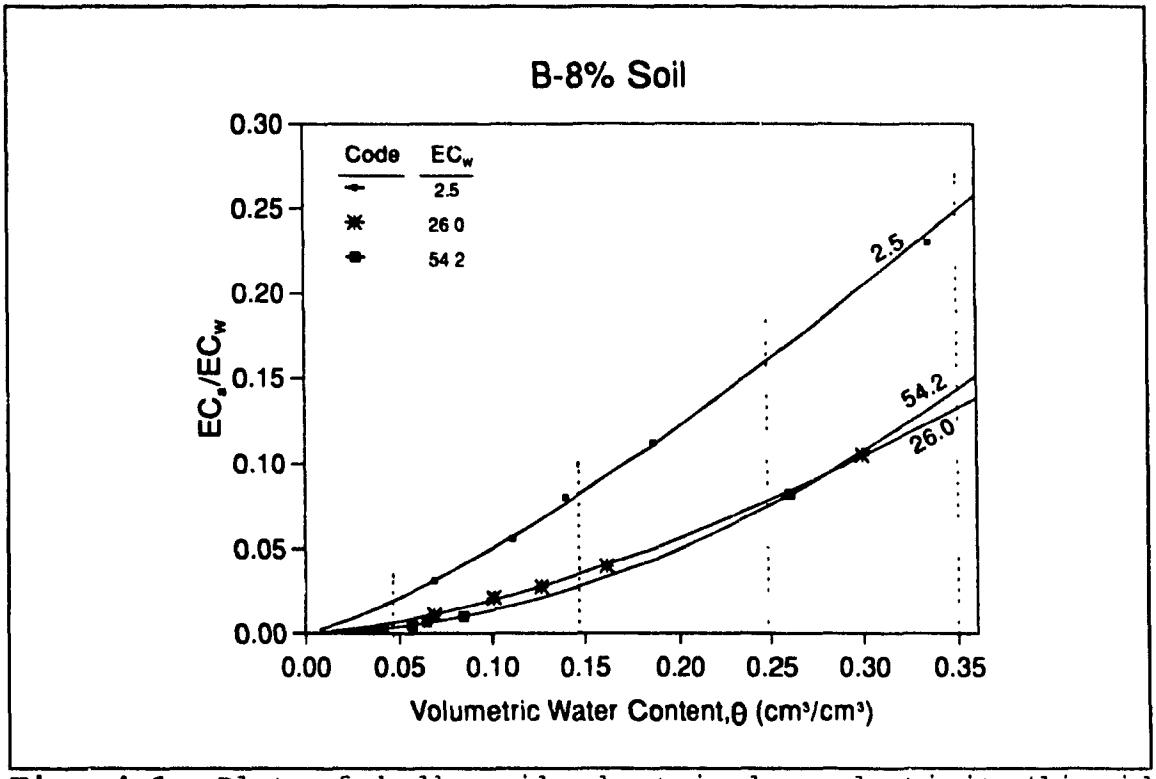

Fig. 4.1: Plot of bulk soil electrical conductivity/liquid phase electrical conductivity, EC_a/EC_w, vs. volumetric water content, θ, for B-8% material.

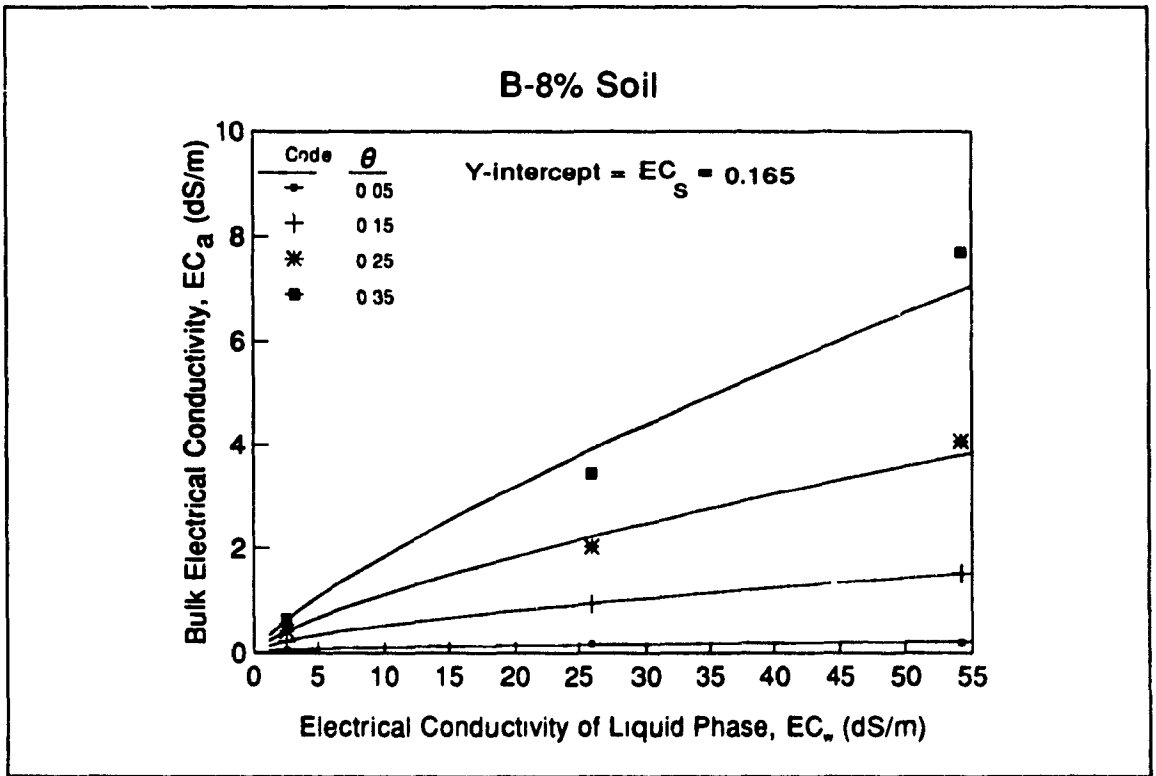

Fig. 4.2: Plot of EC_a vs. EC_w for various chosen volumetric water contents as interpolated from Fig. 4.1 for B-8% material showing the extrapolated value of EC_s as the Y-intercept.

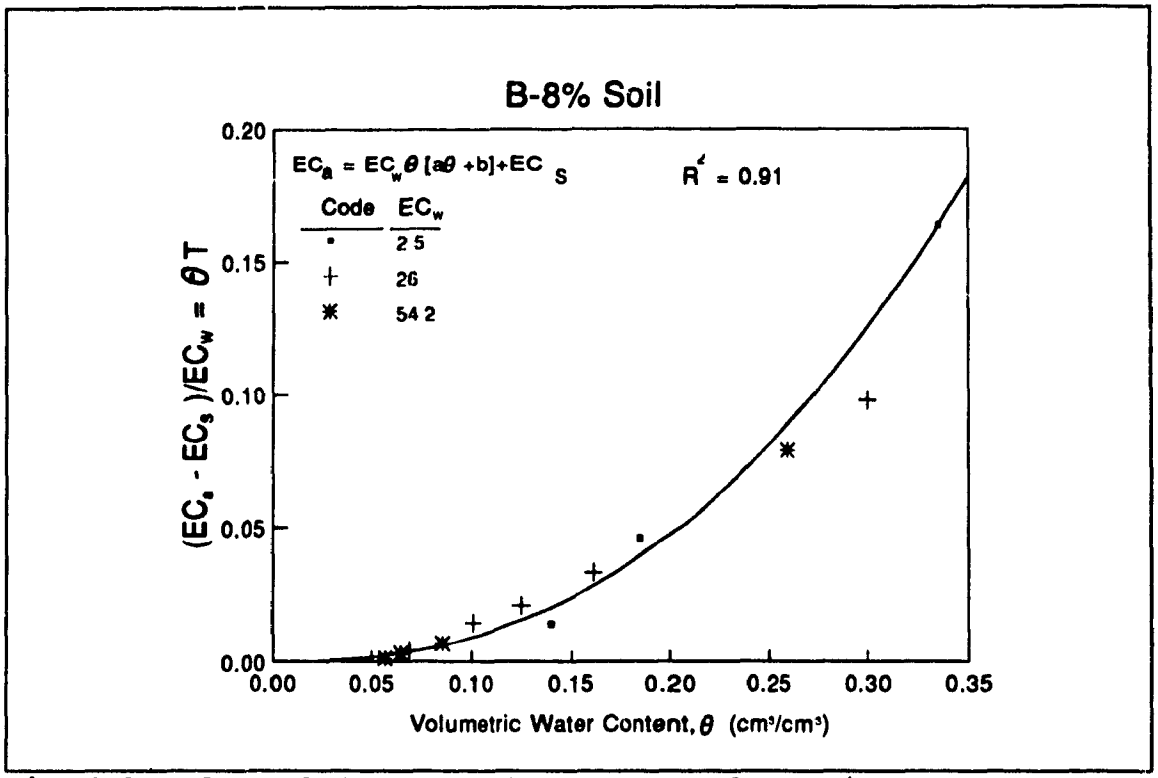

Fig 4.3: Plot of $(EC_a - EC_s)/EC_w$ vs. volumetric water content for data of Fig 4.1 and Fig 4.2.

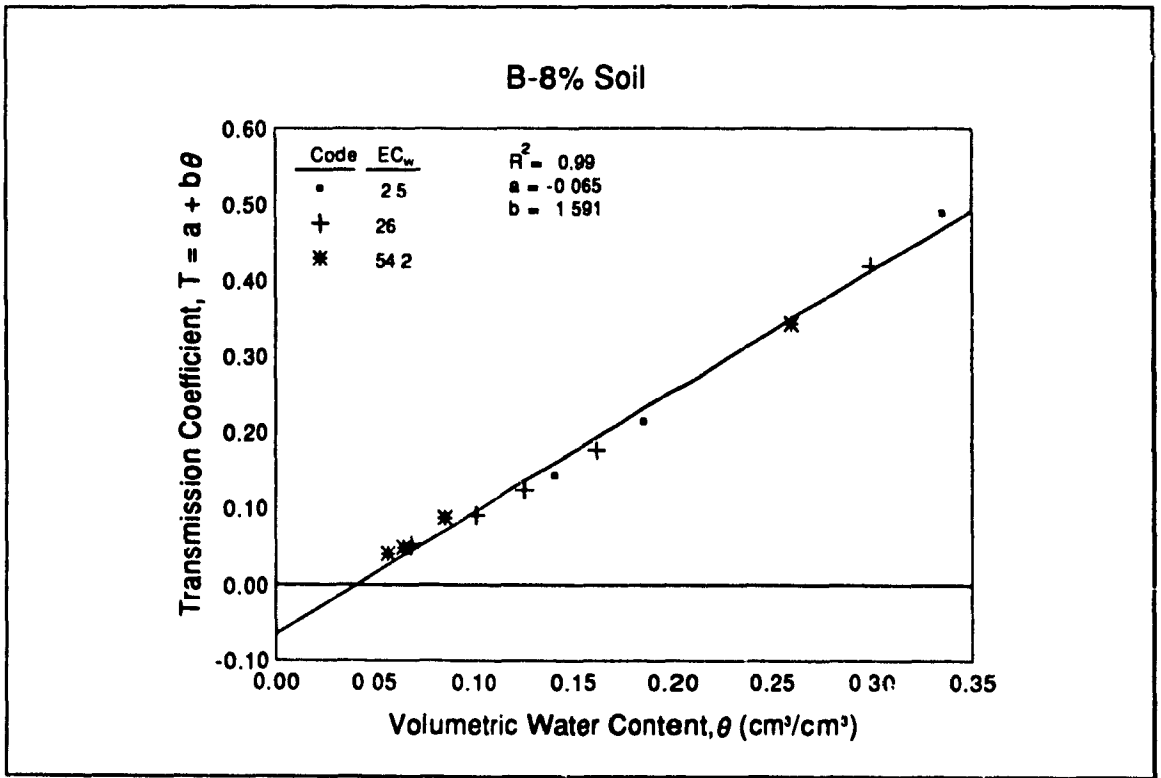

Fig. 4.4: Relation of the transmission coefficient, T, and volumetric water content, θ, determined for B-8% material.

Table 4.1: Determined surface conductivities, transmission coefficient parameters, and threshold water contents of soils.

Soil	EC_S	a^+	b^+	θ_t *	R #
1 H-8%	0.080	0.219	0.53	-	0.98
2 B-8%	0.165	-0.065	1.59	0.04	0.99
3 N-8%	0.035	0.071	0.96	-	0.99
4 H-16%	0.096	0.181	0.96	-	0.98
5 B-16%	0.400	-0.021	1.34	0.020	0.99
6 N-16%	0.050	-0.013	1.06	0.012	0.99
7 H-30%	0.136	0.16	0.28	-	0.97
8 B-30%	0.511	-0.39	2.76	0.140	0.97
9 N-30%	0.075	-0.015	0.82	0.018	0.99

+ Transmission coefficient = $[a + b\theta]$; a = intercept, b = slope.

* θ_t = threshold water content = - (a/b).

\# Linear correlation coefficient between The transmission coefficient and θ.

1 8% Hydrite clay material mixed with 92% coarse sand.

2 8% Bentonite clay material mixed with 92% coarse sand.

3 8% natural (Ste. Rosalie) clay soil mixed with 92% coarse sand.

4 16% Hydrite clay material mixed with 84% coarse sand.

5 16% Bentonite clay material mixed with 84% coarse sand.

6 16% natural (Ste. Rosalie) clay soil mixed with 84% coarse sand.

7 30% Hydrite clay material mixed with 70% coarse sand.

8 30% Bentonite clay material mixed with 70% coarse sand.

9 30% natural (Ste. Rosalie) clay soil mixed with 70% coarse sand.

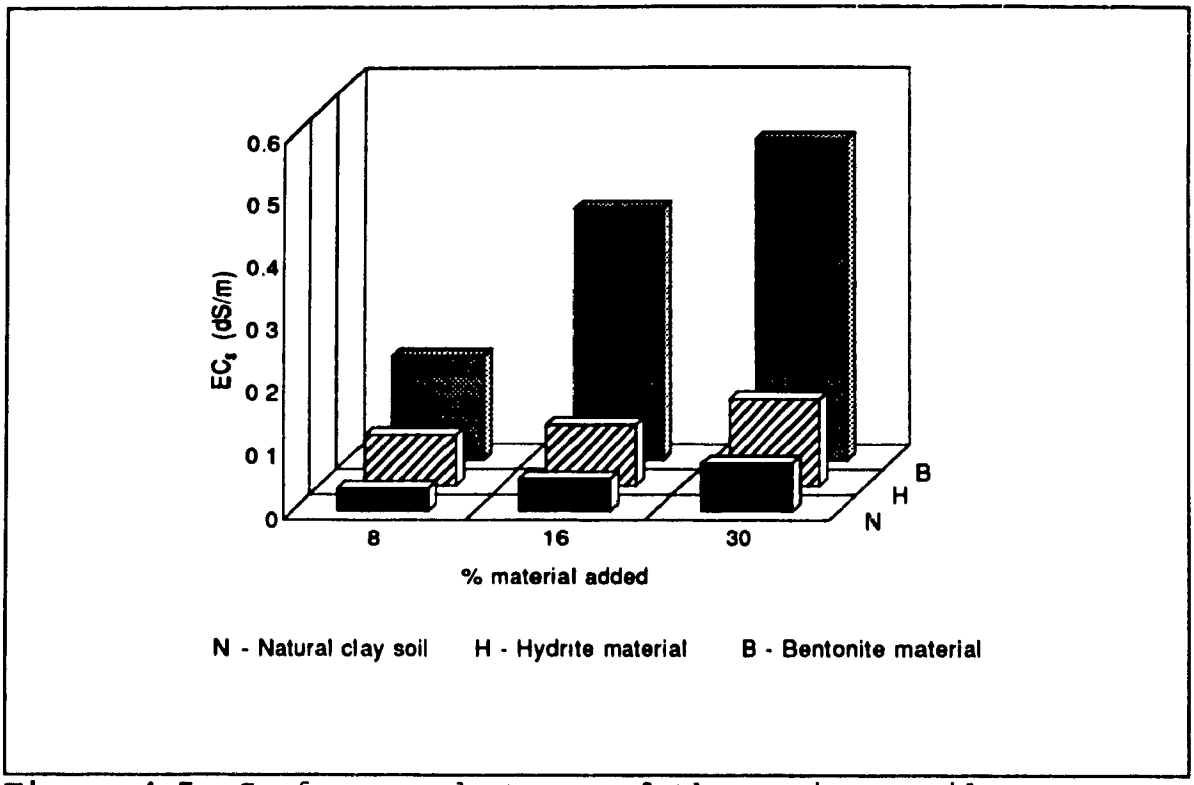

Figure 4.5: Surface conductance of the various soil types.

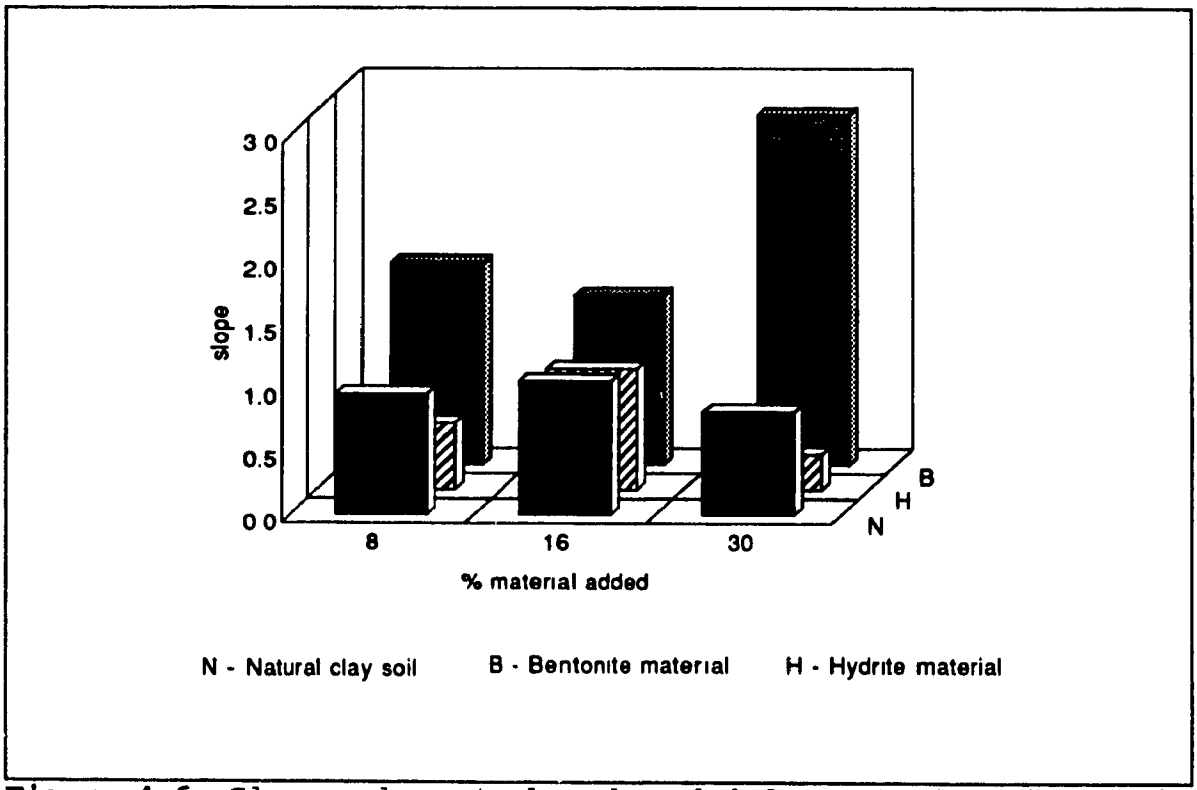

Figure 4.6: Slope values (related to [T] factor) of various soil types.

4.2 Statistical analysis performed

The experimental data of EC_a and θ obtained using TDR, was analysed using a SAS (statistical analysis system) computer program. The experimental design used was a completely randomized design with three sources of clay material (Hydrite, Bentonite and a Ste. Rosalie clay soil), each mixed at three levels (8%, 16% and 30% by weight) with sand. The observed variations in θ-TDR and EC_a-TDR are partly attributable to variations in actual moisture content (moisture content obtained by weight). Thus analysis of covariance was carried out to remove the effect of the covariable (moisture content obtained by weight) and to adjust the treatment means. The three levels of clay content were analyzed within each group seperately. Because they were different for each group (see Table 3.2). The test of heterogeneity of slopes was performed to compare the regression relationships constructed for treatment groups (clay types) and to investigate the effect of clay types on TDR readings. Regression relationships that differ among treatment groups actually reflect an interaction between the treatment groups and the independent variable(s) or covariates (Rudolf J. Freund and Ramon C. Littel, 1981). In SAS this phenomenon is indeed specified and analyzed as an interaction and the Type I sums of squares provide the most useful information.

The clay content and clay type were tested for their effects on θ and EC_a measured by TDR. All of the SAS output files are shown in **Appendix D.**

4.3 Discussion of moisture content

4.3.1 Results of statistical analysis for different clay content

The results of analyses of covariance for different levels of material within each group are presented in **Table 4.2.** As can be seen from Table 4.2 (a, b, c), the effect of

gravimetric moisture content on θ-TDR, as the covariable, is significant at the 1% level. There exist significant differences among the materials (8%, 16% and 30%) within each group at 1% level. This means that clay content has some effect on θ-TDR readings. The contrast tests presented in Table 4.2 (a, b, c) show that there exist significant differences between each pair of materials at the probability level of 1%. One exception is the contrast test between 8% and 16% materials within the Ste. Rosalie group which is not significant at the propability level of 5% or more. This anomaly can be attributed to the low level of clay particle size content (3.48% and 6.96%) corresponded to 8% and 16% Ste. Rosalie soils respectively. It may be that there exists a threshold level of clay size content above which the amount of clay effects the θ-TDR. This threshold level is probably different for different clay types.

The TDR and gravimetric moisture content data, obtained at the same time, are illustrated in **Figures 4.7 to 4.9**. The regression lines, fitted to these data, represent the calibration lines for different material within each group. The intercept, slope and R-square values of all regression lines are shown in **Table 4.3**. These calibration lines visually illustrate that there exists a difference in θ-TDR for different levels of clay material. Further discussion on this point follows.

Physical and chemical properties of a material may be greatly influenced by the extent of its surface area. Soils differ markedly in surface area as a result of differences in types of clay minerals, texture, and amount of caly size content. Such important properties as water retention and cation exchange capacity have been shown to be highly correlated with the surface area of soils. For example, there is an interaction between the water molecules and the clay surface. Some water molecules may be adsorbed on the clay surface through hydrogen bounding, and some may be adsorbed by the exchangeable ions becoming hydrated. The effect of the cation on the water molecules is greater the greater its charge and the smaller its size, that is, the greater its surface charge density.

Table 4.2: Results of analyses of covariance for 8%, 16% and 30% materials within different groups.

a- Hydrite group

Source	DF	SS	Mean Square	F Value	Pr > F
Material	2	0.36240	0.01812	23.56	0.0001 **
Grvmoist	1	0.48989	0.48989	636.97	0.0001 **
Contrast:					
H-16% vs H-30%	1	0.03606	0.03606	46.89	0.0001 **
H-16% vs H-8%	1	0.00608	0.00608	7.90	0.0060 **
H-8% vs H-30%	1	0.01227	0.01227	15.95	0.0001 **

b- Bentonite group

Source	DF	SS	Mean Square	F Value	Pr > F
Material	2	0.11860	0.05930	77.35	0.0001 **
Grvmoist	1	0.41422	0.41422	540.28	0.0001 **
Contrast:					
B-16% vs B-30%	1	0.08748	0.08748	114.11	0.0001 **
B-16% vs B-8%	1	0.00683	0.00683	8.91	0.0037 **
B-8% vs B-30%	1	0.10155	0.10155	132.45	0.0001 **

c- Ste. Rosalie (natural) group

Source	DF	SS	Mean Square	F Value	Pr > F
Material	2	0.04898	0.02450	14.29	0.0001 **
Grvmoist	1	0.66517	0.66517	388.16	0.0001 **
Contrast:					
N-16% vs N-30%	1	0.03616	0.03616	21.10	0.0001 **
N-16% vs N-8%	1	0.00019	0.00019	0.11	0.7423 ns
N-8% vs N-30%	1	0.04030	0.04030	23.52	0.0001 **

** The difference is statistically significant at probability level of 0.01.
ns The difference is not statistically significant at probability of 0.05 or more.
DF Degrees of freedom. SS Sum of squares. Pr Probability
Grvmoist Gravimetric moisture content

Figures 4.7-4.9 tend to show that, as the level of clay material (consequently the clay size content) increases, the TDR technique tends to increasingly underestimate the θ value. This effect can be attributed to the presence of progressively more bounded water as the clay content increases. Since the electrostatically bounded water has a lower dielectric constant (3-5) than does interstitial water (70-80). This phenomenon has been investigated by other researchers (Wang and Schmugge, 1978, 1980; Dobson et al., 1985). All these studies showed that the dielectric constant decreased from coarse to fine textured soils. Thus, there seems to be a need to know the clay content of the soil and the specific surface area of the clay component, and adjusting or calibrating the recorded TDR readings.

Table 4.3: Results of the structural analyses of the regression lines for θ-TDR versus gravimetric moisture content from Figures 4.7 to 4.9.

Soil	Y-intercept	Slope	R-square
H-8%	0.08	1.33	0.91
H-16%	0.07	1.49	0.80
H-30%	0.02	1.56	0.93
B-8%	0.05	1.41	0.84
B-16%	0.08	1.03	0.89
B-30%	0.04	0.87	0.97
N-8%	0.12	1.14	0.80
N16%	0.05	1.55	0.87
N-30%	0.12	0.89	0.88

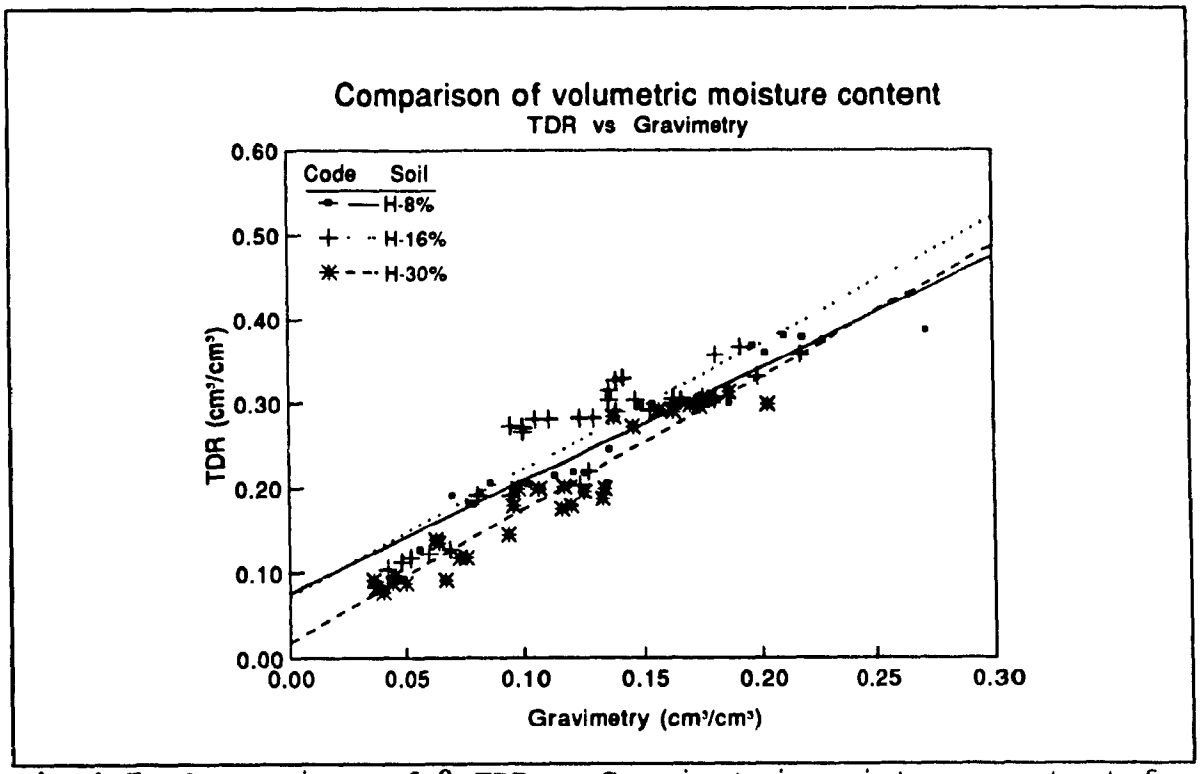

Fig 4.7: Comparison of θ-TDR vs Gravimetric moisture content for Hydrite materials.

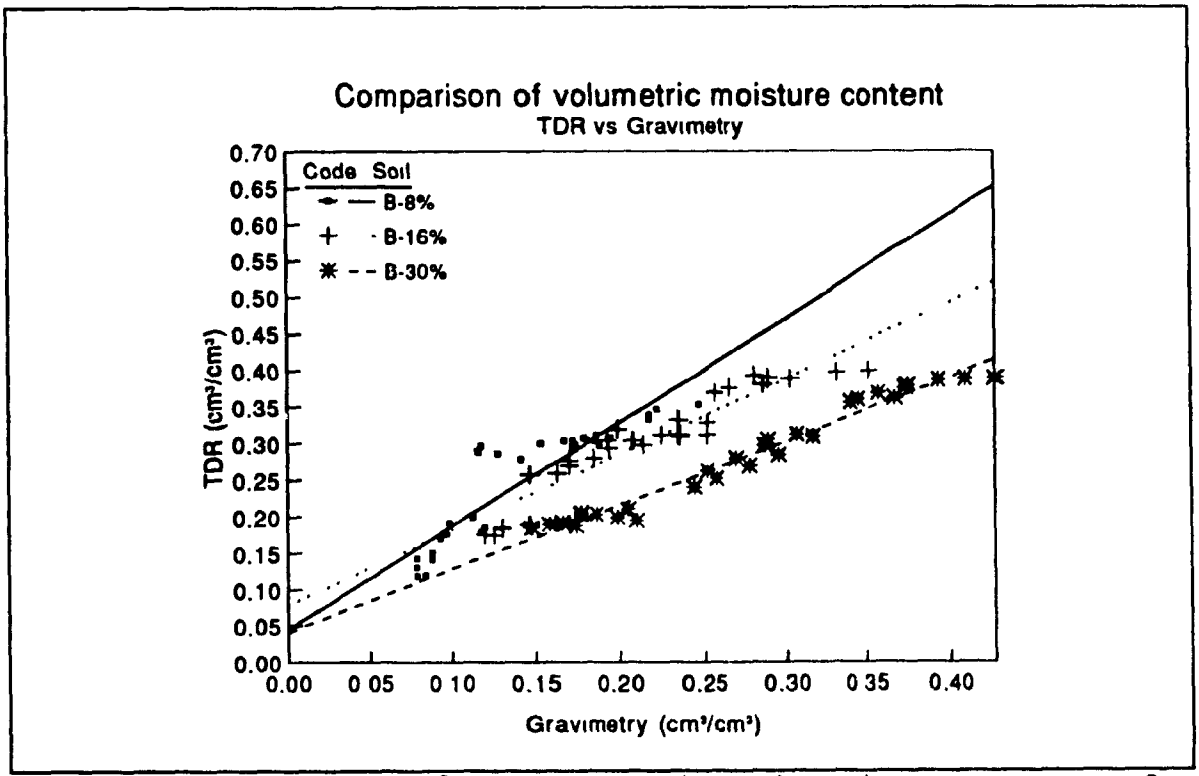

Fig 4.8: Comparison of θ-TDR vs Gravimetric moisture content for Bentonite materials.

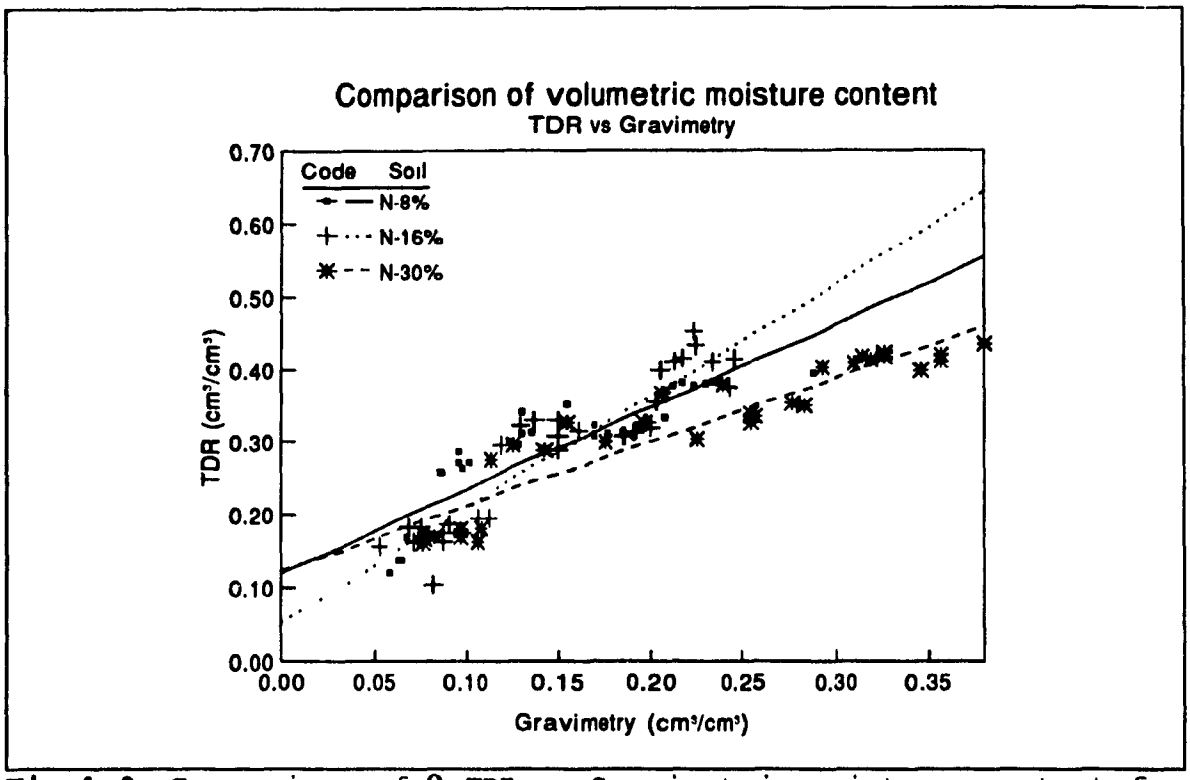

Fig 4.9: Comparison of θ-TDR vs Gravimetric moisture content for Ste. Rosalie (Natural) materials.

4.3.2 Results of statistical analysis for different clay types

The test of heterogenity of slopes was carried out to compare the clay types together assuming the clay content and moisture content as independent variables (covariates) and the clay type as classes. The results of this analysis are presented in **Table 4.4**. As can be seen from Table 4.4 the Type I sums of squares show that the clay content has an effect on θ-TDR, the clay type has an effect on θ-TDR at any given clay content, and there is a significant difference in the θ-TDR / clay content relationship for different clay types at the probability of 1% level.

The estimated values in **Table 4.5** are obtained with ESTIMATE statements using a SAS program that specify construction of the coefficients for different clay types. These

estimated coefficients illustrate the lower level of overall θ-TDR for the Bentonite clay type.

Table 4.4: Results of test of heterogeneity of regression θ-TDR / clay content relationships for different groups (clay types).

Source	DF	Type I SS	Mean Square	F Value	Pr > F
CT	2	0.16513	0.08256	67.16	0.0001 **
Moisture	1	1.41952	1.41952	1154.69	0.0001 **
CC	1	0.22729	0.22729	104.89	0.0001 **
CC*CT #	1	0.03321	0.03321	13.51	0.0001 **
Moisture*CC #	1	0.01288	0.01288	10.48	0.0014 **

** The difference is statistically significant at propability of 1%.

ns The difference is not statistically significant at probability of 0.05 or more.

Interaction between the treatment group and independent variable.

CT Clay type CC Clay content

Table 4.5: Estimate coefficients for different clay types.

Parameter	Estimate	T for H_0: Parameter = 0	PR > T	Std Error of Estimate
CC:CTH	-0.002951	-2.77	0.0059	0.00106443
CC:CTB	-0.000878	-1.25	0.2115	0.00070085
CC:CTN	-0.004437	-4.05	0.0001	0.00109543

CTH Hydrite clay type CTB Bentonite clay type

CTN Ste. Rosalie clay type CC Clay content

The TDR and gravimetric moisture content data are illustrated in **Figures 4.10** to **4.12.** The regression lines, fitted to these data, represent the calibration lines for different clay types. The intercept, slope and R-square values of all regression lines are shown in **Table 4.3.** These calibration lines visually illustrate that there exists a difference in θ TDR for different clay types.

The data points, depicted in Figures 4.7-4.9, as well as lower slope values (the one exception being B-8% soil) shown in Table 4.3 generally exhibit lower θ values for the bentonite soils compared to the hydrite and natural clay soils. These effects can be explained by the fact that the clay minerals differ a great deal in specific surface area. Nonswelling clays like Hydrite clay and Ste. Rosalie clay have only an external surface, but swelling clays like Bentonite clay have a great deal of internal as well as external surface. The specific surface area ranges from 5 to 20 m^2/g for the Hydrite clay, however, it ranges from 700 to 800 m^2/g for the Bentonite clay. This large area of Bentonite clay holds more water in a bounded state which has the lower dielectric constant (3-5) than does interstitial water (70-80). Consequently the type of clay mineral present in soil is of major importance in determining the effect of clay on θ-TDR readings.

Some of the variability observed in the data (see R-squares in Table 4.3) is probably attributable to the small sample volumes and to the physical changes in these samples caused by contact with the probe itself. Thus, more water may be redistributed within the soil matrix at each saturated period due to the physical contact of the probe itself, which could lead to artificially higher dielectric constant measurements. Gap space between the soil and probes may also be a factor; especially for the Bentonite and Hydrite soils with high levels of clay content. As the soils dried, some cracks developed in the soil. Other cracks developed when inserting the probes into the soil. Swelling can be another factor mostly for Bentonite, as the water added into the soil, the volume of the soil changed during the recording period. Also, the length of probe can be other factor,

as inserted into the soil, it is difficult to accurately determine probe length in the soil. All of the above factors may have contributed to some of the variability in the results.

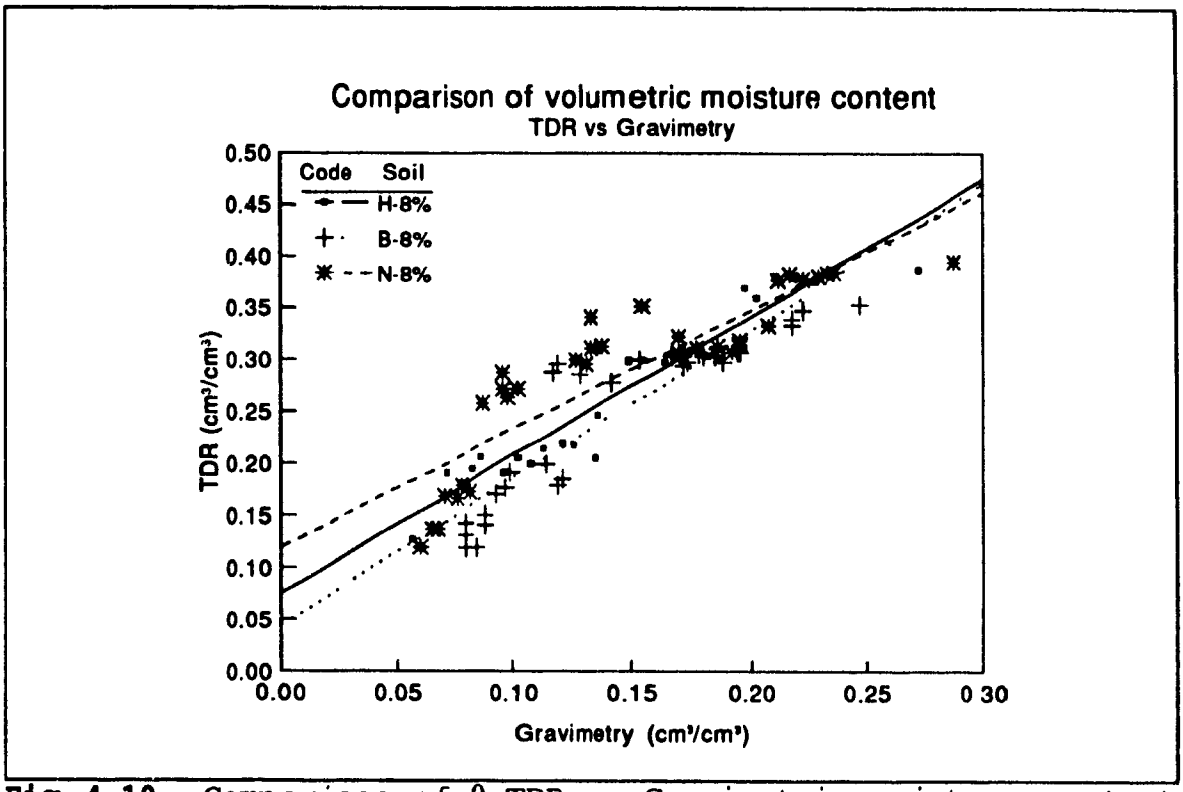

Fig 4.10: Comparison of θ-TDR vs Gravimetric moisture content for Hydrite, Bentonite and Ste. Rosalie (Natural) materials with 8% level.

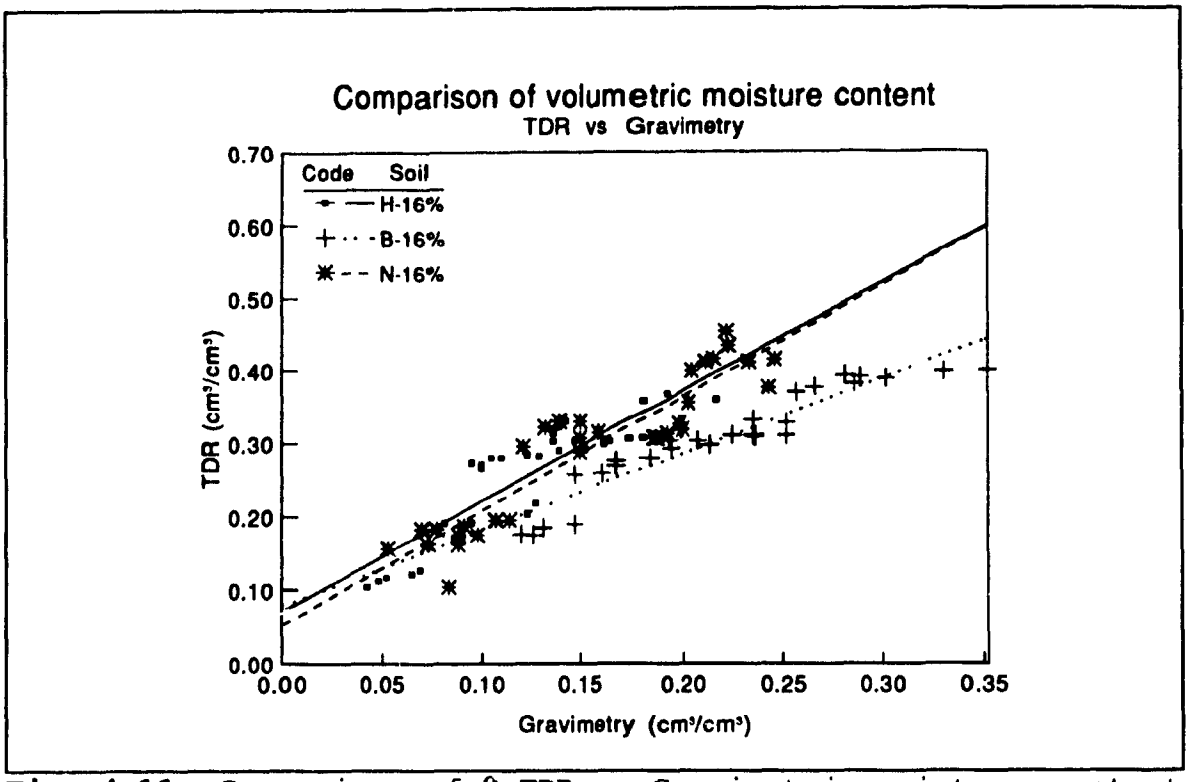

Fig. 4.11: Comparison of θ-TDR vs Gravimetric moisture content for Hydrite, Bentonite and Ste. Rosalie (Natural) materials with 16% level.

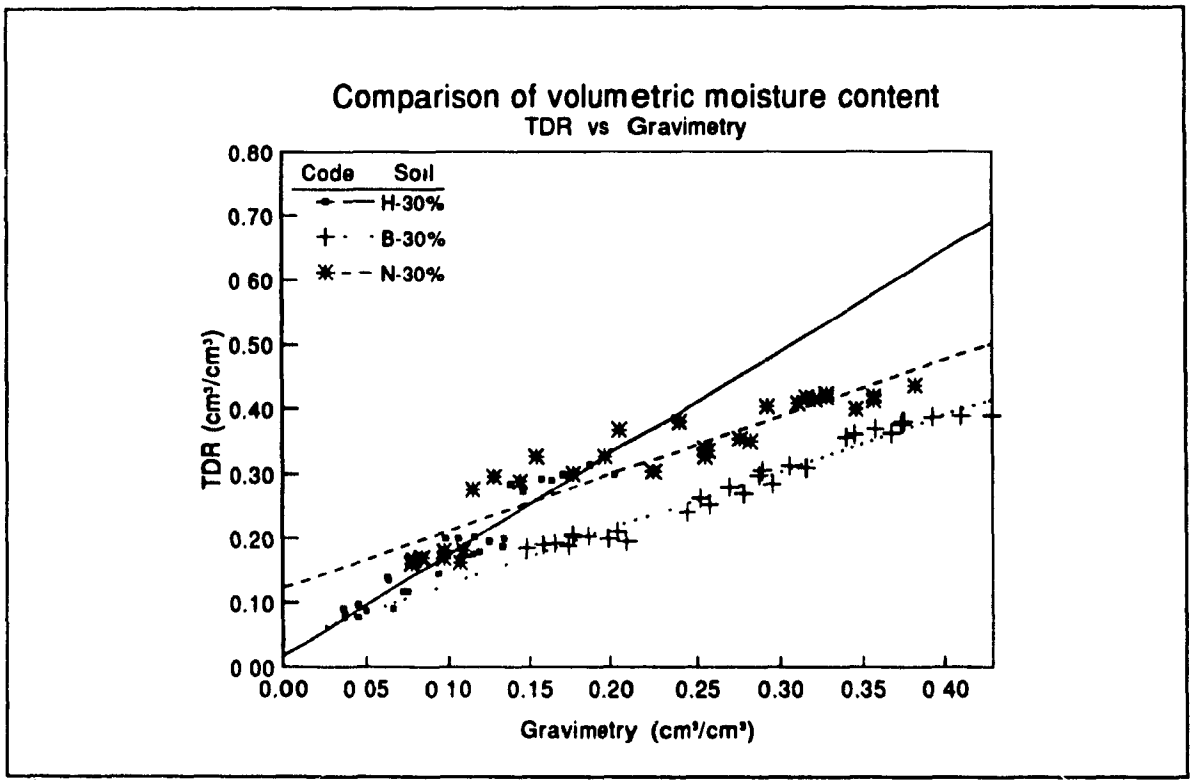

Fig 4.12: Comparison of θ-TDR vs Gravimetric moisture content for Hydrite, Bentonite and Ste. Rosalie (Natural) materials with 30% level.

4.4 Discussion of bulk electrical conductivity

The dependence of EC_a on the electrical conductivity of the soil water (ECw), on volumetric water content (θ), on transmissivity (T) and on surface conductance (EC_s) has been presented by Rhoades et al., 1976 (eq 4.1 and 4.2). He found that the contribution of exchangeable cations (surface conductance, EC_s) compared to EC_a is relatively small and constant in saline soils. The ECw is increased proportionately as θ is reduced by evapotranspiration. Because of this inversely proportional relationship between EC_w and θ, the product ($EC_w.\theta$) is almost constant (Roades et al., 1976). Consequently, the EC_a for different soils will be a function of the [T] factor which is directly related to θ. Therefore, to find the effects of different clay types and clay contents on EC_a-TDR, an analysis of covariance was carried out to remove the moisture content effect and to adjust the treatment means.

4.4.1 Results of statistical analysis for different clay contents

The results of covariance analyses, run for each group, are presented in **Table 4.6 (a, b, c)**. As can be seen from Table 4.6 (a, b, c), the moisture content has an effect on EC_a-TDR which is significant at the 1% level. The material also has an effect on EC_a-TDR which is significant at the 1% level within the Hydrite and Bentonite groups. But the effect of material on EC_a-TDR within the Ste. Rosalie group is not significant. A reason can be attributed to the low level of clay content (3.48%, 6.96%, and 11%) and to the small range of clay content variation within the Ste. Rosalie materials.

The contrast tests in Table 4.6 (a, b) show significant differences between 30% and 16% or 30% and 8% materials at the 0.01 probability level, but there is no significant differences between 8% and 16% materials. These results tend to show that the low level of clay content have little effect on EC_a readings. The fact that the 30% material readings

are significantly different from 8% and 16% materials suggests that at some point (critical clay content) enough clay is present to interact with EC_a readings. More research is required to define the level of critical clay content. Note that this critical clay content may be different for different clay types.

Plots of EC_a-TDR versus Gravimetric moisture content for the different materils are presented in **Figures 4.13-4.15**. The intercept, slope and R-square values for these graphs are shown in **Table 4.7**. Figures 4.13-4.15 visually show differences in the data points depicted for the different materials. These figures tend to demonstrate that the EC_a of the soils at a fixed moisture content decreases, as the clay content increases (one exception being for hydrite material, Fig. 4.13). This effect can be explained by the fact that the transmission factor, [T], is changed for soils with different clay contents. The [T] factor can be affected, especially in structured field soils, by the number, size, and continuity of the soil pores. Considerable differences in the total pore space of various soils occur, depending upon field and management conditions. Sandy soils generally show a range of pore space from 35 to 50%, whereas medium- to fine-textured soils vary from 40-60% or even more for marked granulation clays. Although the total porosity in a sandy soil is low, the movement of air and water is surprisingly rapid because of the dominance of macropores. Fine-textured soils allow relatively slow gas and water movement despite the larger amount of total pore space.

In order to verify this, Figures 4.16-4.18 were plotted to show the [T] values in relation to θ. The [T] values for different soils, used in this experiment, were obtained using the Rhoades' procedure and are presented in Table 4.1. Figures 4.16-4.18 also exhibited lower [T] values for the soils with higher level of clay material (one exception being the 16% hydrite material).

Table 4.6: Results of covariance analyses for 8%, 16% and 30% materials within different groups.

a- Hydrite group

Source	DF	Type III SS	Mean Square	F Value	Pr > F
Material	2	0.29306	0.14653	6.77	0.0018 **
Grvmoist	1	4.10434	4.10434	189.51	0.0001 **
Contrast:					
H-16% vs H-30%	1	0.20240	0.20240	9.35	0.0029 **
H-16% vs H-8%	1	0.00494	0.00494	0.23	0.6342 ns
H-8% vs H-30%	1	0.24063	0.24063	11.11	0.0012 **

b- Bentonite group

Source	DF	Type III SS	Mean Square	F Value	Pr > F
Material	2	0.51373	0.25687	12.74	0.0001 **
Grvmoist	1	7.32819	7.32819	363.44	0.0001 **
Contrast:					
B-16% vs B-30%	1	0.49893	0.49893	24.74	0.0001 **
B-16% vs B-8%	1	0.01504	0.01504	0.75	0.3900 ns
B-8% vs B-30%	1	0.24086	0.24086	11.95	0.0008 **

c- Ste. Rosalie (natural) group

Source	DF	Type III SS	Mean Square	F Value	Pr > F
Material	2	0.04076	0.02038	0.85	0.4310 ns
Grvmoist	1	9.79625	9.79625	408.17	0.0001 **
Contrast:					
N-16% vs N-30%	1	0.01956	0.01956	0.81	0.3690 ns
N-16% vs N-8%	1	0.00404	0.00404	0.17	0.6823 ns
N-8% vs N-30%	1	0.03941	0.03941	1.64	0.2032 ns

** The difference is statistically significant at probability level of 0.01.
ns The difference is not statistically significant at probability of 0.05 or more.
DF Degrees of freedom. SS Sum of squares. Pr Probability
Grvmoist Gravimetric moisture content

Table 4.7: Results of the structural analysis of the regression lines for EC_a-TDR and gravimetric moisture content relationship.

Soil	Y-intercept	Slope	R-square
H-8%	0.20	2.81	0.45
B-8%	-0.22	4.85	0.89
N-8%	-0.05	4.66	0.90
H-16%	-0.10	4.07	0.70
B-16%	-0.11	4.17	0.79
N-16%	-0.14	4.74	0.84
H-30%	-0.20	5.87	0.75
B-30%	-0.23	3.88	0.91
N-30%	-0.13	4.20	0.90

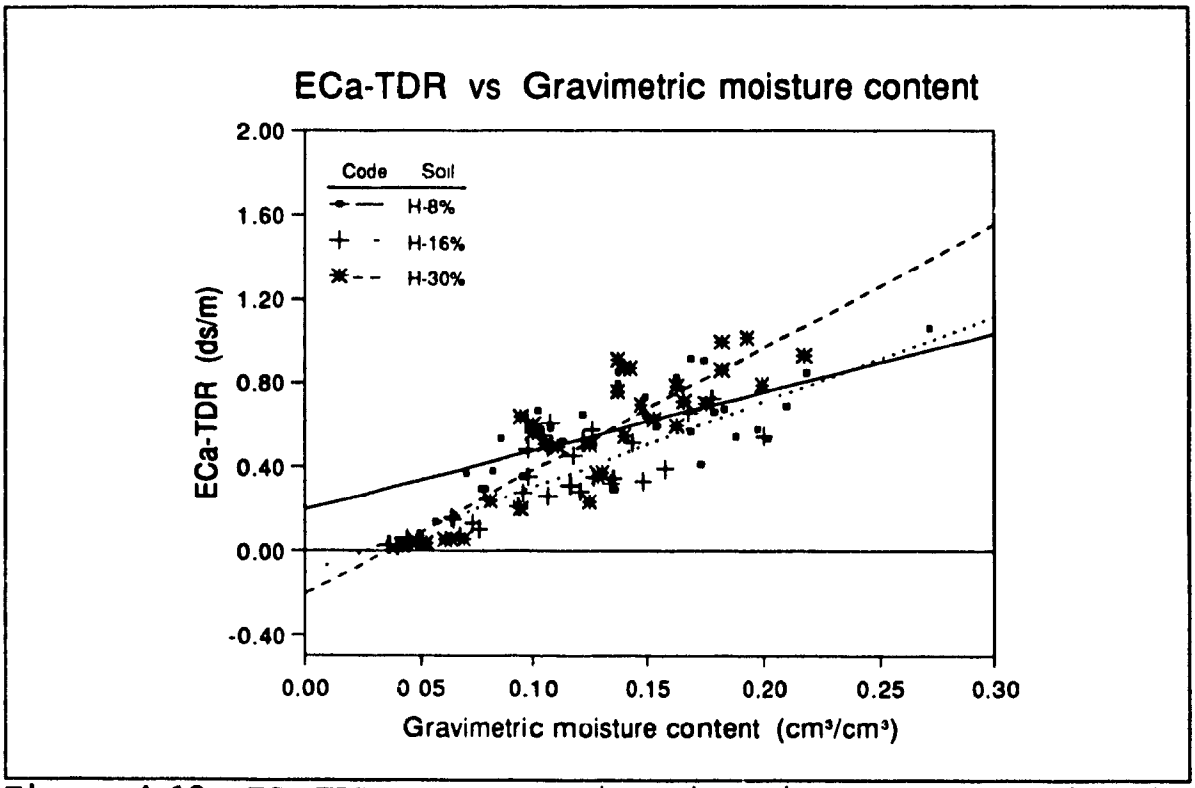

Figure 4.13: EC_a-TDR versus gravimetric moisture content for 8%, 16%, and 30% Hydrite materials used in this experiment.

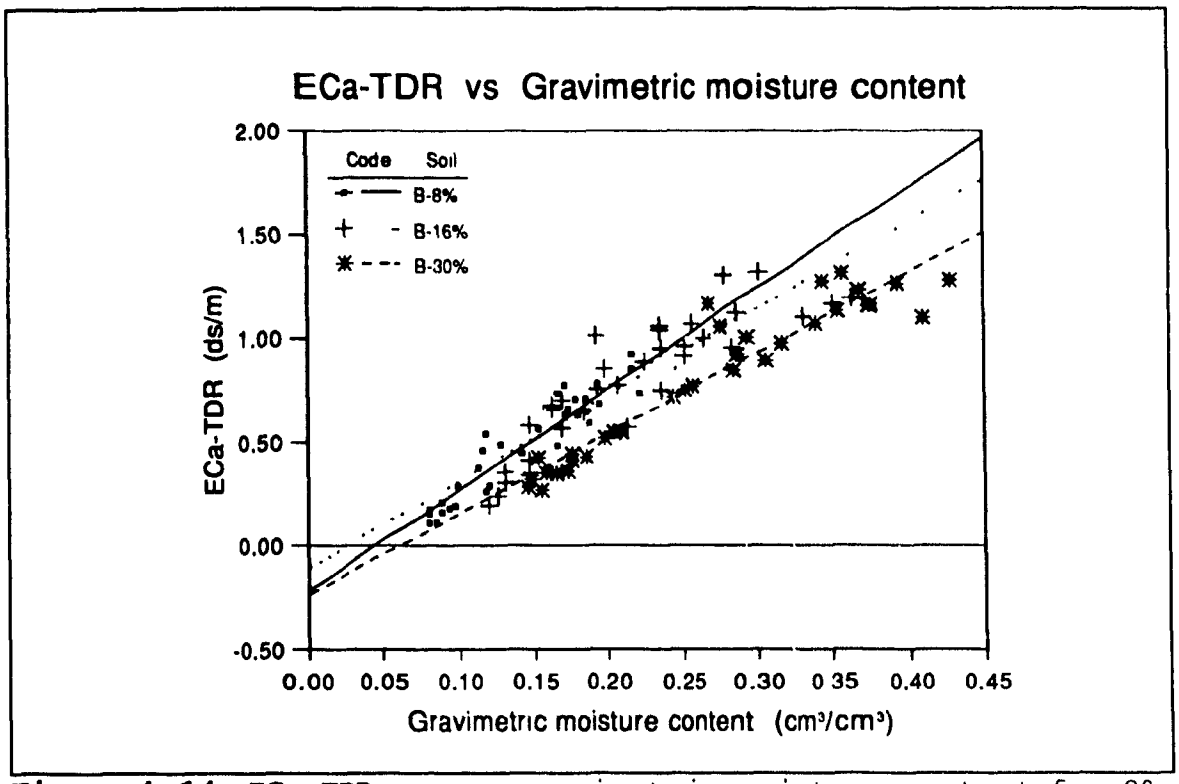

Figure 4.14: EC_a-TDR versus gravimetric moisture content for 8%, 16%, and 30% Bentonite materials used in this experiment.

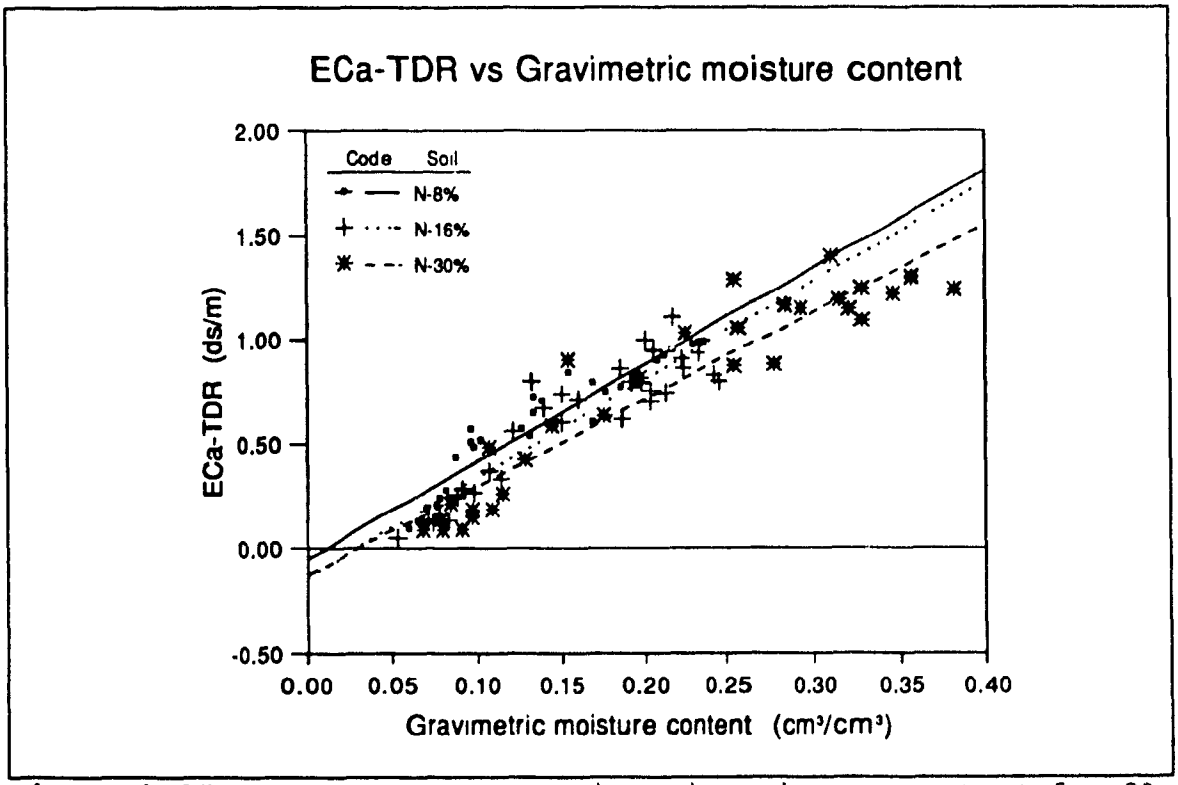

Figure 4.15: EC_a-TDR versus gravimetric moisture content for 8%, 16%, and 30% Ste. Rosalie (Natural) materials used in this experiment.

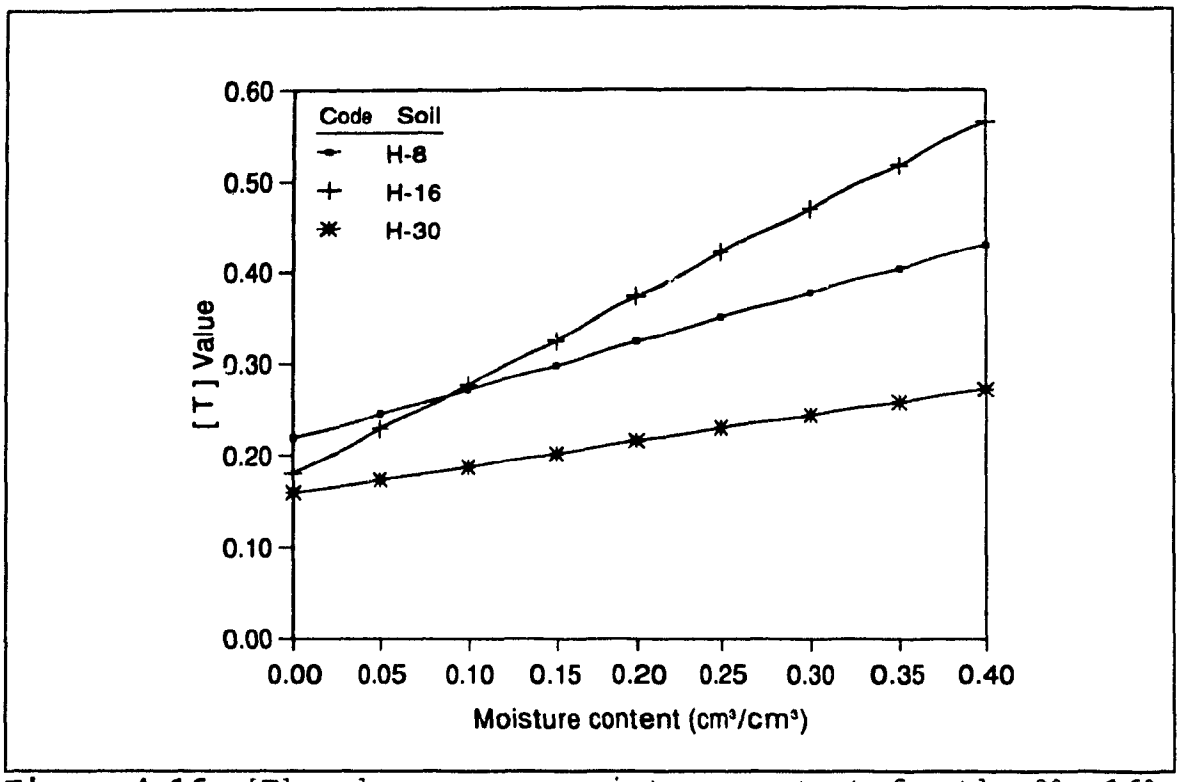

Figure 4.16: [T] values versus moisture content for the 8%, 16%, and 30% Hydrite materials.

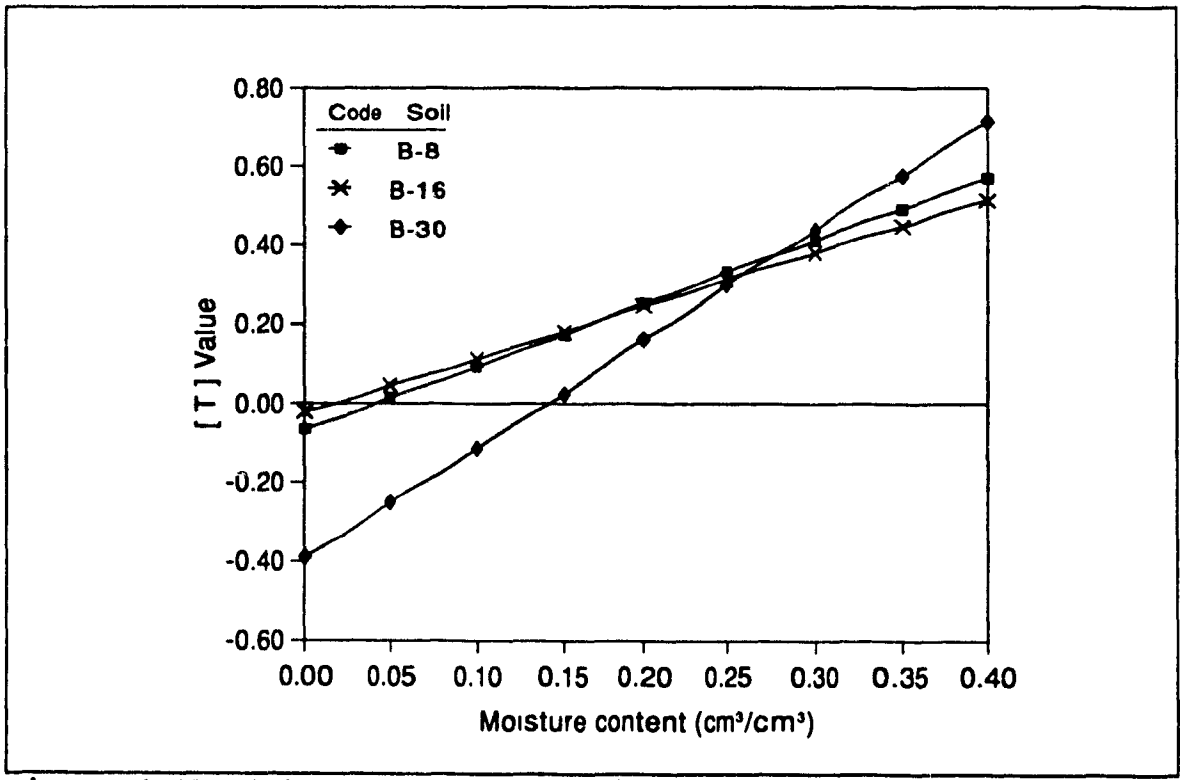

Figure 4.17: [T] values versus moisture content for the 8%, 16%, and 30% Bentonite materials.

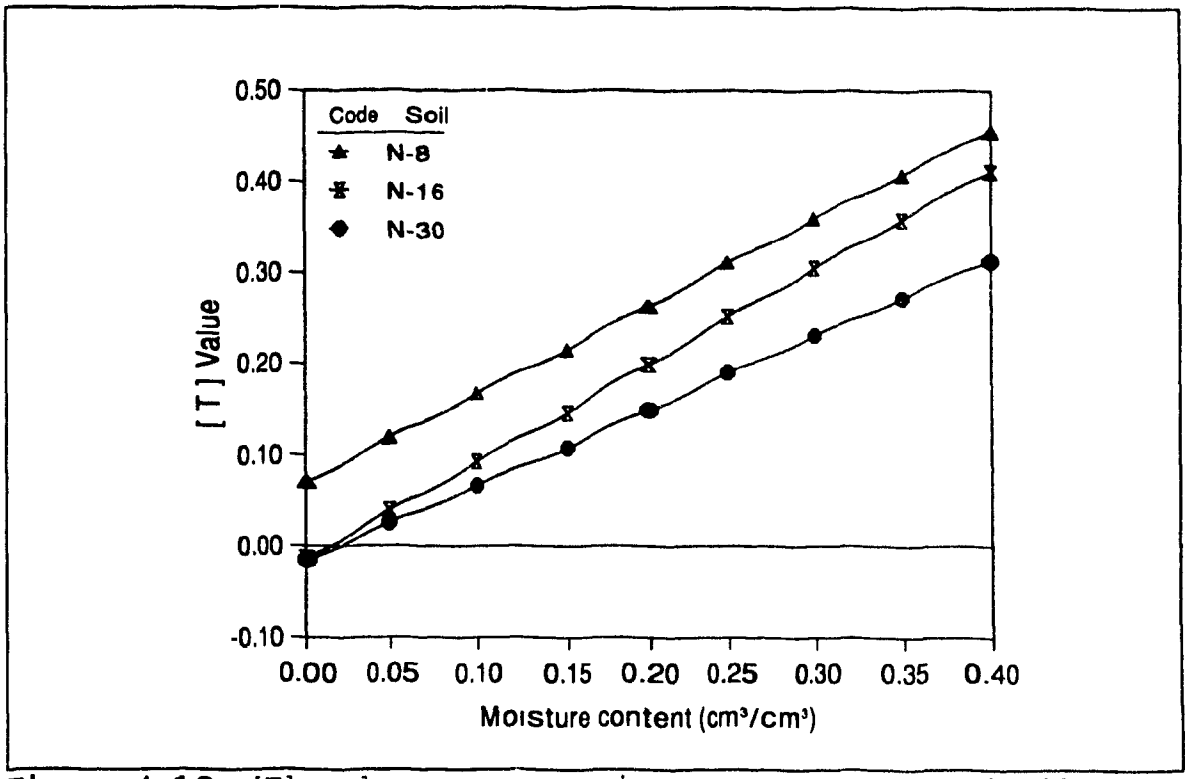

Figure 4.18: [T] values versus moisture content for the 8%, 16%, and 30% Ste. Rosalie (Natural) materials.

4.4.2 Results of statistical analysis for different clay types

The test of heterogeneity of slopes was carried out to look at whether or not the regression coefficients of EC_a / clay content relationship are constant over groups (different clay types). The results of this analysis are given in Table 4.8. The Type I sums of squares show that the clay type is significant at the probability level of 0.01. Thus the clay type has an effect on EC_a-TDR at any given clay content. Note that the clay content percentages are different for all materials (see Table 3.2). The Type I sums of squares also show that the clay content has an effect on EC_a-TDR, and there is a significant differences in the EC_a-TDR / clay content relationship for different clay types. This means that when working with different materials a calibration curve with regard to clay type and clay content is required for EC_a-TDR determinations. Without calibration

only relative values of EC_a can be obtained. This in itself is often sufficient when monitoring changes in soil profile EC_a over time, but if absolute values of EC_a are required, calibration for these factors must be performed.

The estimate coefficients of EC_a-TDR / clay content relationships for different clay types obtained using the SAS program are presented in **Table 4.9**. These estimate coefficients are used to investigate the effect of each treatment (clay type) on EC_a-TDR readings. As given in Table 4.9 the absolute value of estimated coefficients show the lower level of overall EC_a-TDR for the Bentonite clay. Bentonite clay is the one which has the larger surface area and exhibits the largest degree of swelling and the largest CEC values (see Table 3.1). Therefore, it is this clay type which can be expected to be the most interactive with respect to electromagnetic propagation.

Table 4.8: Results of test of heterogeneity of regression EC_a-TDR / clay content relationships for different groups (clay types).

Source	DF	Type I SS	Mean Square	F Value	Pr > F
CT	2	2.56663	1.28331	53.45	0.0001 **
Moisture	1	24.79295	24.79295	1032.61	0.0001 **
CC	1	0.22719	0.22719	9.46	0.0023 **
CC*CT #	1	0.34537	0.17269	7.19	0.0009 **
Moisture*CC #	1	0.00809	0.00809	0.34	0.5619 ns

** The difference is statistically significant at propability of 1%.

ns The difference is not statistically significant at probability of 0.05 or more.

Interaction between the treatment group and independent variable.

CT Clay type CC Clay content

Table 4.9: Estimated coefficients for different clay types.

Parameter	Estimate	T for H_0: Parameter = 0	PR > T	Std Error of Estimate
CC:CTH	-0.007471	-1.69	0.0913	0.00441
CC:CTB	0.002937	0.95	0.3451	0.00311
CC:CTN	-0.004474	-0.95	0.3442	0.00472

CTH Hydrite clay type CTB Bentonite clay type

CTN Ste. Rosalie clay type CC Clay content

The EC_a-TDR and Gravimetric moisture content data, obtained at the same time, are illustrated in **Figures 4.19-4.21**. The data points in these Figures tend to show the lower level of overall EC_a-TDR for the bentonite material compared to the hydrite and Ste. Rosalie materials. This difference is visually most evident for the 30% bentonite material shown in Fig. 4.21. Since low clay contents have a small effect on the ECa readings, this difference is less evident within the 8 and 16% mixtures. The slope value for the 30% Bentonite material is 3.88, as compared to 5.87 and 4.20 for the 30% Hydrite and Ste. Rosalie materials respectively. This effect might be attributed to bound water which has a lower dielectric constant (K_d = 3-5) and to the surface charge of clay minerals (surface charge density) which is related to the cation exchange capacity (CEC) of the material. Because of the abundance of negative electrical charges at their surfaces, the Bentonite material adsorbs more positively charged ions (cations) than does the Hydrite and Ste. Rosalie materials. The Bentonite clay typically has a cation exchange capacity of 80-100 meq/100g of soil, the Hydrite clay, in the range of 3-15 meq/100g and the natural clay (Ste. Rosalie) 5-20 meq/100g of soil.

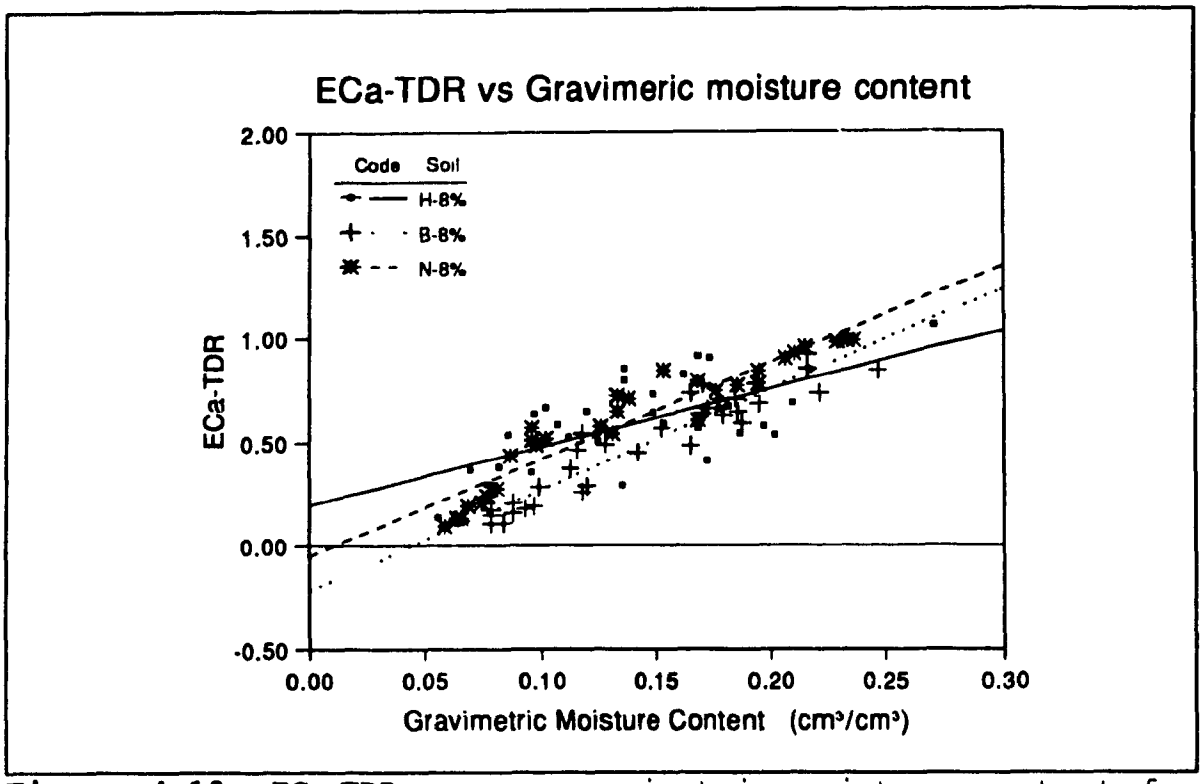

Figure 4.19: EC_a-TDR versus gravimetric moisture content for different clay types at 8% level.

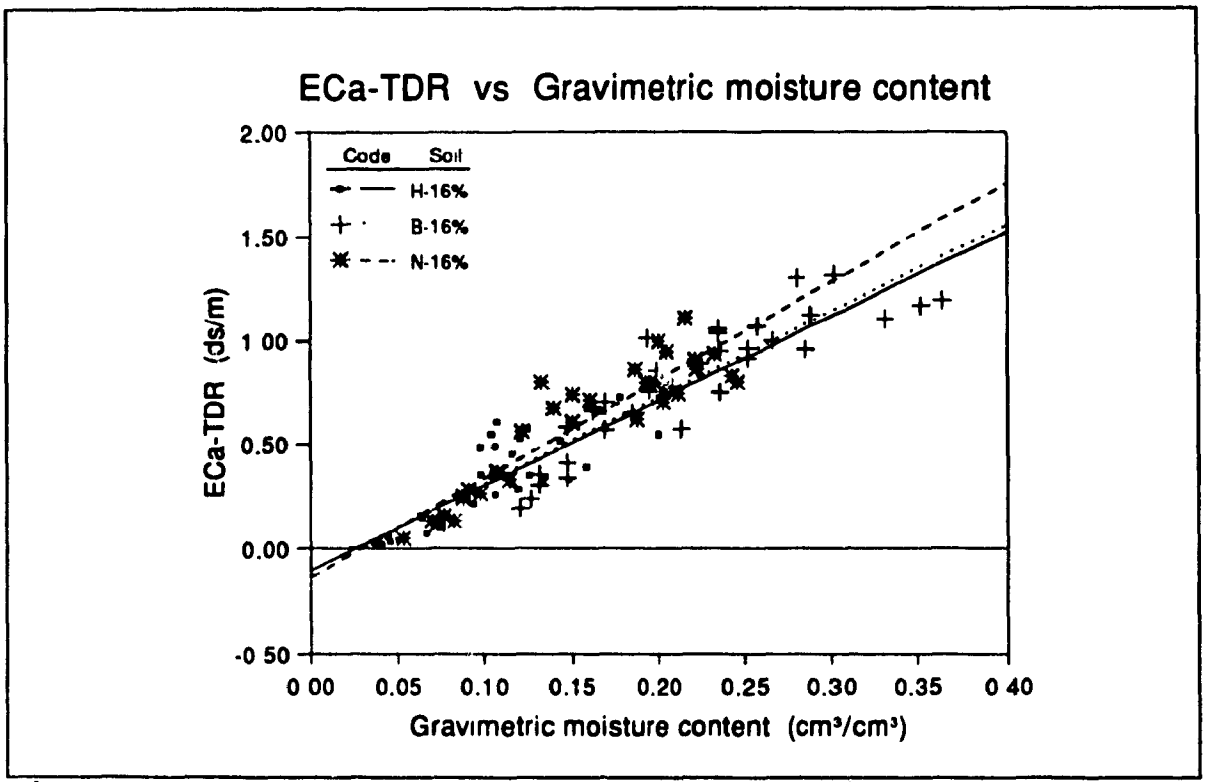

Figure 4.20: EC_a-TDR versus gravimetric moisture content for different clay types at 16% level.

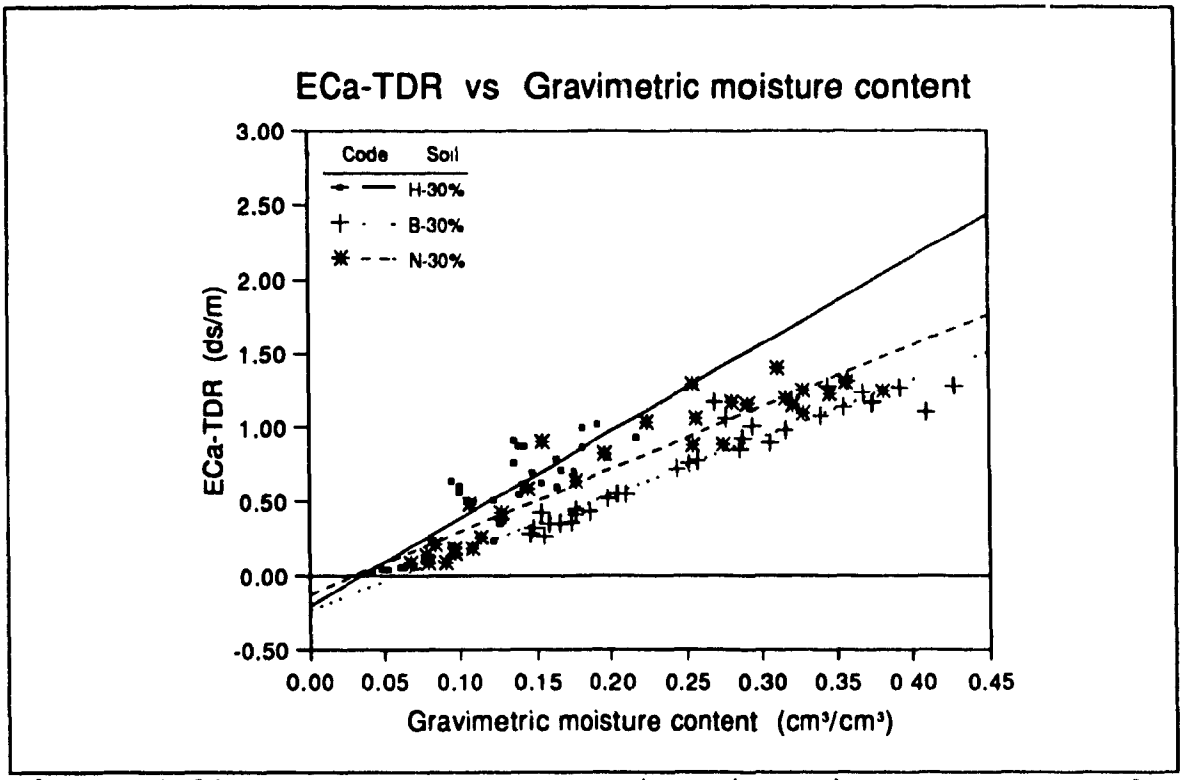

Figure 4.21: EC_a-TDR versus gravimetric moisture content for different clay types at 30% level.

4.5 Calibration curves for EC_a-TDR

As discussed above, clay type and clay content effect EC_a as measured by TDR. Thus, a calibration curve is necessary to compensate for different clay types and different clay contents. In this experiment the EC_a-TDR and EC_a-4p were recorded at the same time for calibration purposes. Figures 4.22-4.27 illustrate the calibration curves for the soils used. As can be seen, the curves are very close together and the data points in each Figure generally tend to fall on one curve (R-squares range from 85 to 90 for the different clay types and from 83 to 87 for the different levels of clay material). This similarity can be explained by the fact that the different clay types and clay contents also effect the EC_a measured by the 4-Probe technique. Therefore, it is necessary to determine the actual effects of clay type and clay content on the 4-Probe technique as well. If it is effected,

a calibration curve for the EC_a-4P technique also seems to be required. Then other methods have to be used to calibrate the EC_a-TDR. In practice, EC_a-4P determinations are often calibrated for different soils by comparison with saturated paste extract EC determinations. It is suggested that for accurate data requirements, EC_a-TDR determinations will need to be calibrated for any one field site by the same extract method. For reconnaissance work or for monitoring relative changes in soil salinity, less rigorous calibration is required.

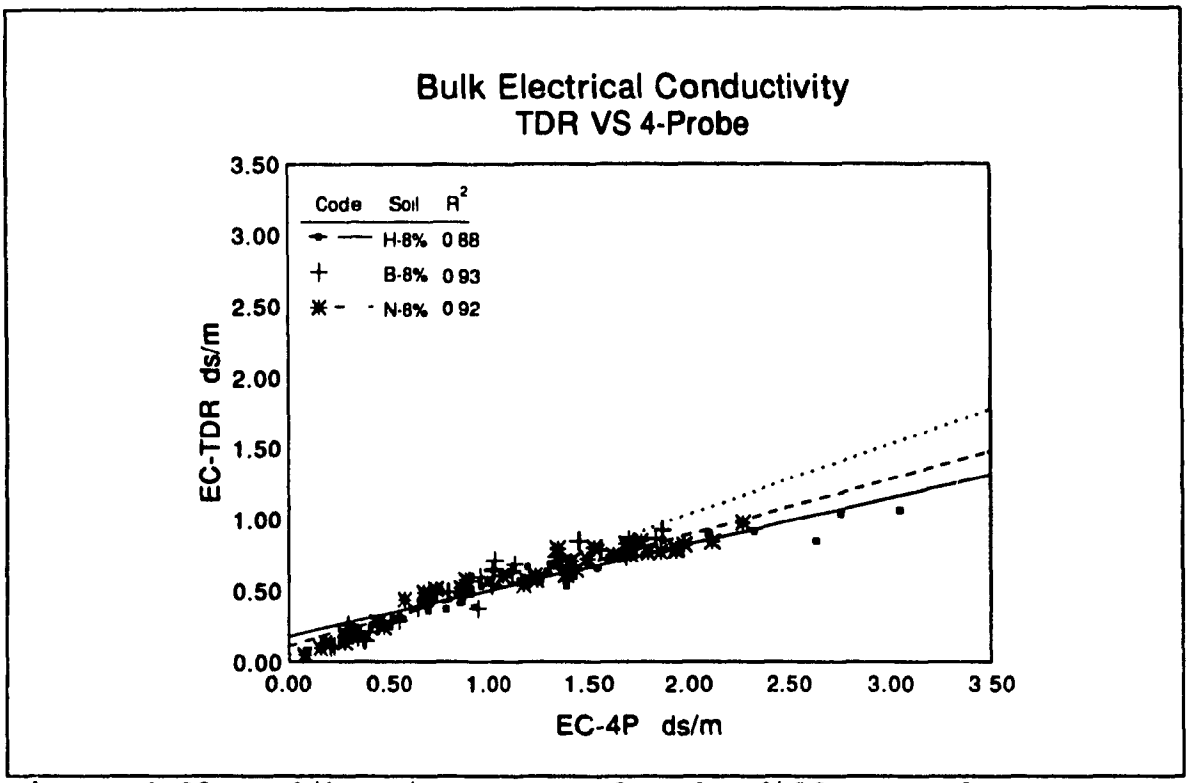

Figure 4.22: Calibration curves for the different clay types at 8% level.

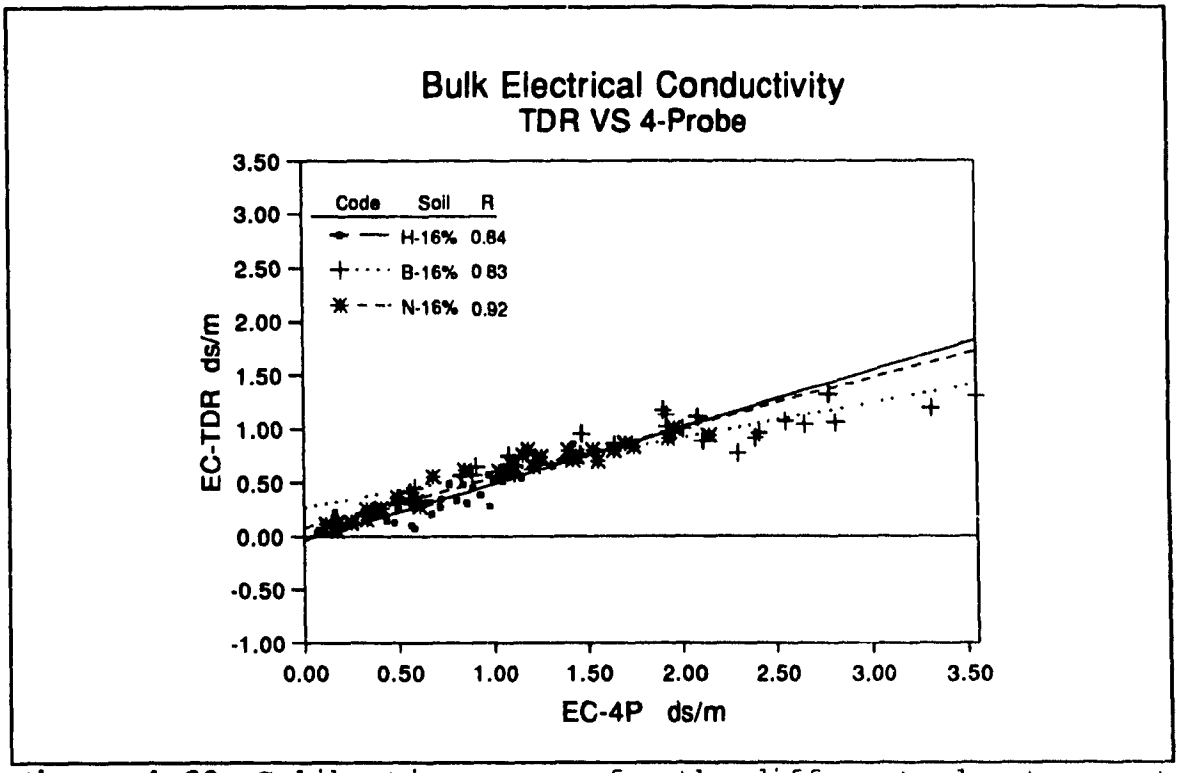

Figure 4.23: Calibration curves for the different clay types at 16% level.

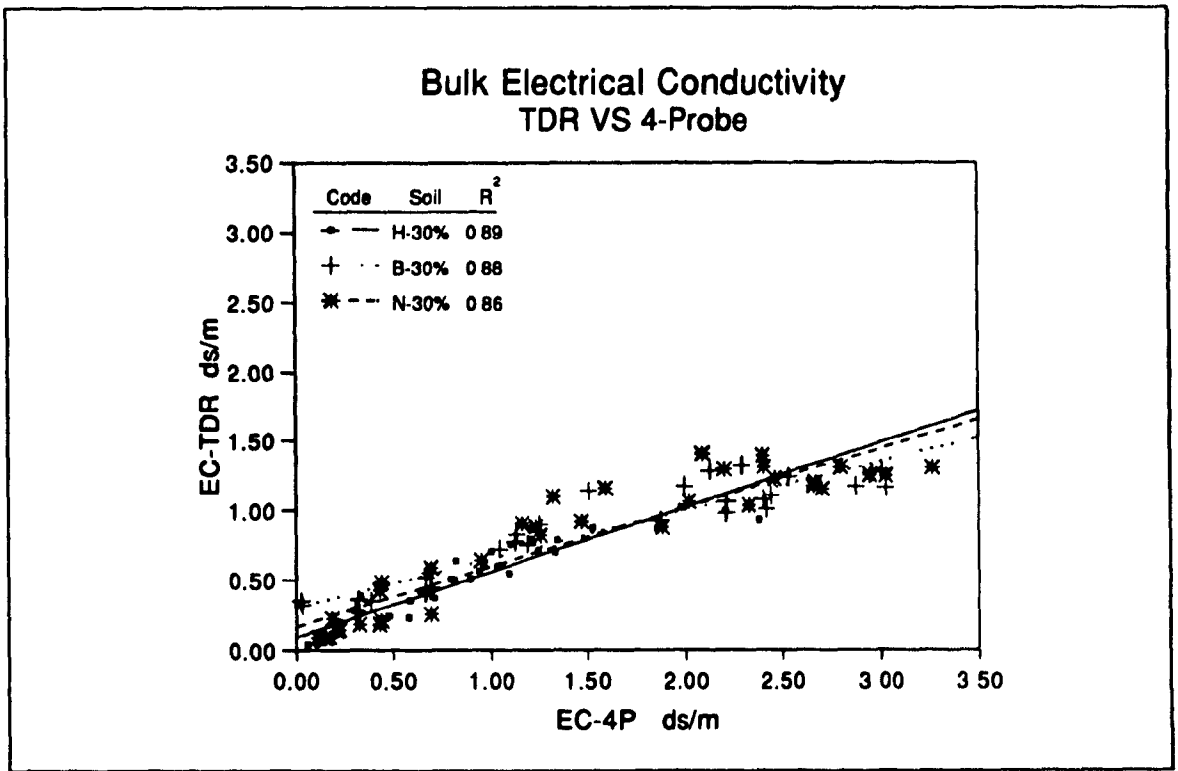

Figure 4.24: Calibration curves for the different clay types at 30% level.

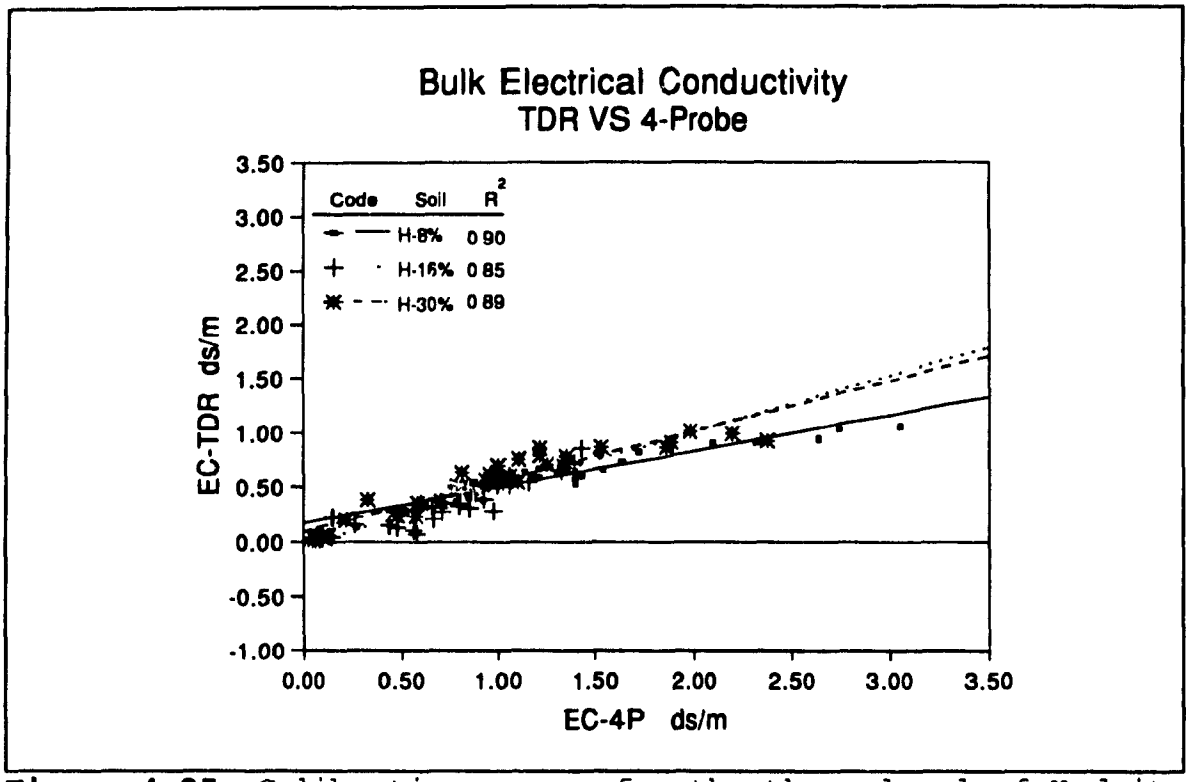

Figure 4.25: Calibration curves for the three level of Hydrite materials.

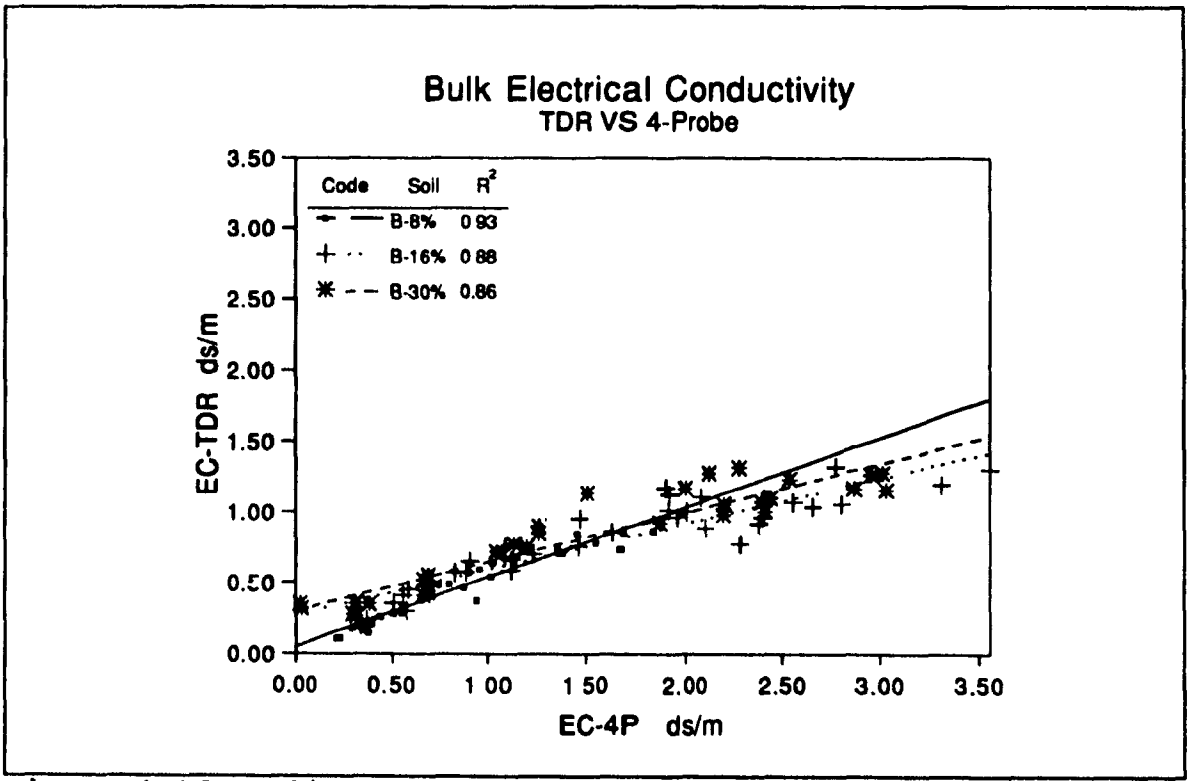

Figure 4.26: Calibration curves for the three level of Bentonite materials.

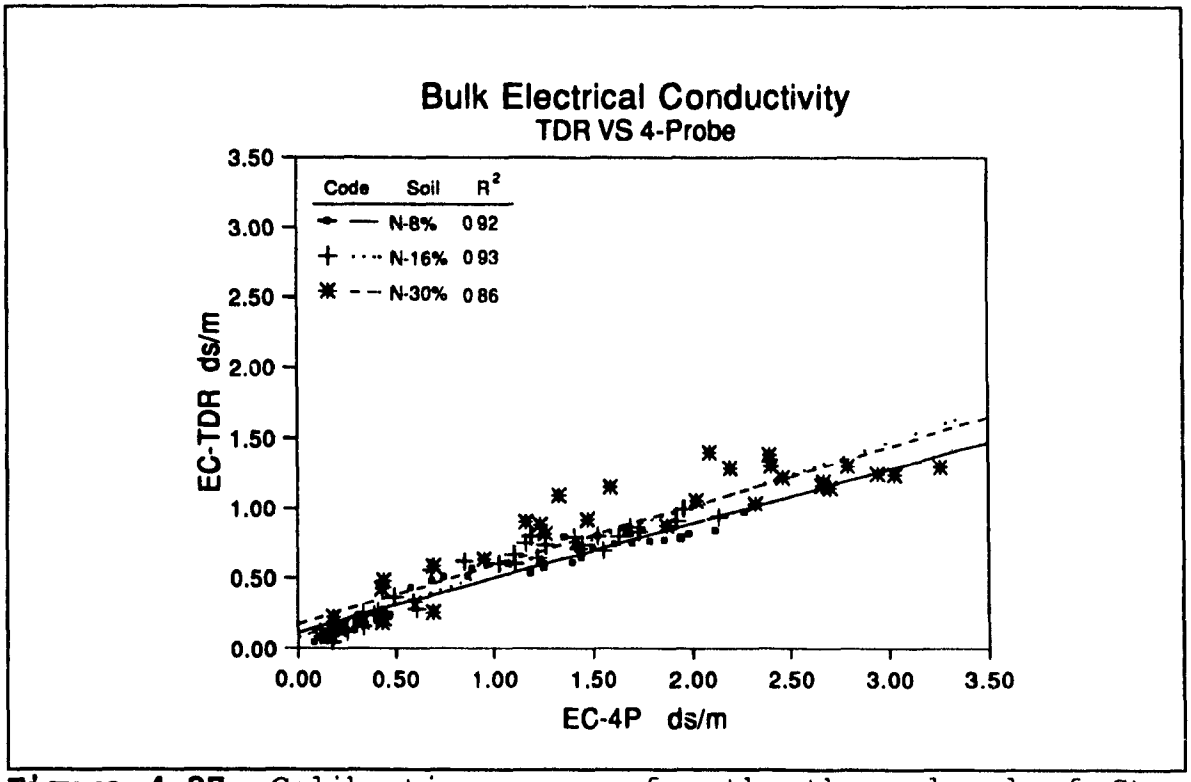

Figure 4.27: Calibration curves for the three level of Ste. Rosalie (Natural) materials.

CHAPTER V

5.1 SUMMARY AND CONCLUSION

This study was carried out in an attempt to quantify the effects of clay content and clay type in a soil matrix on the results obtained when measuring θ and EC_a using the TDR technique. To achieve this, 27 cylinders (150 mm diameter and 200 mm in length) were packed with various soil mixtures. These soil mixtures consisted of three replicates of three clay materials (Hydrite, Bentonite and Ste. Rosalie clay source) and three levels of materials (8, 16 and 30% by weight).

A salt solution of 10 dS/m was added to the cylinders and the moisture content and bulk soil electrical conductivity were recorded as the cylinders of soil were allowed to air dry. For θ recording two independent methods, gravimetric and TDR, were used and for EC_a recording two independent methods, 4-Probe and TDR, were used.

The results obtained in this study are presented in this thesis. The conclusions are as follows:

1. Although application of time domain reflectometry (TDR) has become an acceptable method for nondestructive estimation of soil water content (θ) and appears to be essentially independent of soil type, it has been found that the different clay types have some effects on θ-TDR. The TDR technique tended to show the lower level of overall θ-TDR for the Bentonite materials compared to the Hydrite and Ste. Rosalie (Natural) materials.
2. Low fractions of clay (in this case less than 13.05%, 12.8%, and 14.4% for the Ste. Rosalie, Hydrite, and Bentonite materials respectively) do not effect

EC_a-TDR. Once a calibration curve is performed, it can be used for all the mineral soils with clay fractions less than their threshold level of clay content.

3. Clay types and clay contents were found to have some effects on estimation of EC_a using TDR and 4-Probe techniques. Bentonite material, which exhibits the largest particle surface areas and the largest CEC values compared to Hydrite and Ste. Rosalie (natural) material, tended to show lower values for EC_a estimated by the two methods.

4. It was found that the bulk electrical conductivity of the soils at a fixed moisture content tends to decrease as the clay content increases (one exception being for hydrite soil).

5. To estimate θ- and EC_a-TDR, a calibration curve is necessary to compensate for different clay types and clay contents. Without a calibration only relative values of θ and EC_a can be obtained. Relative values are useful for monitoring changes in soil profile θ and EC_a over time.

CHAPTER VI

6.1 RECOMMENDATIONS FOR FUTURE RESEARCH

With regard to the results of this study, the following items are recommended for further research:

1. As discussed in section 4.3.1, low clay contents do not effect θ-TDR. But further research is required to find the threshold level of clay content above which the amount of clay effects the θ-TDR. This threshold level is probably different for different clay types.

2. As discussed in section 4.4.1, small changes of clay content do not effect the EC_a-TDR. Thus, further research is necessary to define the point (critical clay content) in which enough clay is present to interact with EC_a readings.

3. For accurate data requirements, EC_a-TDR determinations will need to be calibrated against standard methods known to be little effected by soil clay type or content percent (such as the saturated paste extract method).

CHAPTER VII

REFERENCES

Baker, J.M. and R.R. Allmaras. 1990. A system for automating and multiplexing soil moisture measurements by TDR. Soil Sci. Soc. Amer. J. 54: 1-6.

Bonnell, R.B., R.S. Broughton, and P. Enright. 1991. The measurement of soil moisture and bulk soil salinity using time domain reflectometry. Canadian Agricultural Engineering. 33(2): 225-230.

Bonnell, R.B. 1993. "Subsurface Irrigation with Saline Water". Ph.D. Thesis. Department of Agricultural Engineering. Macdonald Campus, McGill University. Montreal, Quebec.

Brady, N.C. 1974. "The Nature and Properties of Soils ". 8th Edition, Macmillan Publ. Inc., N.Y.

Brisco, B. and T.J. Pultz. 1992. Soil moisture measurement using portable dielectric probes and time domain reflectometry. Water Res. Res., 28(5): 1339-1346.

Bucci, O.M., G. Cortucci, G. Franceschetti, C. Savarese and R. Tiberie. 1972. Time domain techniques for measuring the conductivity and permittivity spectrum of materials. IEEE Trans. on Instrum. and Meas. IM-21: 237-243.

Campbell, J.E. 1990. Dielectric properties and influence of conductivity in soils at one to fifty megahertz. Soil Sci. Soc. Amer. J. 54: 332-341.

Clarkson, T.S., L. Glasser, R.W. Tuxworth and G. Williams. 1977. An appreciation of experimental factors in time_domain spectroscopy. Adv. in Molecular Relaxation and Interaction Processes. 10: 173-202.

Dalton, F. N. 1987. Measurement of soil water content and electrical conductivity using time domain reflectometry. Int. Conf. on Measurement of Soil and Plant Water Status. Utah State University, Logan, Utah.

Dalton, F.N. and M.Th. Van Genuchten. 1986. The time domain reflectometry for measuring soil water content and salinity. Geoderma 38: 237-250.

Dalton, F.N., W.N. Herkelrath, D.S. Rawlins, and J.D. Rhoades. 1984. Time-domain reflectometry: simultaneous measurement of soil water content and electrical conductivity with a single probe. Science 224: 988-990.

Dasberg, S. and F.N. Dalton. 1985. Time-domain reflectometry field measurements of soil water content and electrical conductivity. Soil Sci. Soc. Amer. J. 49: 293-297.

Dasberg, S. and J.W. Hopmans. 1992. Time domain reflectometry calibration for uniformly and nonuniformly wetted sandy and clayey loam soils. Soil Sci. Soc. Amer. J. 56: 1341-1345.

Davis, J.L. and W.J. Chudobiak. 1975. In-situ meter for measuring relative permittivity of soils, Geol. Surv. Can., Ottawa, Paper 75-IA: 75-79.

Davis, J.L. and A.P. Annan. 1977. Electromagnetic detection of soil moisture: Progress report 1. Can. J. Remote Sensing, 1: 7-86.

Davis, J.L. 1980. Electrical property measurements of sea ice in situ using a wide-band borehole radar and a time-domain reflectometer. Proc. Int. workshop Remote Estimation Sea Ice Thickness, St. John's, Newfoundland 80(5): 155-187.

Dobson, M. C., F. T. Ulaby, M. T. Hallikainen, and M. A. El-Rayes. 1985. Microwave dielectric behaviour of wet soil, II, Dielectrio mixing models, IEEE Trans. Geosci. Remote Sens., 23: 35-46.

Fellner-Feldegg, H. 1969. The measurement of dielectrics in time domain reflectometry. J. Phys.Chem., 73: 616-623.

Giese, K. and R. Tiemann. 1975. Determination of the complex permittivity from thin-sample time domain reflectometry: Improved analysis of the step response waveform. Adv. Mol. Relaxation Processes, 7: 45-49.

Gupta, S.C. and R.J. Hanks. 1971. Influence of water content on electrical conductivity of the soil. Soil Sci. Soc. Amer. Proc. 36: 855-857.

Halvorson, A.D. and J.D. Rhoades. 1974. Assessing soil salinity and identifying potential saline seep areas with field soil resistance measurement. Soil Sci. Soc. Amer. J. Proc. 38: 576-581.

Hayhoe, H. N. and W. G. Bailey. 1985. Monitoring changes in total and unfrozen water content in seasonnnally frozen soil using time domain reflectometry and neutron moderation technique. Water Resour. Res. 8: 1077-1083.

Hayhoe, H.N., G.C. and W.G. Bailey. 1983. Measurement of soil water contents and frozen soil depth during a thaw using time domain reflectometry. Atoms. Ocean 21: 299-311.

Heimovaara, T., F.N. Dalton and J.A. Poss. 1988. Time domain reflectometry, a method for measuring volumetric water content and bulk electrical conductivity of soils. USA Salinity Research Report 88, Riverside, Calif.

Herkelrath, W.N., S.P. Hamburg, and F. Murphy. 1991. Automatic, real-time monitoring of soil moisture in a remote field area with time domain reflectometry, Water Resour. Res., 27(5): 857-864.

Hook, W.R., N.J. Livingston, Z.J. Sun, and P.B. Hook. 1992. Remote diode shorting improves measurement of soil water by time domain reflectometry. Soil Sci. Soc. Amer. J. 56: 1384-1391.

Kachanoski, R. G., E. Pringle and A.Ward. 1992. Field measurement of solute travel time using time domain reflectometry. Soil Sci.Soc. Amer. J., 56: 47-52.

Keng, J.C.W. and G.C. Topp. 1983. Measuring water content of soil columns in the laboratory: A comparison of gumma ray attenuation and TDR techniques. Can. J. Soil Sci. 63: 37-43.

Knight, J.H. 1992. Sensitivity of time domain reflectometry measurements to lateral variations in soil water content. Water Resour. Res., 28(9): 2345-2352.

Lajoie, P.G. 1960. Soil Survey of Argenteuil, Two Mountains and Terrebonne Counties, Quebec. Research Branch, Canada Department of Agriculture in Co-operation with Quebec Department of Agriculture and Macdonald College, McGill University.

Malicki, M. A. and J. Skierucha. 1989. A manually controlled TDR soil moisture meter operating with 300ps rise-time needle pulse. Irri. Sci. 10: 153-163.

Malicki, M.A. 1990. A reflectometric (TDR) meter of moisture content in soils and other capillary-porous materials. Zeszyty Problemowe Postepow Nauk Rolniczych 388:107.

Nadler, A., S. Dasberg and I. Lapid. 1991. Time domain reflectometry measurements of water content and electrical conductivity of layered soil columns. Soil Sci. Soc. Amer. J. 55: 938-943.

Nadler, A. and H. Frenkel. 1980. Determination of soil solution electrical conductivity from bulk soil electrical conductivity measurements by the four-electrode method. Soil Sci. Soc. Amer. J. 44: 1216-1221.

Nadler, A. and H. Frenkel. 1981. Field application of the Fore-Electrode Technique for Determining Soil Solution Conductivity. Soil Sci. Soc. Amer. J. 45: 30-34.

Nadler, A. 1991. Effect of soil structure on bulk soil electrical conductivity (EC_a) using the TDR and 4P techniques. Soil Sci. J. 1[illegible]3): 199-203.

Newton, R.W. 1977. Microwave remote sensing and its application to soil moisture detection. Texas A&M University Tech. Rep. RSC-81, College Station.

Patterson, D.E. and M.W. Smith. 1981. The measurement of unfrozen water content by time domain reflectometry: Results from laboratory tests. Can.Geotech.J. 18: 131-144.

Pepin, S., A.P. Plamondon, and J. Stein. 1992. Peat water content measurement using time domain reflectometry. Can. J. For. Res. 22: 534-540.

Quirk, J.P. 1968. Particle interaction and soil swelling. Israel Jour. Chemistry, 6: 213-234.

Rhoades, J.D. and J. van Schilfgaarde. 1976. An electrical conductivity probe for determining soil salinity. Soil Sci. Soc. Amr. J. 40: 647-651.

Rhoades, J.D.,P.A.C. Raats and R.J. Prather. 1976. Effects of liquid phase electrical conductivity, water content and surface conductance on bulk soil electrical conductivity. Soil Sci. Soc. Amer. J. 40: 651-655.

Rhoades, J.D., M.T. Kaddah, A.D. Halvorson and R.J. Prather 1977. Establishing soil electrical conductivity - salinity calibration using four-electrode cells containing undisturbed soil cores. Soil Sci. 123: 137-141.

Rhoades, J.D. and A.D. Halvorson. 1977. Electrical conductivity methods for detecting and delineating saline seeps and measuring salinity in northern great plains soils. ARS-W-42, USDA, Washington, D.C. publ. #60.

Rhoades, J.D., N.A. Mongeghi, P.J. Shouse, and W.J. Alves. 1989. Soil electrical conductivity and soil salinity: New formulations and calibrations. Soil Sci. Soc. Amr. J. 53: 433-439.

Russell, E.W., 1973. "Soil Conditions and Plant Growth ". 10th Edition, Longman Pub. Inc., N.Y.

Selig, E.T. and S. Mansukhani. 1975. Relationship of soil moisture to the dielectric property. J. Geotech. Eng. Div., Amer. Soc. Civil Eng., 101: 755-769.

Simpson, J.R. and J.J. Meyer. 1987. Water content measurements comparing a TDR array to neutron scattering. Proc. of Int. Conf. on measurement of Soil and Plant Water Status. Utah State U., Logan, Utah.

Steel, G.D. and J.H. Torrie. 1980. "Principles and Procedures of Statistics ". McGraw-Hill Book Co. Inc., Toronto, Canada.

Stein, J. and D.L. Kane. 1983. Monitoring unfrozen water content of soil and snow using time domain reflectometry. Water Resources. Res., 19: 1573-1584.

Toikka, M.V. and M. Hallikainen. 1989. A practical electric instrument for in situ measurement of peat properties. In Land and water use. Agricultural Engineering: Proceedings of the 11th International Congress on Agricultural Engineering, 4-8 Sept. 1989, Dublin. Edi. V.A. Dodd and P.M. Grace. Balkema, Rotterdam, Netherlands. pp.: 101-105.

Topp, G.C. J.L. Davis and A.P. Annan. 1980. Electromagnetic determination of soil water content: Measurements in coaxial transmission lines. Water Resources Res. 16: 574-582.

Topp, G.C. and J.L. Davis 1982. Measurement of soil water content using time domain reflectometry. Nat'l. Res. Coucil of Can., Can. Hydrol. Symp., Ottawa pp. 269-287.

Topp, G.C. and J.L. Davis 1985. Time domain reflectometry (TDR) and its application to irrigation. In "Advances in Irrigation" (D. Hillel, ed.). Academic Press, New York,pp. 107-127.

Topp, G.C., M. Yanuka, W.D. Zebchuk and S. Zegelin 1988. Determination of electrical conductivity using time domain reflectometry: Soil and water experiments in coaxial lines. Water Resources. Res. 24: 945-952.

U.S. Salinity Laboratory Staff. 1954. In L. A. Richards (ed.) Diagnosis and improvement of saline and alkali soils. USDA Handbook 60, U.S. Government Printing Office,

Washington, D.C.

Van Gemert, M.J.C. 1971. Dielectric measurements with time domain reflectometry when large conductivities are involved. J. Phys. Chem. 75: 1323-1324.

Van Loon, W.K.P., E. Perfect, P.H. Groenevelt, and B.D. Kay. 1990. A new method to measure bulk electrical conductivity in soils with time domain reflectometry. Can. J. Soil Sci. 70: 403-410.

Wang, J.R. and T.J. Schmugge. 1980. An empirical model for the complex permittivity of soil as a function of water content, IEEE Trans. Geosci. Electron., 18: 288-295.

Wraith, J.M. and J.M. Baker. 1991. High resolution measurement of root water uptake using automated time domain reflectometry. Soil Sci. Soc. Amer. J., 55: 928-932.

Yanuka, M., G.C. Topp, S. Zeglin and W.D. Zebchuk 1988. Multiple reflection and attenuation of TDR pulses: Theoretical considerations for applications to soil and water. Water Resources. Res. 24: 939-944.

Zeglin, S. 1988. The determination of electrical conductivity using TDR: Soil and Water experiment in Coaxial lines. Water Resources. Res. 24: 945-952.

Zegelin, S.J., I. White and D.R. Jenkins. 1989. Improved field probes for soil water content and electrical conductivity measurements using time domain reflectometry. Water Resources. Res. 25: 2367-2376.

APPENDIX A

SOIL PROPERTIES

Source of pages 63-64: Dry Branch Kaolin Company, R.R.1, P.O. Box 468-D, Dry Branch, Georgia 31020-9798

Tel: 912 743-7474 Fax: 912 746-0217

Source of pages 66-67: Kaopolite, Inc. 2444 Morris Avenue Union, New Jersey 07083

Tel: 908 789-0609 Fax:908 851-2974

HYDROUS KAOLIN CLAYS

HYDRITE®

Dry Branch Kaolin is one of the largest producers of fine clays with a solid reputation for quality and service. That tradition continues with HYDRITE kaolin clays — the largest selection of filler and extender pigments for the paint, adhesive, ink, plastic and rubber industries

HYDRITE kaolin clays are carefully processed to meet rigid specifications By using centrifugal fractionation techniques, Dry Branch Kaolin offers a wide range of products with precisely controlled particle size distributions The chart below describes the HYDRITE grade best suited to individual applications Dry Branch Kaolin technical sales representatives or distributors will be pleased to provide additional information on specific applications

Typical Uses of HYDRITE Kaolin Clays

Applications	Grades	Properties	Advantages
Paints — gloss and semi-gloss emulsions, primer systems **Adhesives** — thixotropic aid **Caulks** — thixotropic aid **Inks** — letterpress **Engineering plastics**	**HYDRITE UF**	Finest particle size kaolin commercially available, highest water and oil demand	Highest gloss characteristics, best suspension Highest thixotropic characteristics Least abrasion
Paints — interior emulsions, primer systems, emulsion floor paints **Plastics** — bulk molding compounds, gel coats **Inks** — letterpress	**HYDRITE PX**	Good brightness, fine particle size, high water and oil demand	Excellent gloss, color stain removal, hiding power and suspension Excellent rheological properties Excellent flow control
Rubber — mechanical goods	**HYDRITE PXS**	Predispersed form of Hydrite PX	High modulus characteristics
Paints — interior emulsions, primer systems, universal tints **Plastics** — bulk molding compounds **Adhesives** — water base **Inks** — letterpress	**HYDRITE R**	Good brightness, free of coarse particles, medium oil demand	Excellent color, stain removal, hiding power and suspension Rheological control Strike-in control Reduces cost with good finish
Rubber — mechanical and electrical goods **Plastics** — bulk molding compounds, thermoplastic calendered goods	**HYDRITE RS**	Predispersed form of Hydrite R	Good physical, electrical and flow characteristics
Paints — interior emulsions, primer systems **Plastics** — polyester premix	**HYDRITE 121-S**	Intermediate particle size, intermediate water and oil demand Predispersed	Good stain removal, hiding power and suspension Flow control
Paints — interior emulsions, primer systems, exterior emulsions, exterior oleoresinous **Plastics** — bulk molding compounds and preform epoxy molding, phenolic molding **Rubber** — mechanical goods **Adhesives** — epoxy type, water type	**HYDRITE FLAT D**	Large particle size, lower water and oil demand	Good enamel hold-out, suspension and hiding power Low chalking rate Improves physical properties, non-reactive, permits high loadings Reduces shrinkage Very low modulus characteristics Non-reactive, thixotropic Controls penetration

Typical Chemical Properties

Aluminum Oxide (Al_2O_3) (combined)	38.8
Silicon Dioxide (SiO_2) (combined)	45.2
Iron Oxide (Fe_2O_3)	0.3
Titanium Dioxide (TiO_2)	1.4
Calcium Oxide (CaO)	0.05
Magnesium Oxide (MgO)	0.3
Sodium Oxide (Na_2O)	0.3
Potassium Oxide (K_2O)	0.05
Loss on Ignition at 950°C	13.6

Chemical Reactivity

HYDRITE kaolin clays are chemically inert and react with acids and bases only under extreme conditions. These clays are water processed to reduce soluble salt contents to extremely low levels

Physical Constants

Refractive Index*	1.56
Density lbs./solid gallon	21.66
Bulking Value gallon/lb	0.046
Hardness Index (Mohs' Scale)	2.0
Specific Gravity	2.58

Physical Properties

In their natural state, kaolin particles exist as a mixture of plates and stacks. Those finer than 2 microns are thin, flat, hexagonal plates The greater than 2 micron particles occur as stacks of those plates and are bound together as a single particle. Optical and physical characteristics of HYDRITE kaolin clays are greatly affected by changes in particle size and shape

Typical Particle Size Distribution

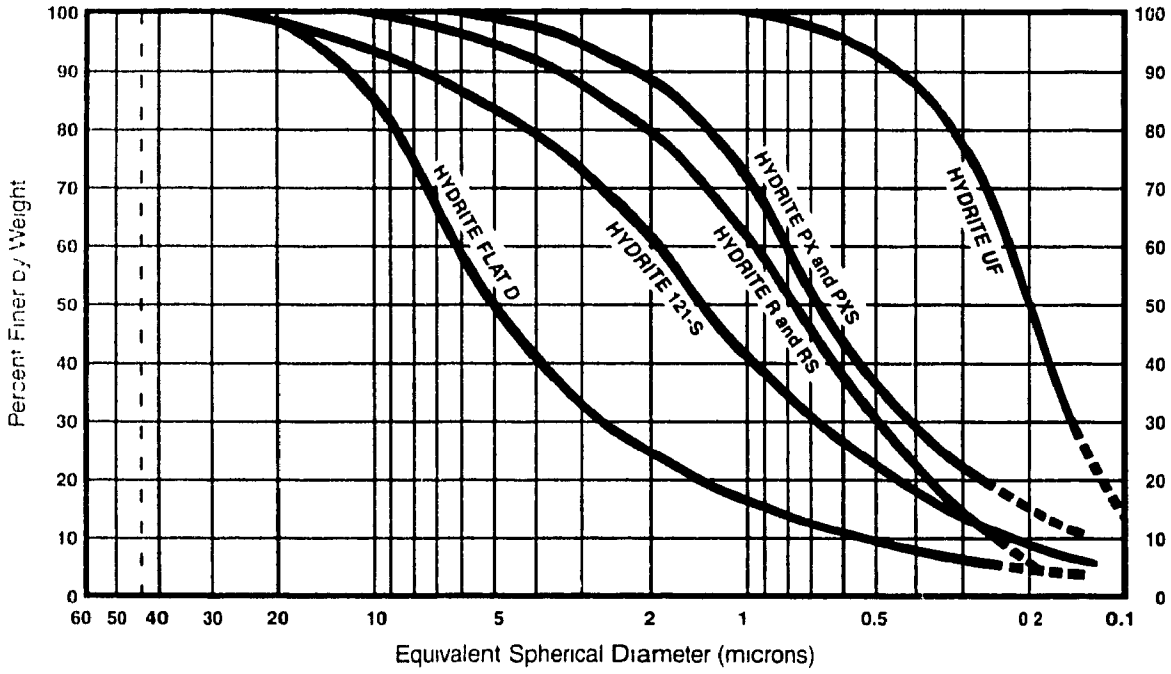

Typical Physical Test Results

Grade	Median Particle Size (Microns)	Brightness (G.E % of MgO)	pH*	325-Mesh Residue (Max. %)	Oil** Absorption (%)	Surface Area B.E.T. N_2 Adsorption (M^2/g)
HYDRITE UF	0.20	82.0 - 85.0	4.2 - 5.2	0.03	47	21
HYDRITE PX	0.68	87.0 - 90.0	4.2 - 5.2	0.03	43	12
HYDRITE PXS***	0.68	87.0 - 90.0	6.5 - 7.5	0.03	42	12
HYDRITE R	0.77	85.0 - 86.5	4.2 - 5.2	0.03	41	10
HYDRITE RS***	0.77	85.0 - 86.5	6.5 - 7.5	0.03	38	10
HYDRITE 121-S***	1.5	83.0 - 84.5	6.5 - 7.5	0.15	39	8
HYDRITE Flat D	5.0	80.2 - 83.0	4.2 - 5.2	0.25	34	7

*pH of a 20% aqueous slurry

** ASTM D1483 84 (Gardner Coleman technique)

***Available as slurry

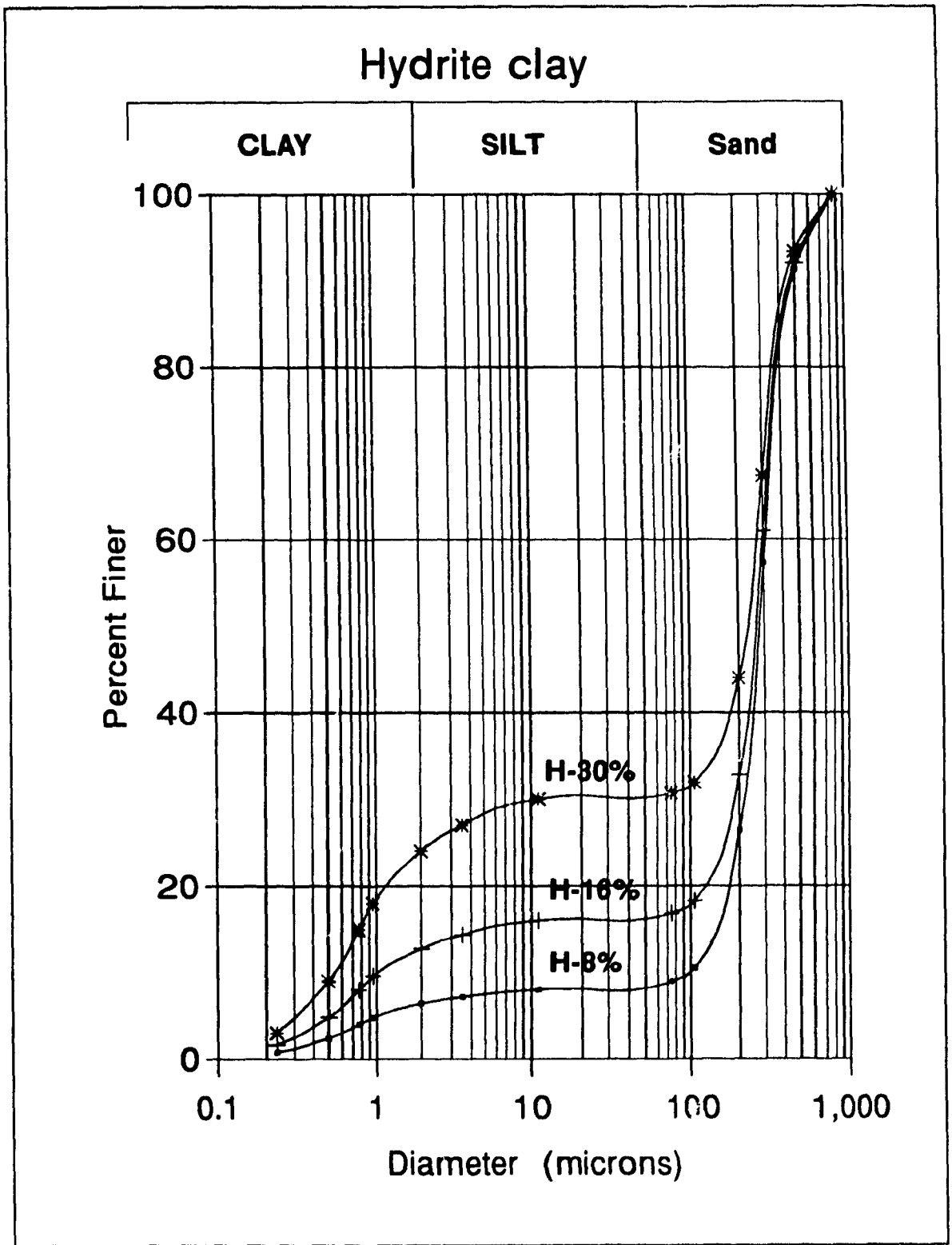

Figure A1: Particle Size Analyses of the three levels of Hydrite materials.

KORTHIX™ H

BENTONITE

KORTHIX™ H Thickening Agent is a modified, refind, white bentonite that generates outstanding rheological characteristics in water based systems. KORTHIX™ H bentonite achieves one the highest viscosities of any mineral thickener. It also exibits a good, clean, white color and ease of dispersion.

TYPICAL PHYSICAL PROPERTIES

Color	White
Form	Fine powder
Moisture (% Max.)	10
pH (2% solids in distilled water)	9.0-10.0
Wet Screen Residue (% retained on 325 Mesh)	0.0

TYPICAL CHEMICAL ANALYSIS

SIO_2	67.20
AL_2O_3	15.20
MgO	3.20
CaO	1.92
Fe_2O_3	1.87
TiO_2	0.16
Na_2O	2.58
K_2O	0.96
Loss on Ignition (1050°C)	5.70
Cation Exchange Capacity (Meq/100 g.)	80

AQUEOUS PROPERTIES

Dispersion: KORTHIX[tm] H Thickening Agent disperses easily in water to form a smooth, colloidal suspension. For best results, and slowly to water, with good agitation.

PARTICLE SIZE ANALYSIS

Due to the chemical (CEC) and swelling properties of this material, the standard methods used by soil scientists for determining particle distribution will no produce meaningfulresults. The Korthix[tm] H Bentonite used in this thesis contain at a minimum of 90% clay size particles (less than 2 micron) (verbal communication with George Larson of Kaopolite Inc.).

Soil type and location	Ste. Rosalie clay; 3/4 mile south of Browns Gore			Ste. Rosalie clay; 2.5 miles northwest of St. Placide			Ste. Rosalie clay; St. Hermas Station		
Horizon	A_o	G	C	A_o	G	C	A_o	G	C
Depth in inches	0-6	8-16	16-22	0-6	6-24	24-30	0-8	8-15	15-24
pH	5.2	6.5	7.8	5.7	6.6	7.3	6.0	6.2	7.1
Physical Analysis									
Gravel percentage of total soil	0	0	0	0	0	0	0	0	0
Sieve fractions									
Coarse sand (%)									
Medium sand (%)									
Fine sand (%)									
Very fine sand (%)									
Bouyoucos									
Sand (total) (%)	27	12	9	26	12	10	20	15	13
Silt (%)	37	29	31	30	36	27	32	35	22
Clay (%)	36	59	60	44	62	63	48	50	65
Chemical Analyses									
Calculated on oven-dried soils-									
Total C (%)	2.41	0.44	0.09	2.39	0.63	0.16	4.85	1.04	0.24
Total N (%)	.15	.04	.04	.17	.05	.03	.27	.06	.03
Total K_2O (%)	2.41	2.83	2.64	2.66	2.92	3.11	2.45	2.44	2.77
Total P_2O_5 (%)	.14	.10	.12	.17	.15	.17	.26	.13	.13
Calculated on air-dried soils-									
Available P_2O_5 (p.p.m.)	51	445	630	92	515	750	220	760	760
Exchangeable K (m.e./100 gms)	.93			.29			.82		
Exchangeable Ca (m.e./100 gms)	4.32			7.88			11.54		
Exchangeable Mg (m.e./100 gms)	2.13			4.12			6.16		

Table A1: Physical / Chemical Analyses of Natural clay (Ste. Rosalie clay).
Source: Lajoie, P.G. 1960.

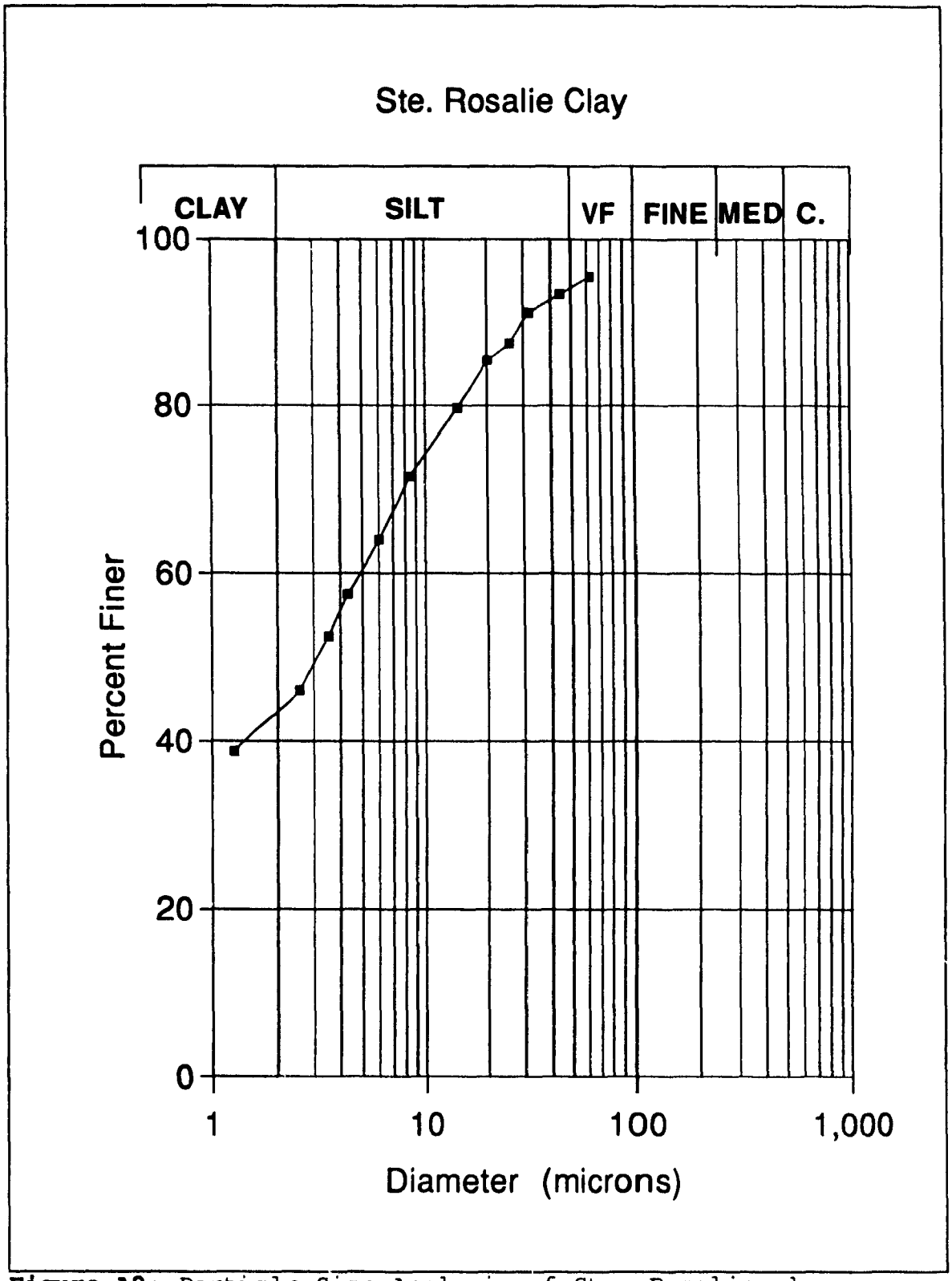

Figure A2: Particle Size Analysis of Ste. Rosalie clay.

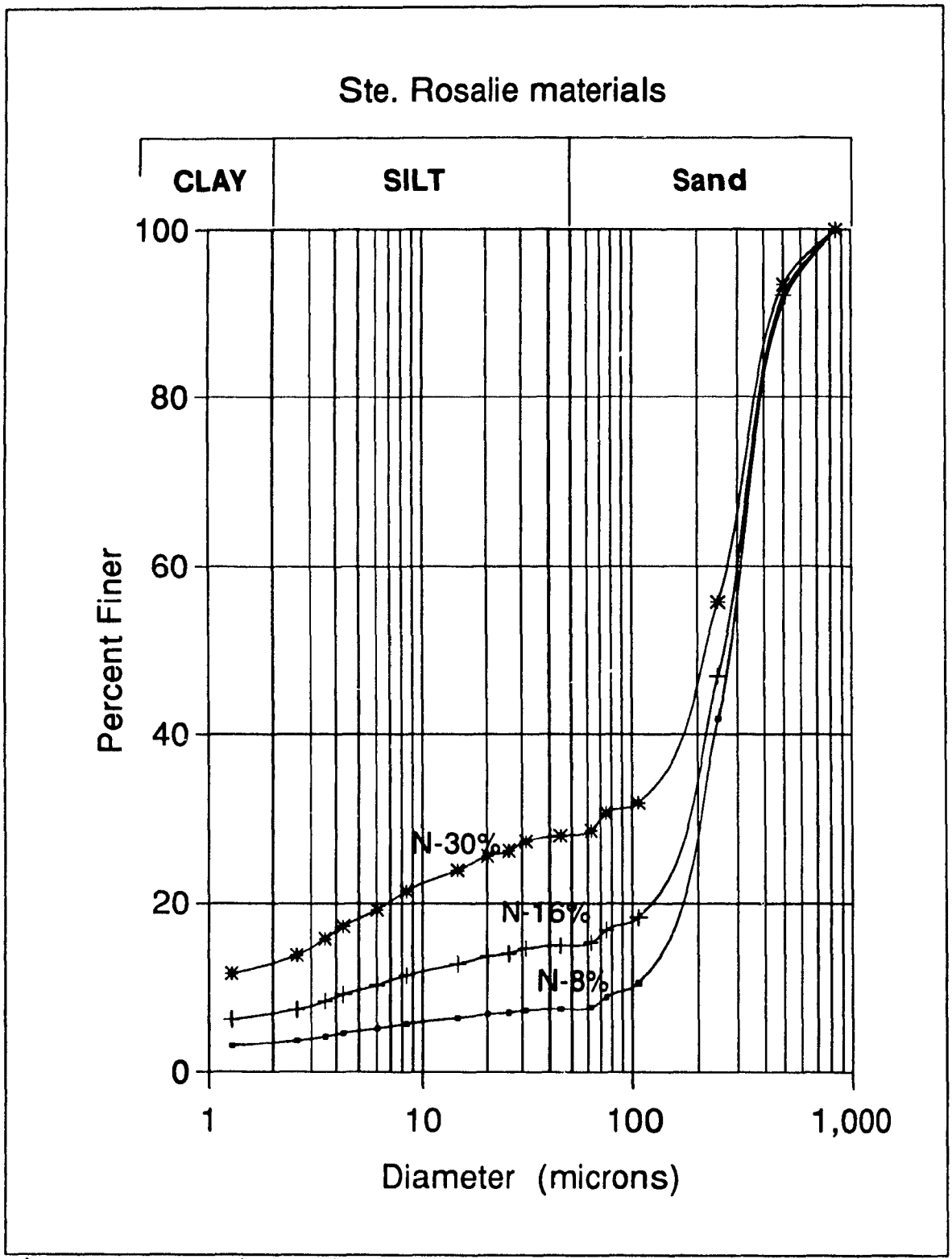

Figure A3: Particle Size Analyses of the three levels of Ste. Rosalie (natural) materials.

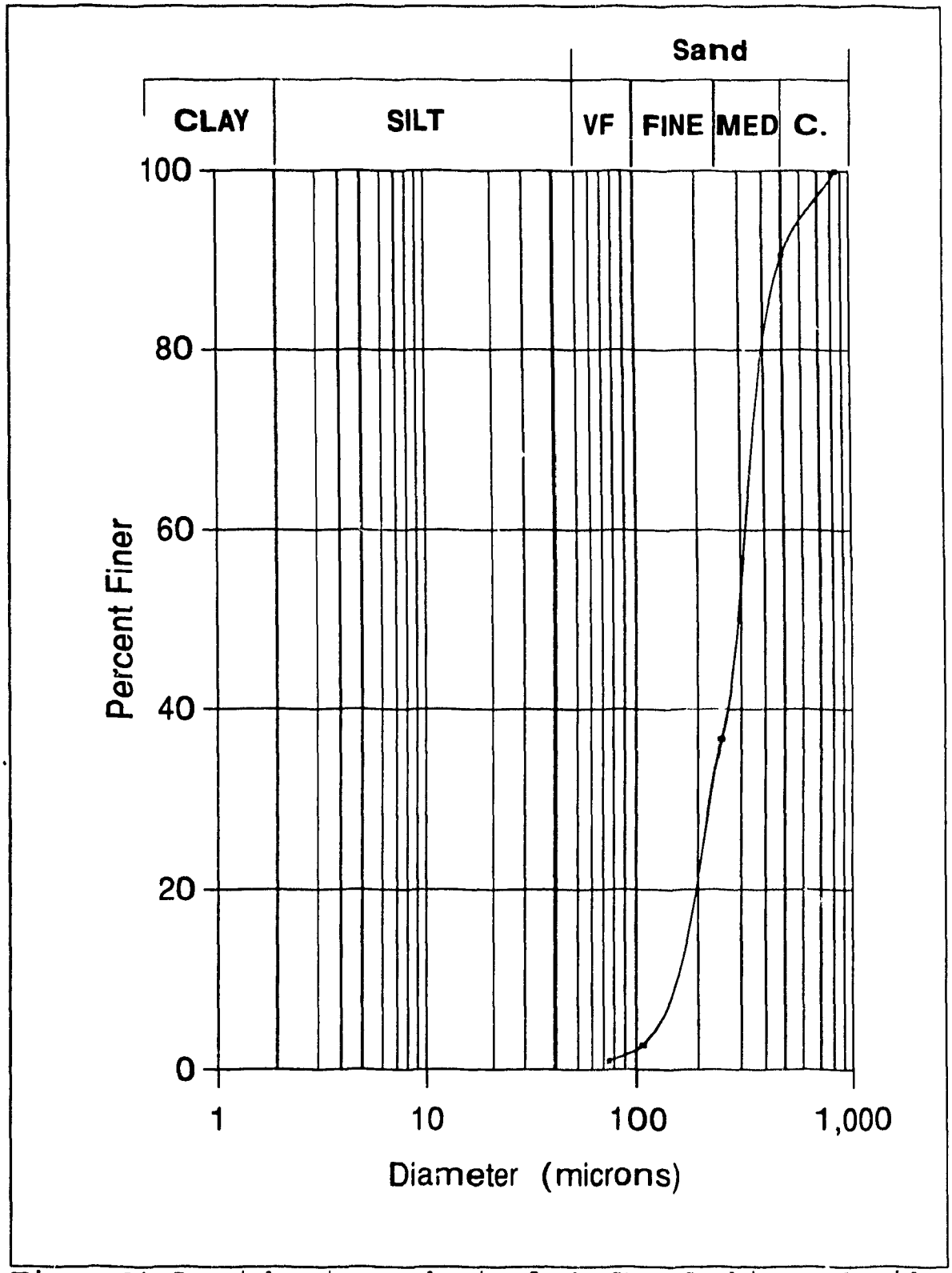

Figure A4: Particle size analysis of the Ste. Sophie sand soil.

APPENDIX B

Temperature factors

Table B1: Temperature factors (f_t) for correcting resistance and conductivity data on soil extracts to the standard temperature of 25° C.

$EC_{25} = EC_t \times f_t$; $EC_{25} = (k/R_t) \times f_t$; $R_{25} = R_t/f_t$

°C.	° F.	f_t	° C.	° F.	f_t	° C.	° F.	f_t
3.0	37.4	1.709	22.0	71.6	1.064	29.0	84.2	.925
4.0	39.2	1.660	22.2	72.0	1.060	29.2	84.6	.921
5.0	41.0	1.613	22.4	72.3	1.055	29.4	84.9	.918
6.0	42.8	1.569	22.6	72.7	1.051	29.6	85.3	.914
7.0	44.6	1.528	22.8	73.0	1.047	29.8	85.6	.911
8.0	46.4	1.488	23.0	73.4	1.043	30.0	86.0	.907
9.0	48.2	1.448	23.2	73.8	1.038	30.2	86.4	.904
10.0	50.0	1.411	23.4	74.1	1.034	30.4	86.7	.901
11.0	51.8	1.375	23.6	74.5	1.029	30.6	87.1	.897
12.0	53.6	1.341	23.8	74.8	1.025	30.8	87.4	.894
13.0	55.4	1.309	24.0	75.2	1.020	31.0	87 8	.890
14.0	57.2	1.277	24.2	75.6	1.016	31.2	88.2	.887
15.0	59.0	1.247	24.4	75.9	1.012	31.4	88.5	.884
16.0	60.8	1.218	24.6	76.3	1.008	31.6	88.9	.880
17.0	62.6	1.189	24.8	76.6	1.004	31.8	89.2	.877
18.0	64.4	1.163	25.0	77.0	1.000	32.0	89.6	.873
18.2	64.8	1.157	25.2	77.4	.996	32.2	90.0	.870
18 4	65.1	1.152	25.4	77.7	.992	32.4	90.3	.867
18.6	65.5	1.147	25.6	78.1	.988	32.6	90.7	.864
18.8	65.8	1.142	25.8	78.5	.983	32.8	91.0	.861
19.0	66.2	1.136	26.0	78.8	.979	33.0	91.4	.858
19.2	66.6	1.131	26.2	79.2	.975	34.0	93.2	.843
19.4	66.9	1.127	26.4	79.5	.971	35.0	95.0	.829
19.6	67.3	1.122	26.6	79.9	.967	36.0	96.8	.815
19.8	67.6	1.117	26.8	80.2	.964	37.0	98.6	.801
20.0	68.0	1.112	27.0	80.6	.960	38.0	100.2	.788
20.2	68.4	1.107	27.2	81.0	.956	39.0	102.2	.775
20.4	68.7	1.102	27.4	81.3	.953	40.0	104.0	.763
20.6	69.1	1.097	27.6	81.7	.950	41.0	105.8	.750
20.8	69.4	1.092	27.8	82.0	.947	42.0	107.6	.739
21.0	69.8	1.087	28.0	82.4	.943	43.0	109.4	.727
21.2	70.2	1.082	28.2	82.8	.940	44.0	111.2	.716
21.4	70.5	1.078	28.4	83.1	.936	45.0	113.0	.705
21.6	70.9	1.073	28.6	83.5	.932	46.0	114.8	.694
21.8	71.2	1.068	28.8	83.8	.929	47.0	116.6	.683

Source: USDA Handbook No. 60.

APPENDIX C

Surface Conductance and Transmission Factor of various soils

Surface Conductivity, EC_S, and Transmission Coefficient, T, for H-8% Soil

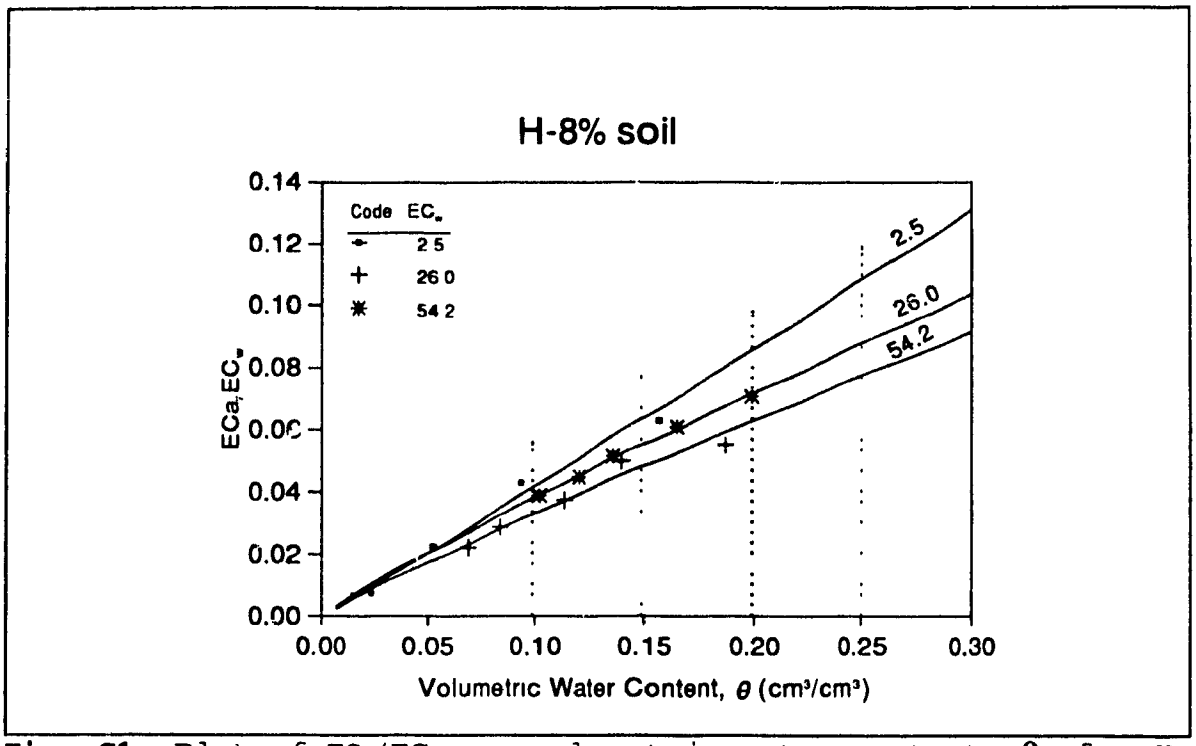

Fig. C1: Plot of EC_a/EC_w vs. volumetric water content, θ, for H-8% soil.

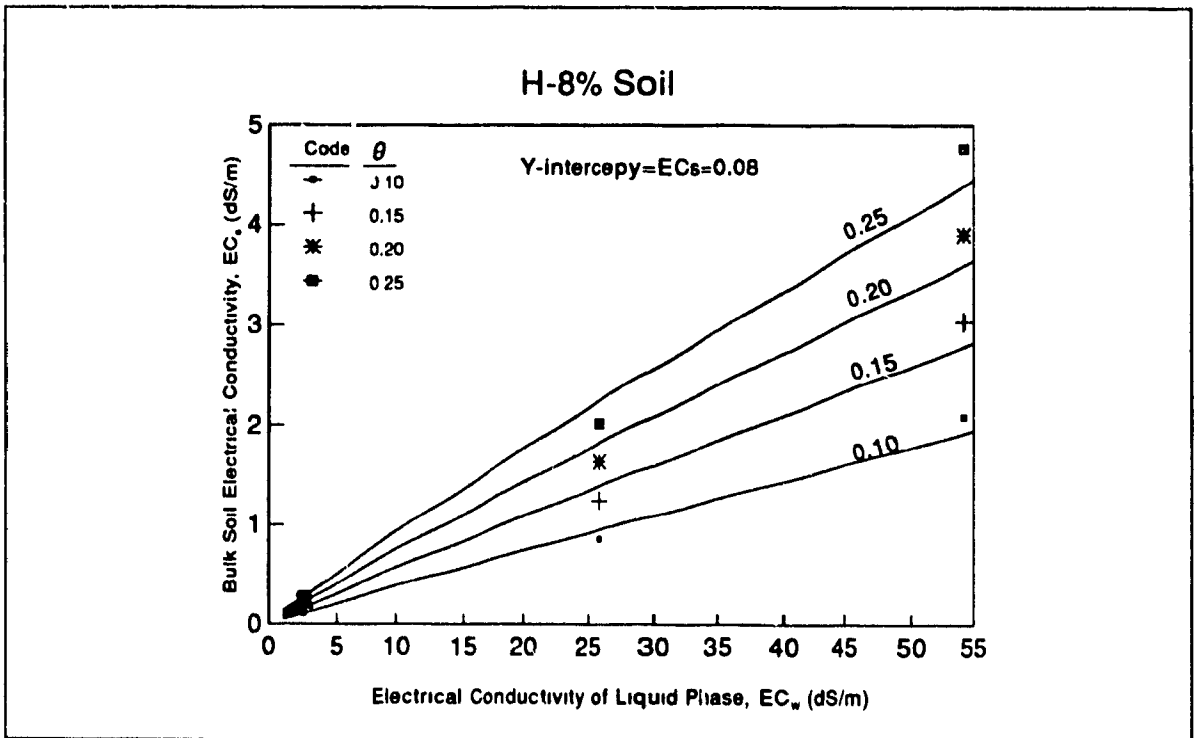

Fig. C2: Plot of EC_a vs. EC_w for various fixed volumetric water contents as interpolated from Fig. C1 for H-8% soil showing the extrapolated value of EC_s.

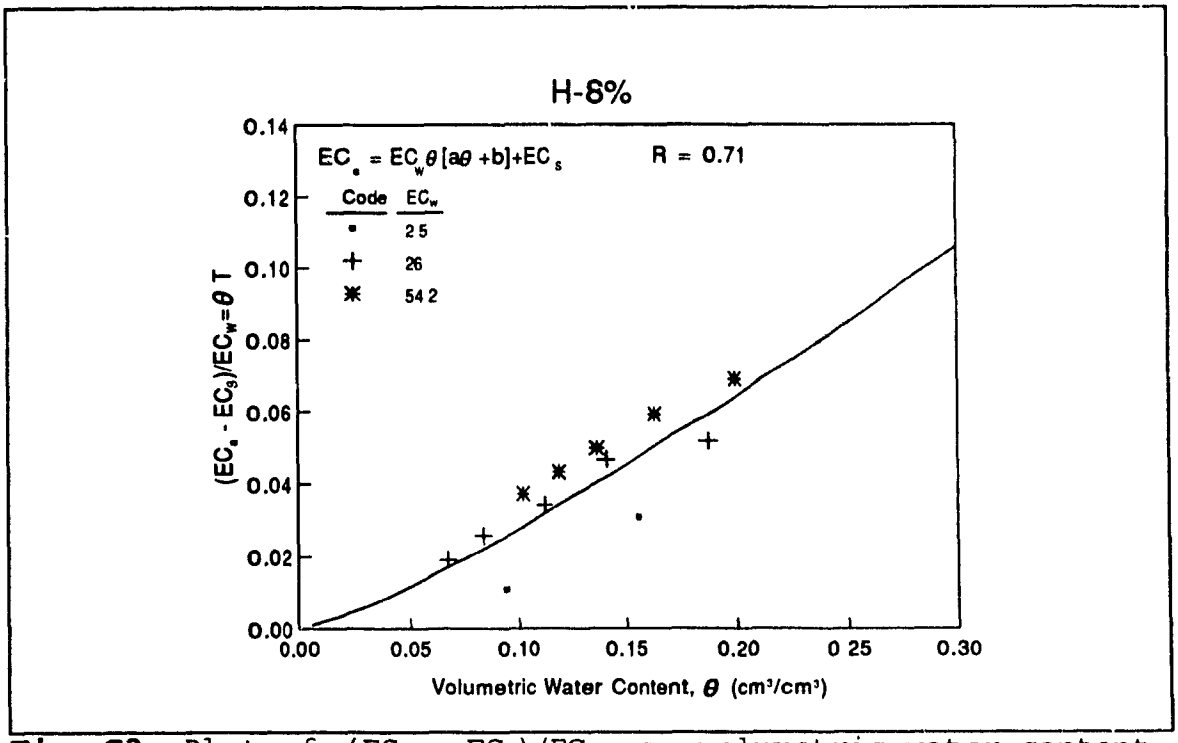

Fig. C3: Plot of $(EC_a - EC_s)/EC_w$ vs. volumetric water content, θ, for data of fig. C1 and C2.

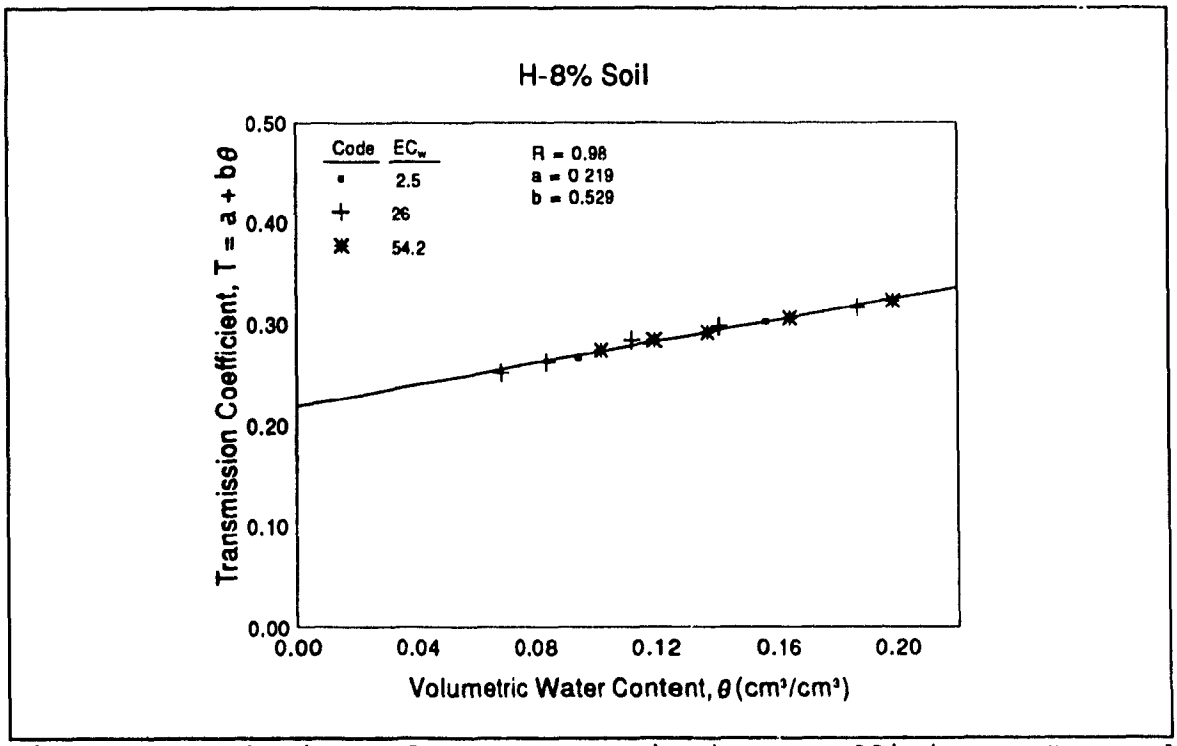

Fig. C4: Relation of the transmission coefficient, T, and volumetric water content for H-8% soil.

Surface Conductivity, EC_s, and Transmission Coefficient, T, for N-8% Soil

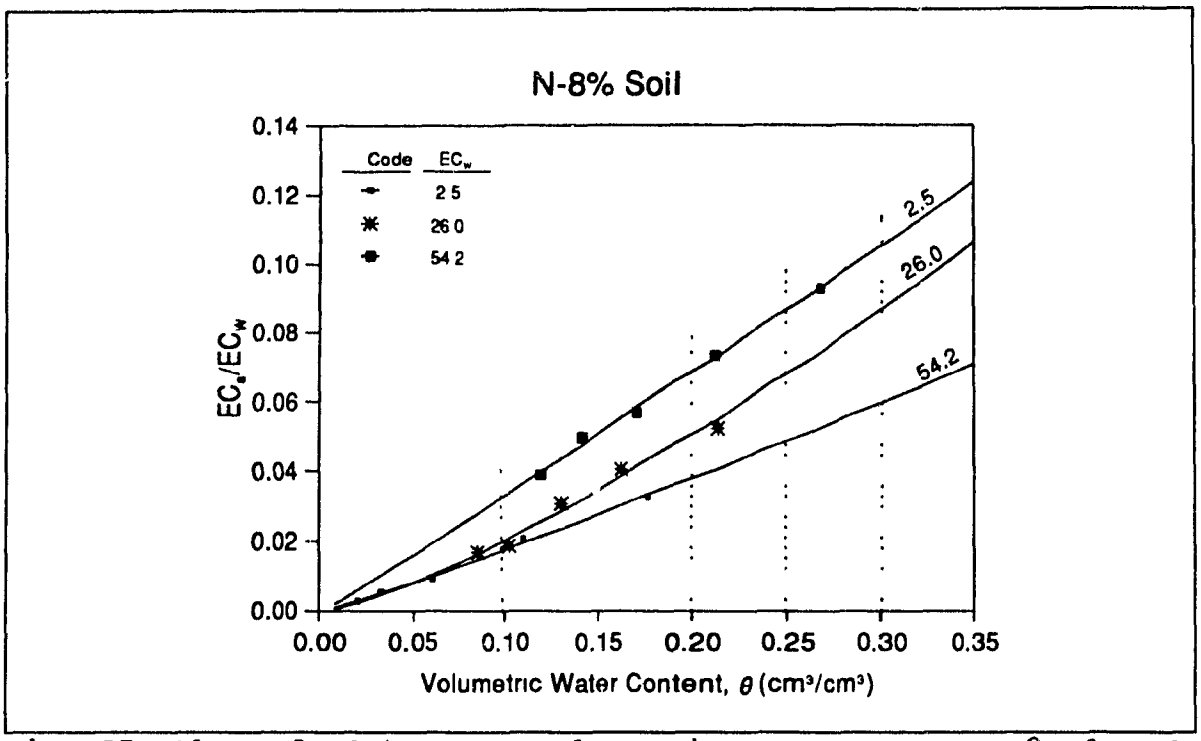

Fig. C5: Plot of EC_a/EC_W vs. volumetric water content, θ, for N-8% soil.

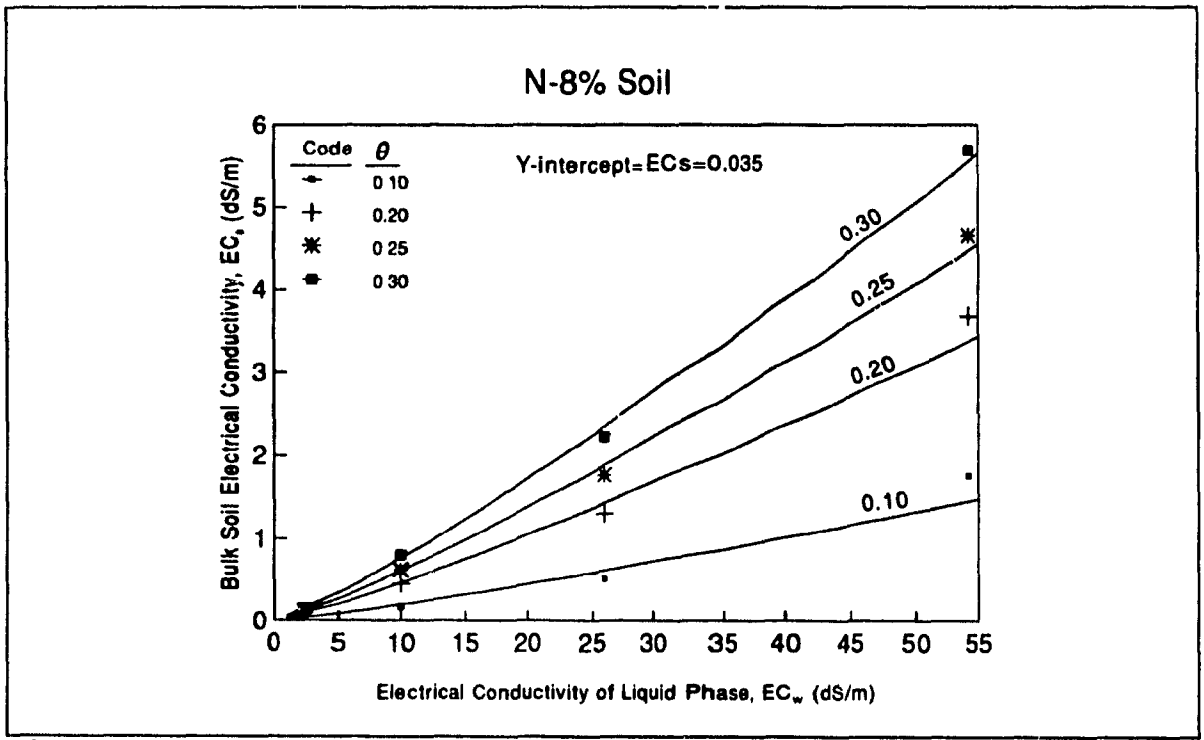

Fig. C6: Plot of EC_a vs. EC_W for various fixed volumetric water contents as interpolated from Fig. C5 for N-8% soil showing the extrapolated value of EC_s.

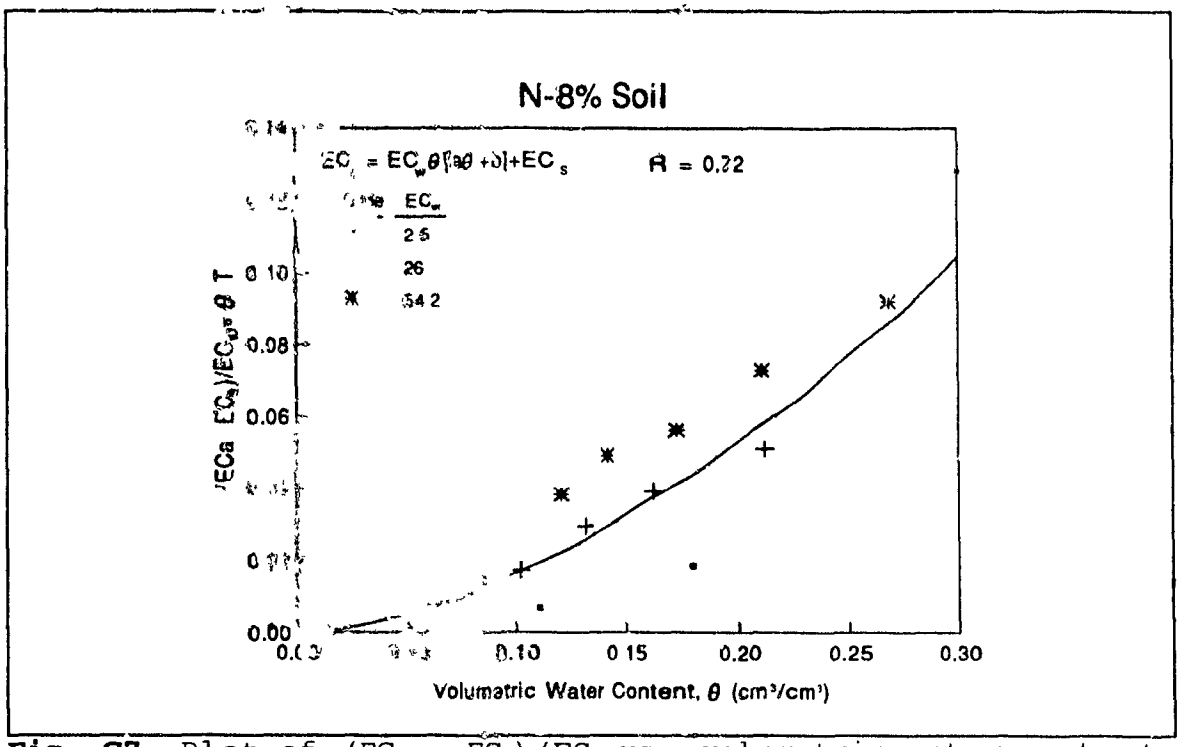

Fig. C7: Plot of $(EC_a - EC_s)/EC_w$ vs. volumetric water content, θ, for data of fig. C5 and C6.

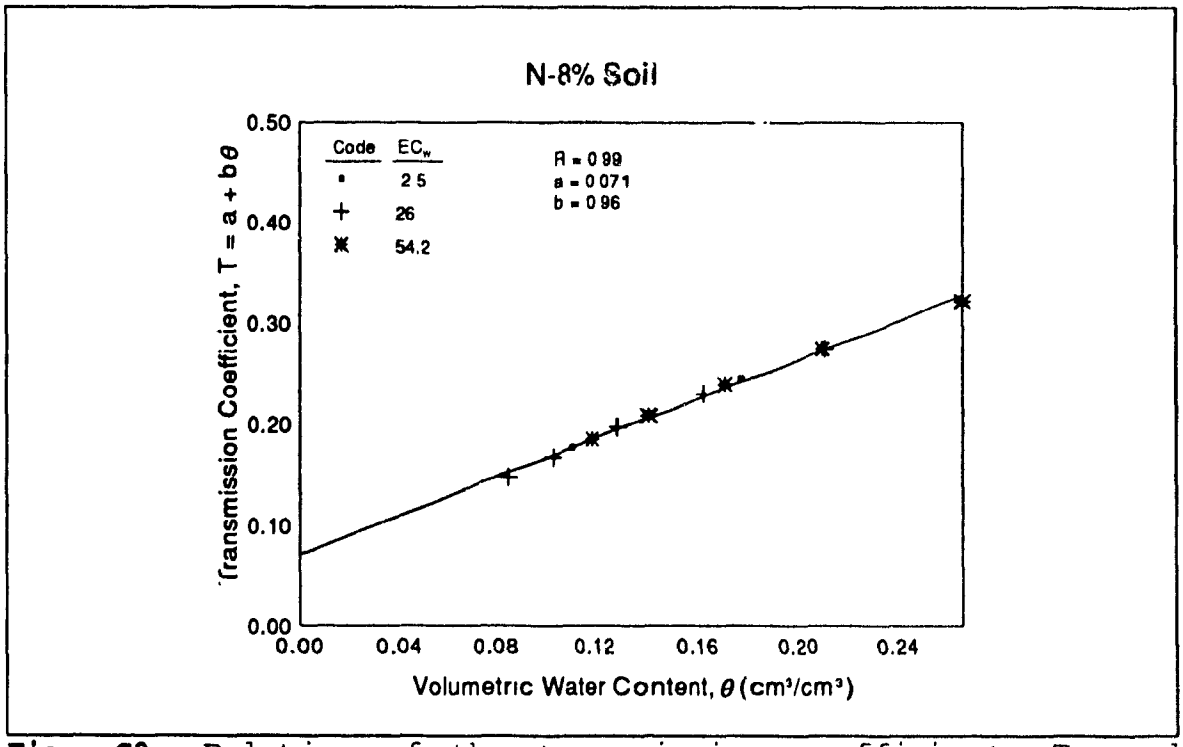

Fig. C8: Relation of the transmission coefficient, T, and volumetric water content for N-8% soil.

Surface Conductivity, EC_S, and Transmission Coefficient, T, for H-16% Soil

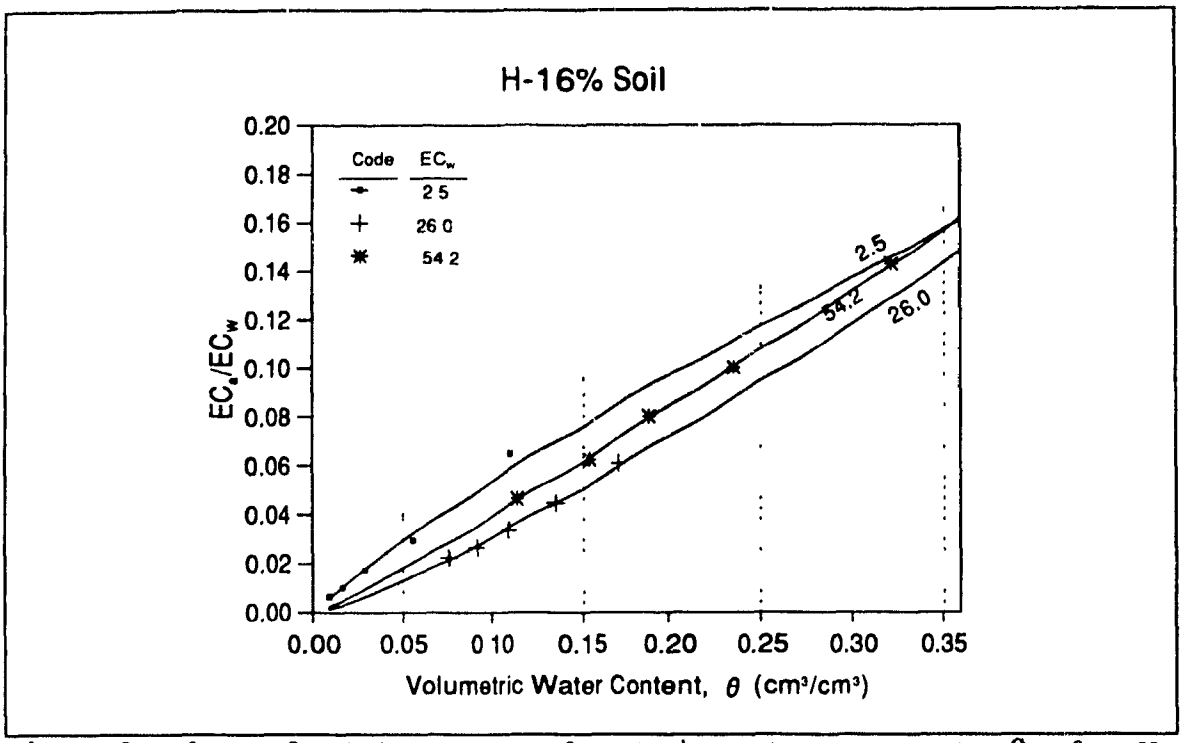

Fig. C9: Plot of EC_a/EC_w vs. volumetric water content, θ, for H-16% soil.

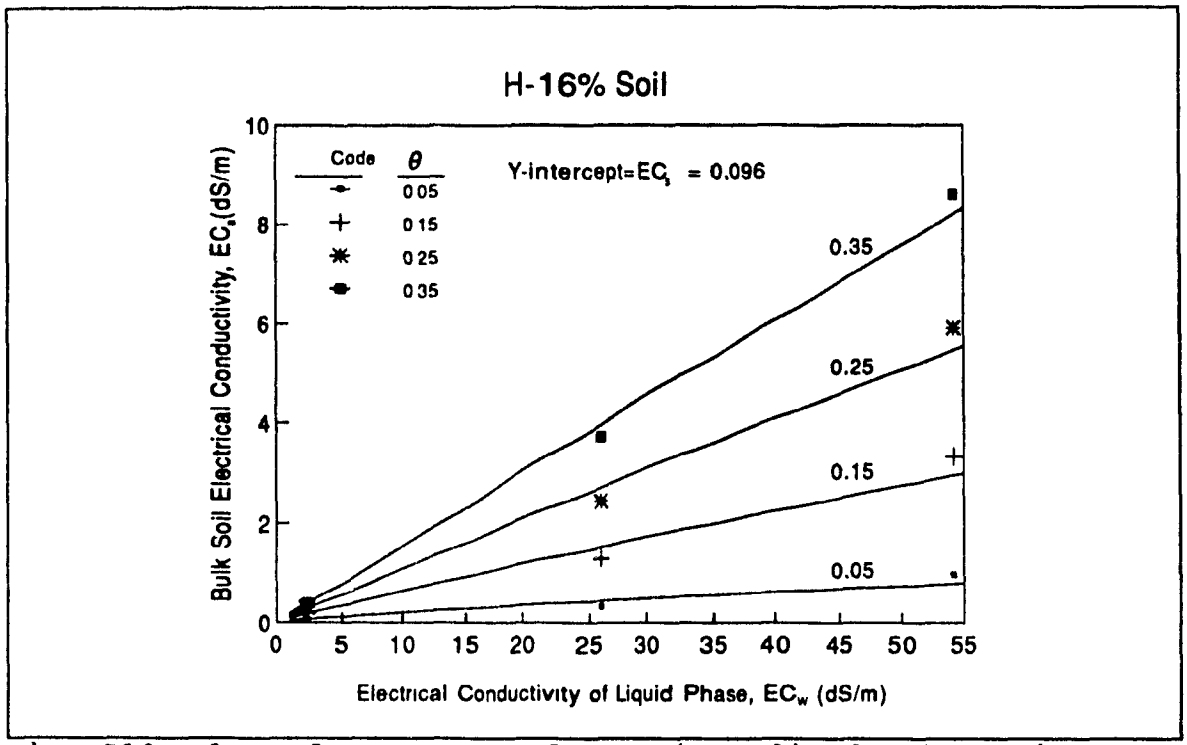

Fig. C10: Plot of EC_a vs. EC_w for various fixed volumetric water contents as interpolated from Fig. C9 for H-16% soil showing the extrapolated value of EC_s.

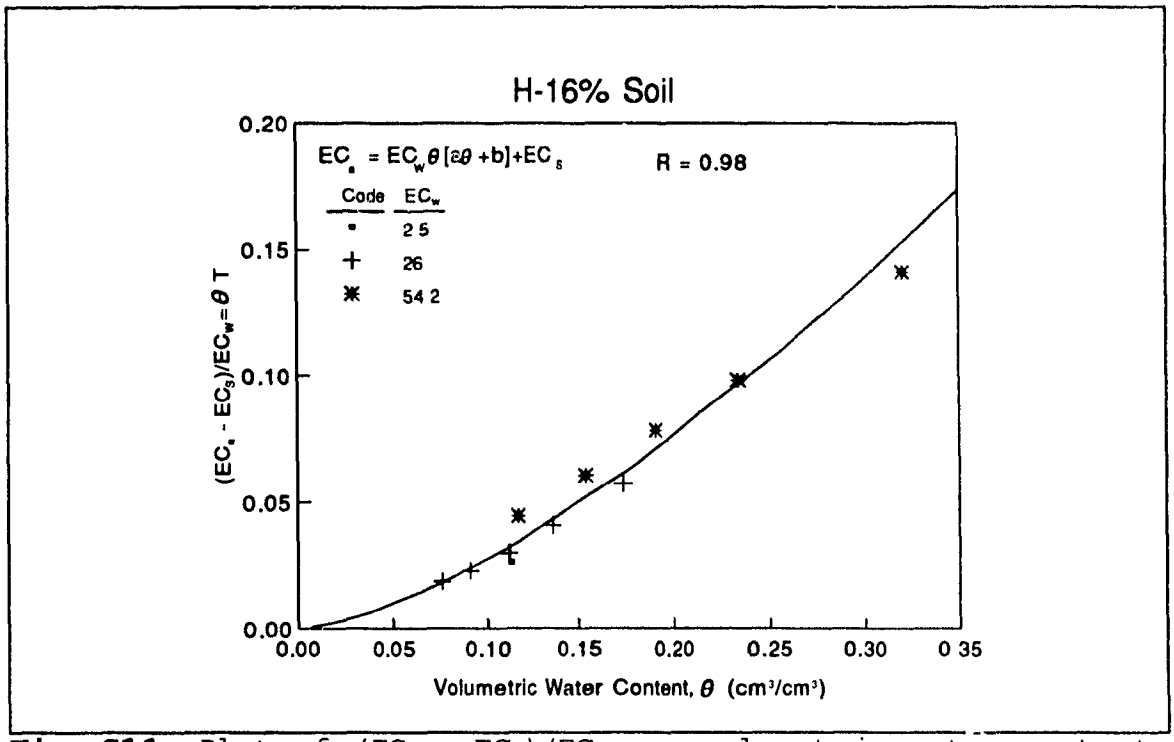

Fig. C11: Plot of $(EC_a - EC_s)/EC_w$ vs. volumetric water content, θ, for data of fig. C9 and C10.

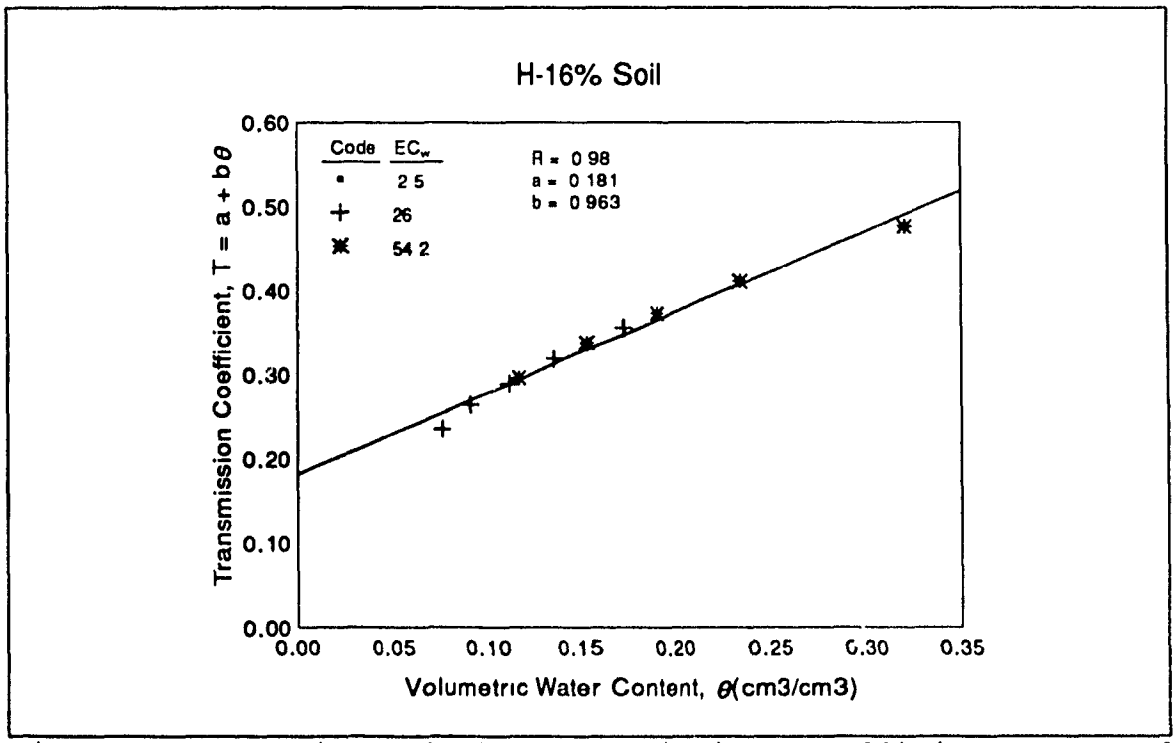

Fig. C12: Relation of the transmission coefficient, T, and volumetric water content for H-16% soil.

Surface Conductivity, EC_s, and Transmission Coefficient, T, for B-16% Soil

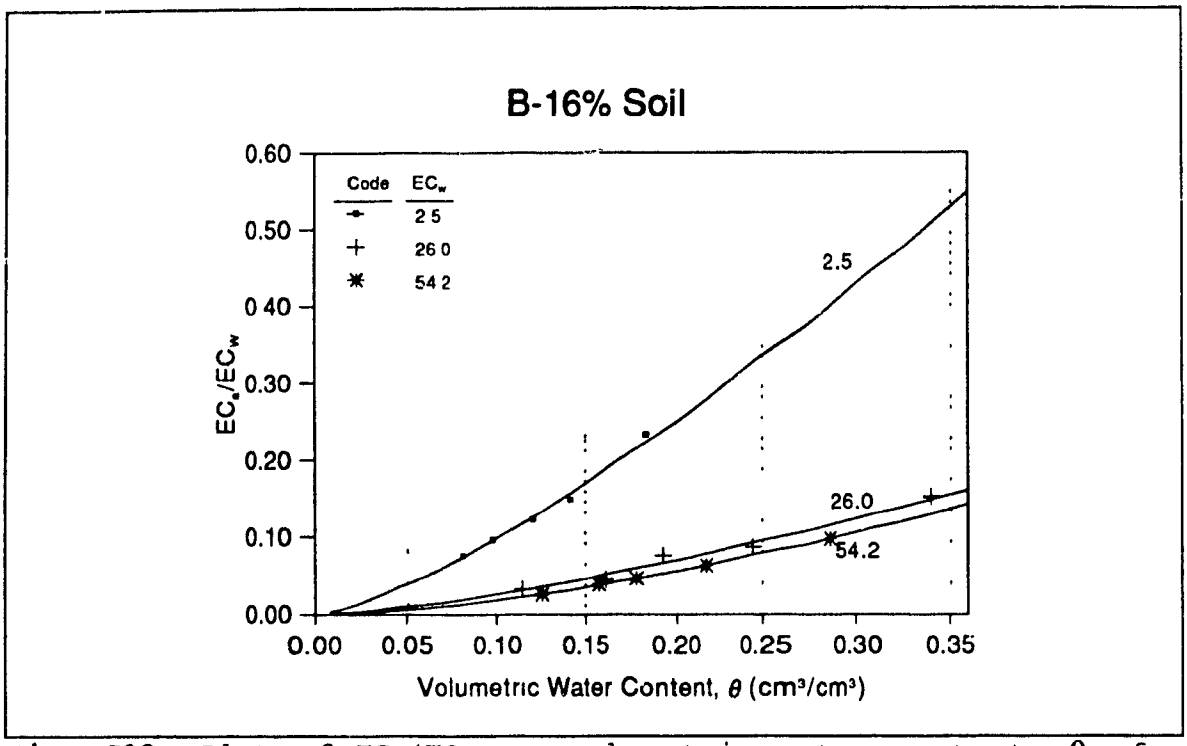

Fig. C13: Plot of EC_a/EC_w vs. volumetric water content, θ, for B-16% soil.

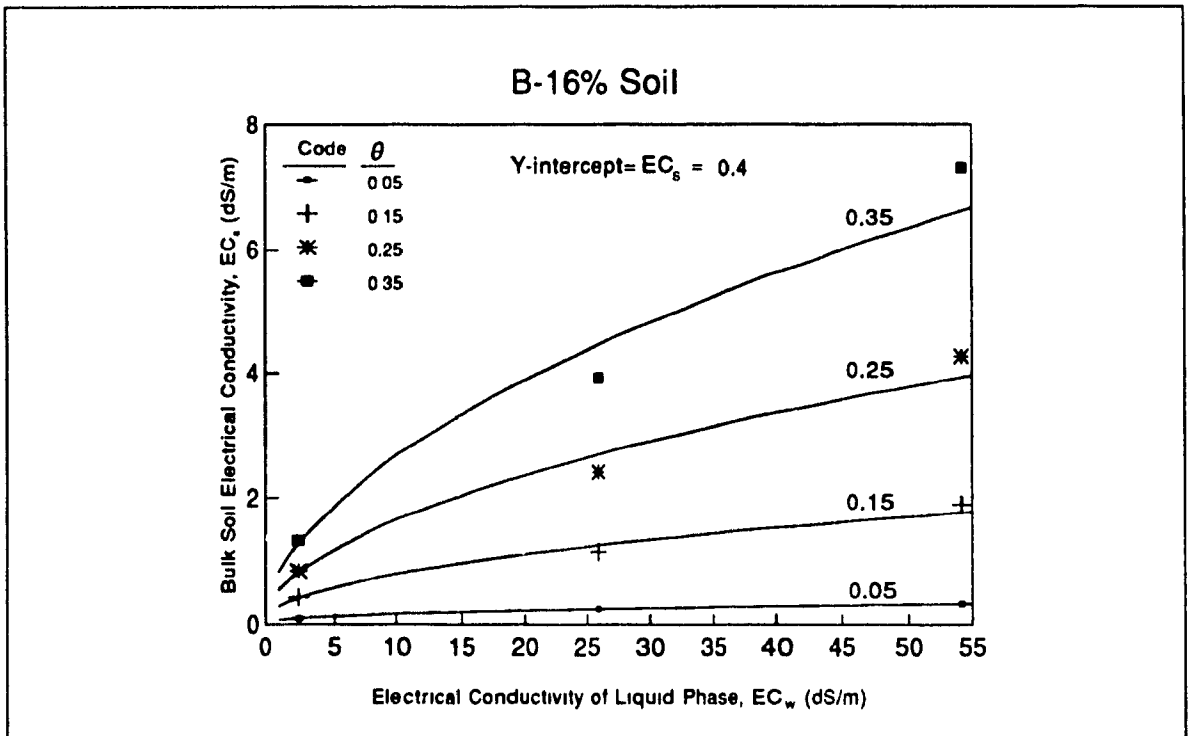

Fig. C14: Plot of EC_a vs. EC_w for various fixed volumetric water contents as interpolated from Fig. C13 for B-16% soil showing the extrapolated value of EC_s.

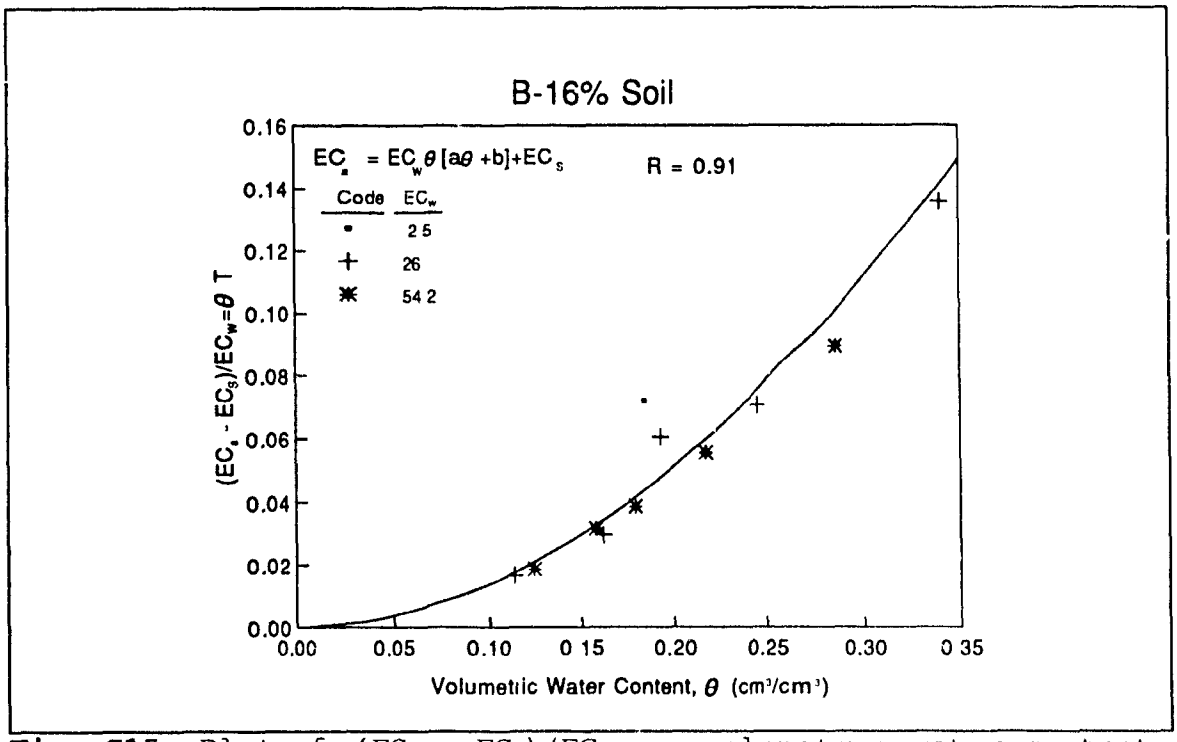

Fig. C15: Plot of $(EC_a - EC_S)/EC_W$ vs. volumetric water content, θ, for data of fig. C13 and C14.

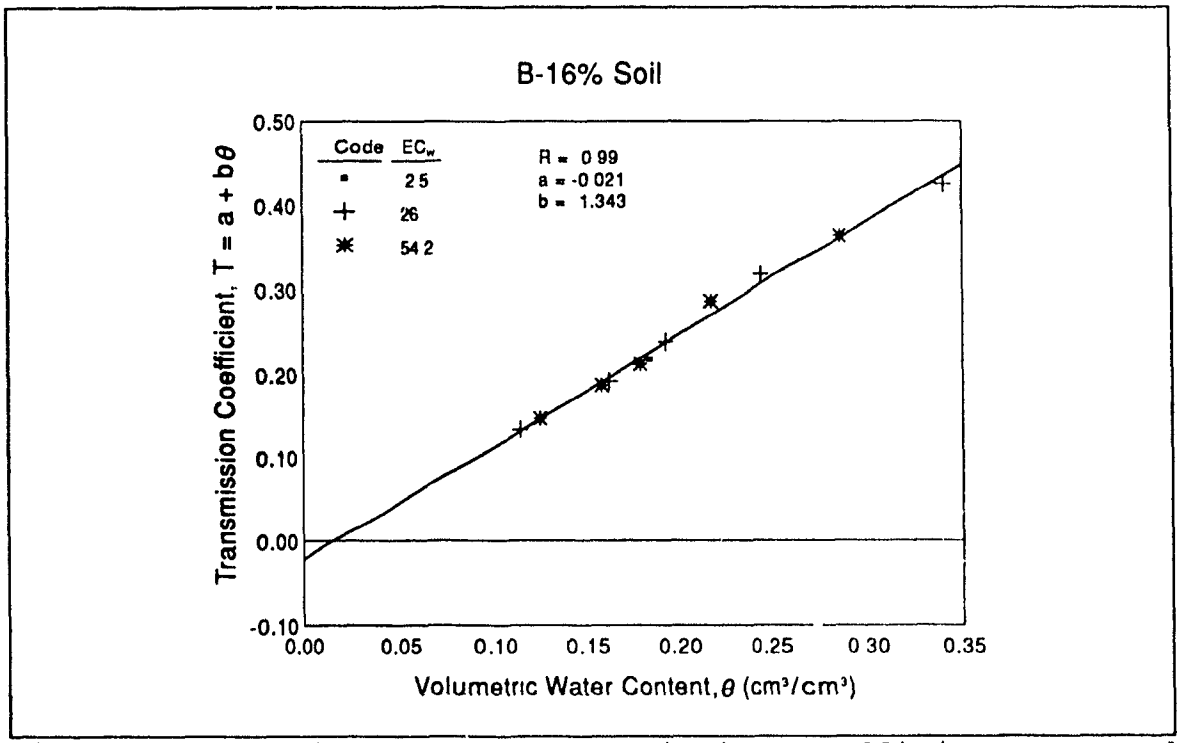

Fig. C16: Relation of the transmission coefficient, T, and volumetric water content for B-16% soil.

Surface Conductivity, EC_S, and Transmission Coefficient, T, for N-16% Soil

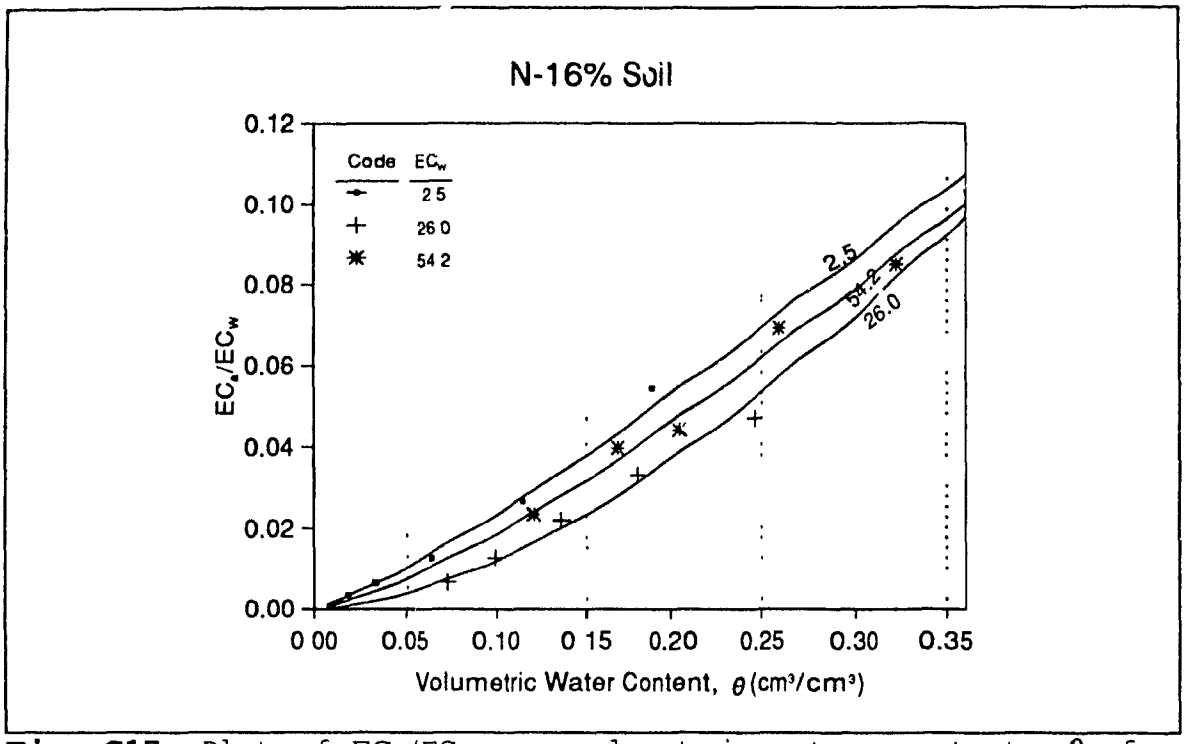

Fig. C17: Plot of EC_a/EC_w vs. volumetric water content, θ, for N-16% soil.

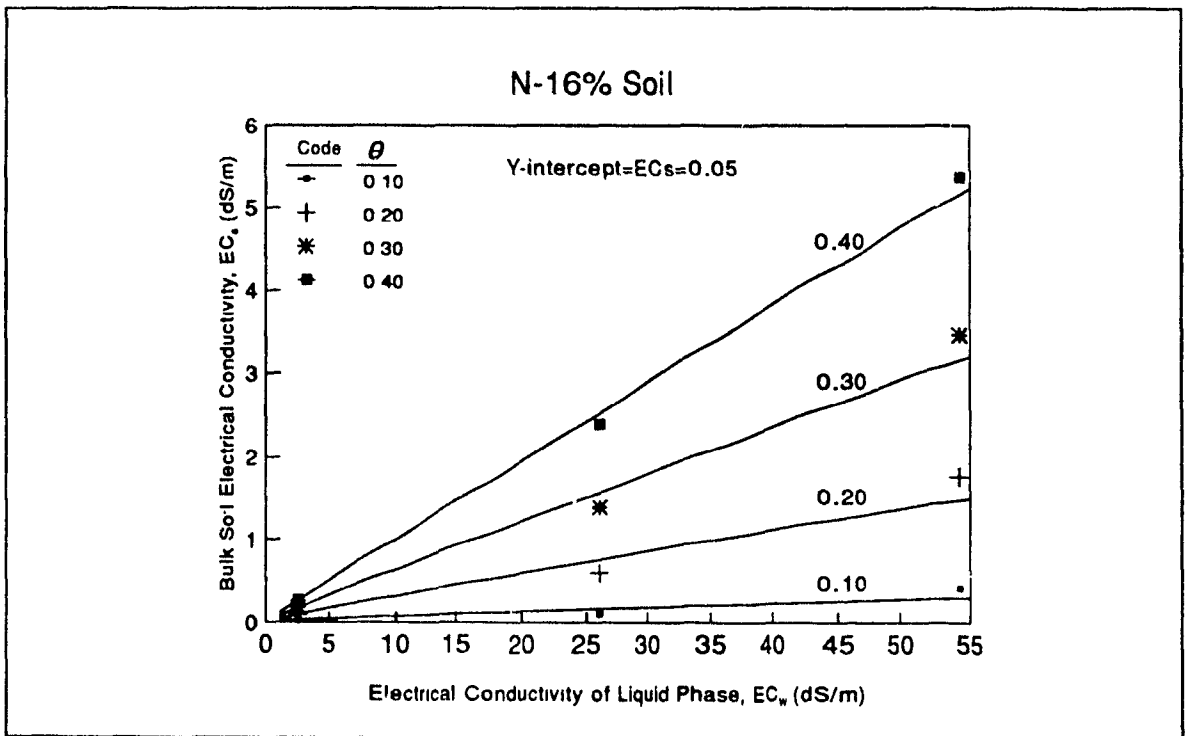

Fig. C18: Plot of EC_a vs. EC_w for various fixed volumetric water contents as interpolated from Fig. C17 for N-16% soil showing the extrapolated value of EC_s.

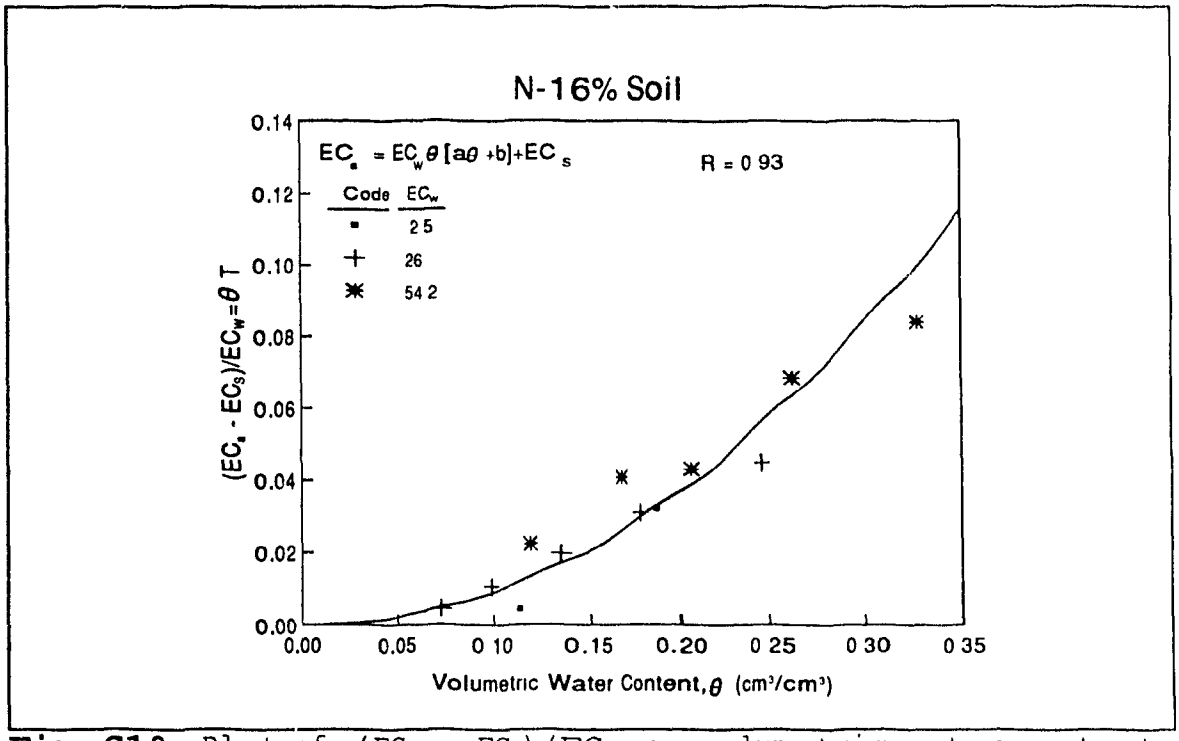

Fig. C19: Plot of $(EC_a - EC_s)/EC_w$ vs. volumetric water content, θ, for data of fig. C17 and C18.

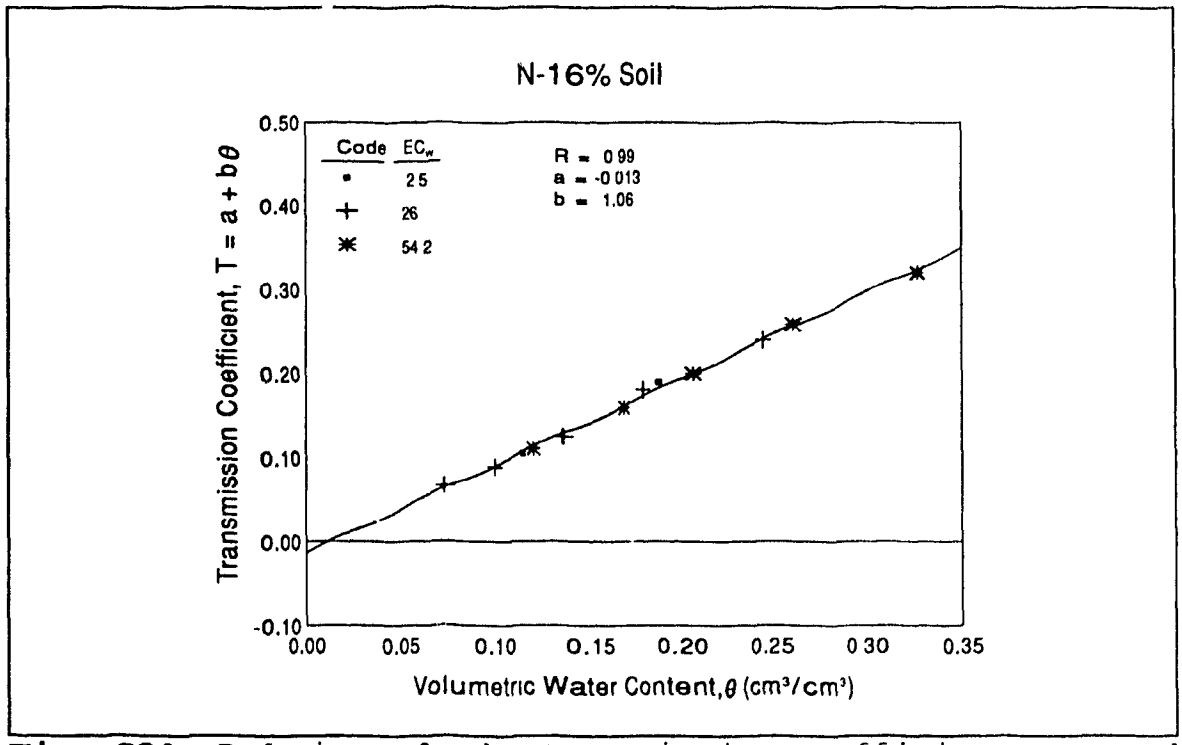

Fig. C20: Relation of the transmission coefficient, T, and volumetric water content for N-16% soil.

Surface Conductivity, EC_s, and Transmission Coefficient, T, for H-30% Soil

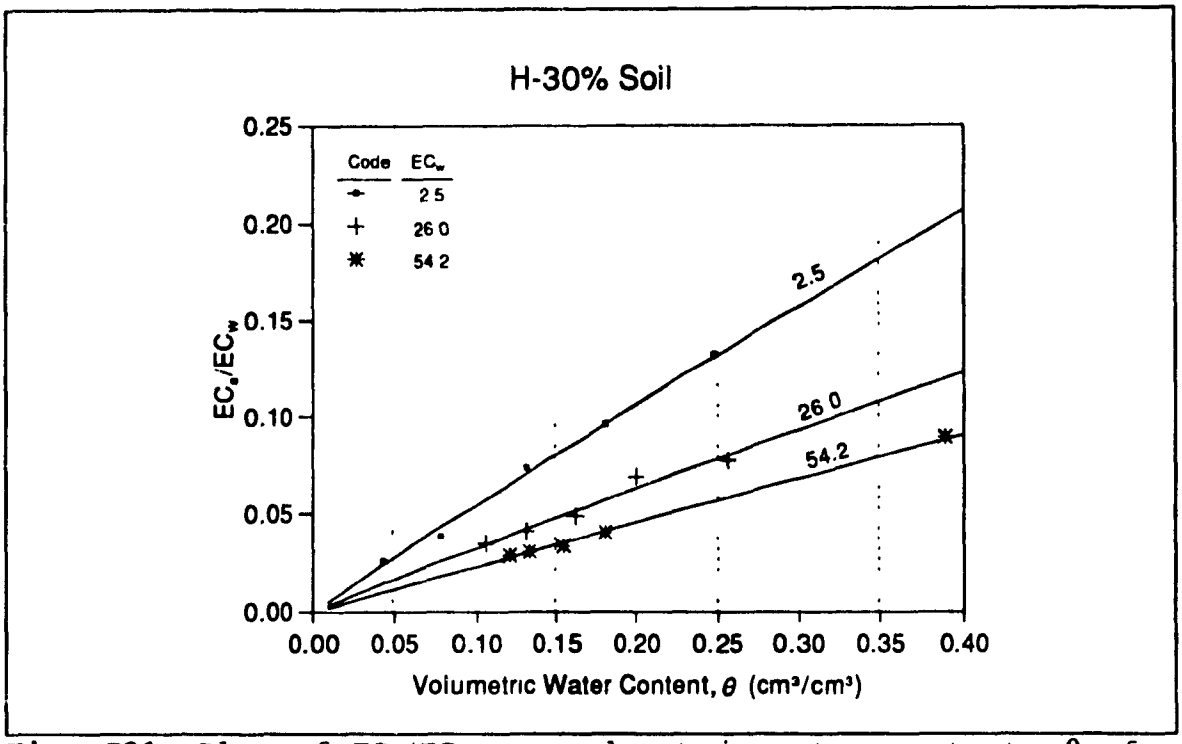

Fig. C21: Plot of EC_a/EC_w vs. volumetric water content, θ, for H-30% soil.

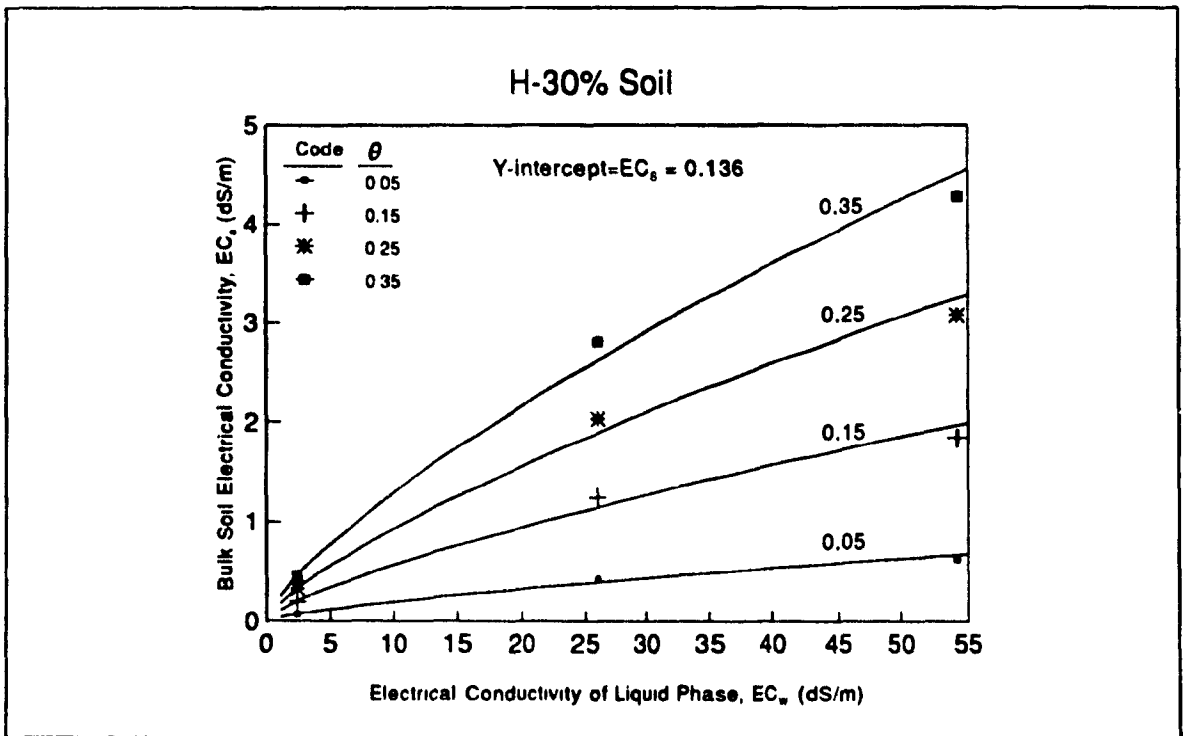

Fig. C22: Plot of EC_a vs. EC_w for various fixed volumetric water contents as interpolated from Fig. C21 for H-30% soil showing the extrapolated value of EC_s.

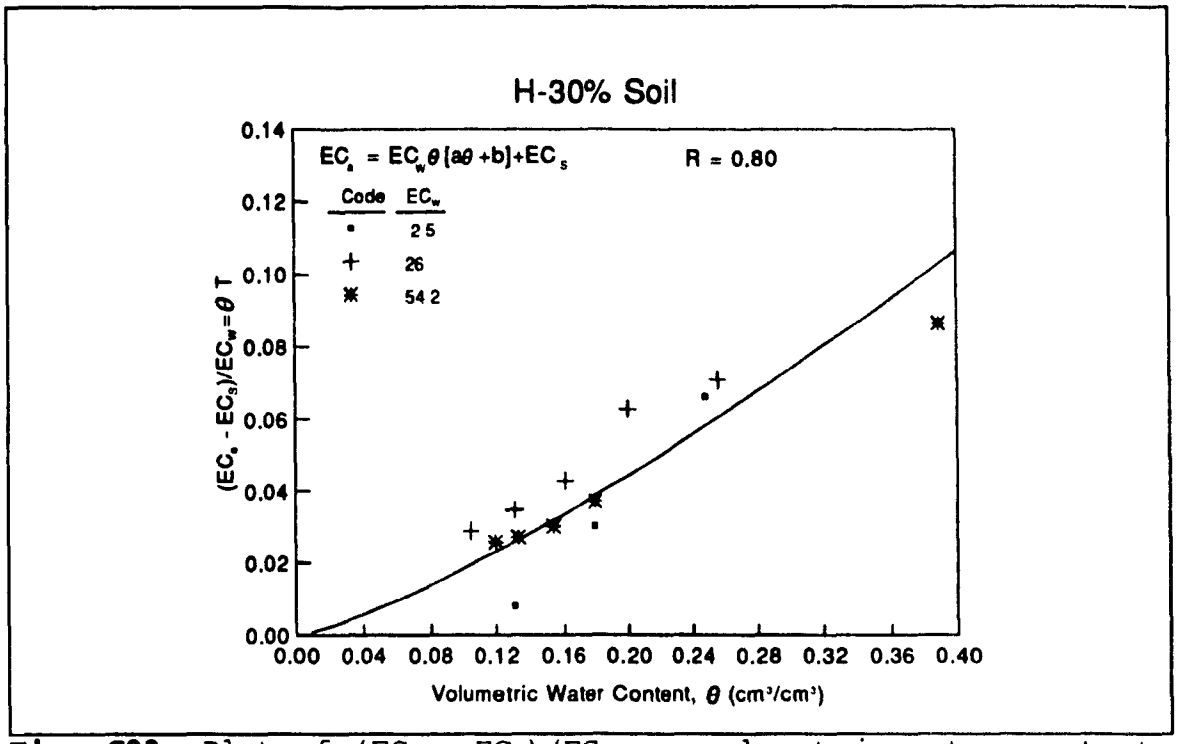

Fig. C23: Plot of $(EC_a - EC_S)/EC_W$ vs. volumetric water content, θ, for data of fig. C21 and C22.

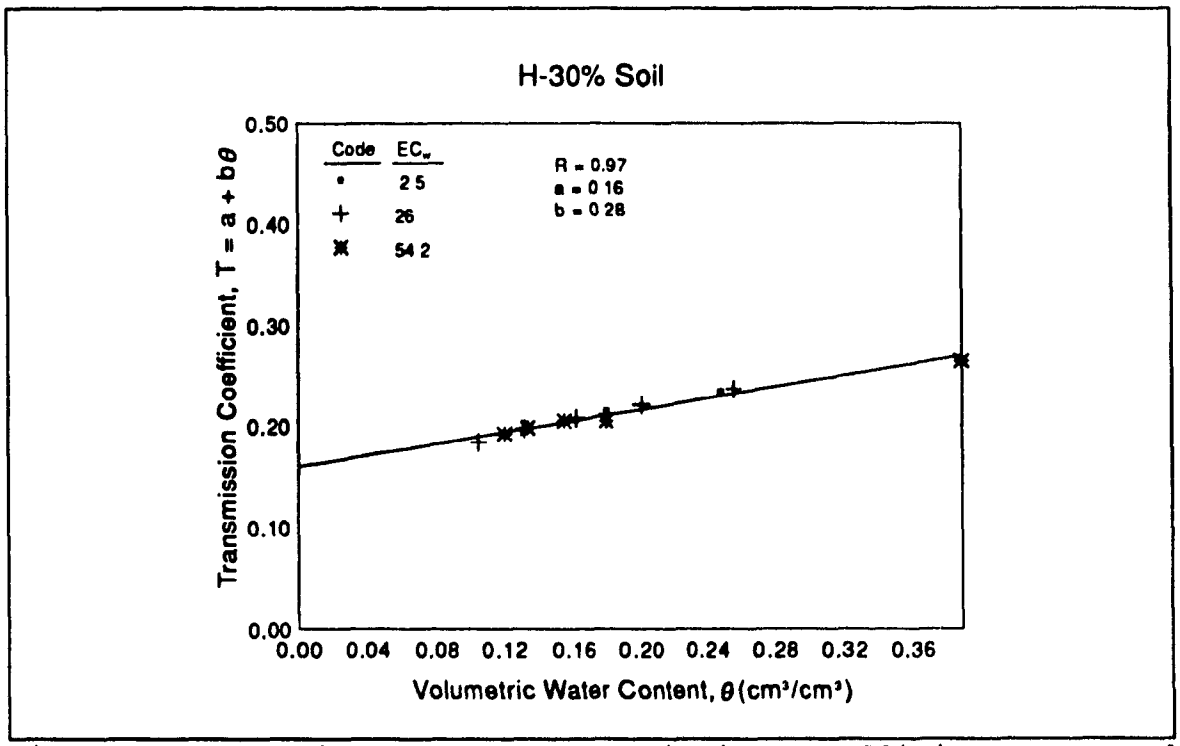

Fig. C24: Relation of the transmission coefficient, T, and volumetric water content for H-30% soil.

Surface Conductivity, EC_s, and Transmission Coefficient, T, for B-30% Soil

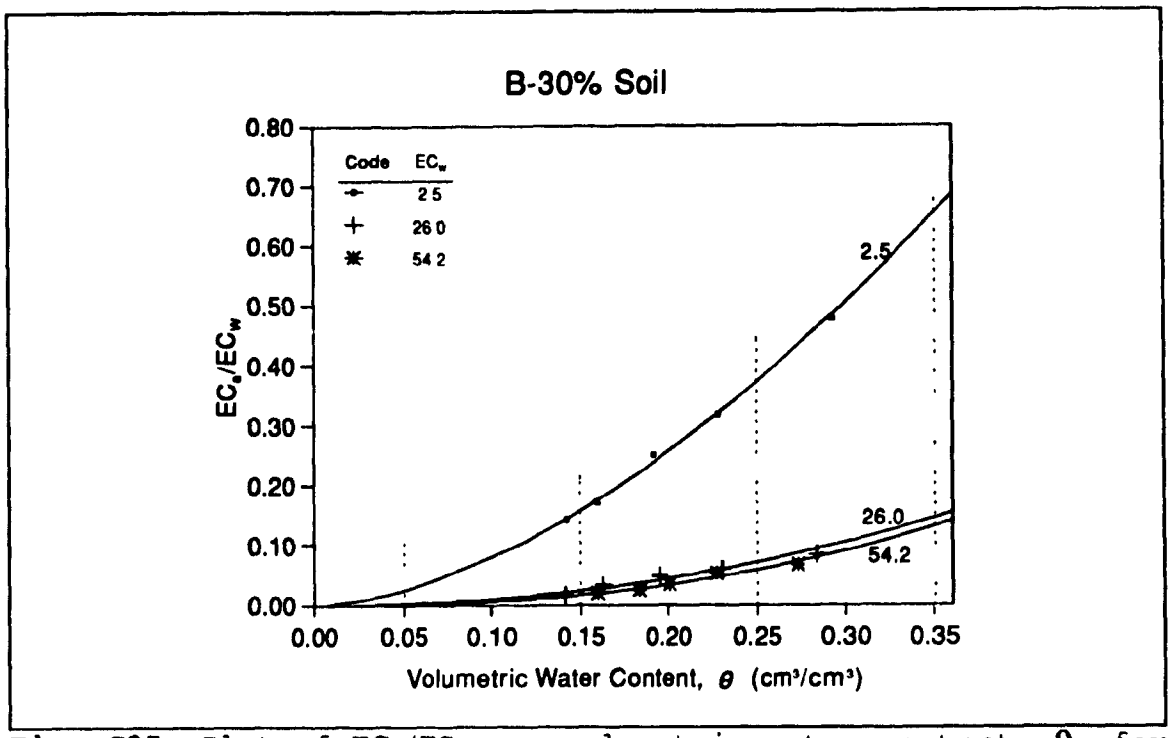

Fig. C25: Plot of EC_a/EC_w vs. volumetric water content, θ, for B-30% soil.

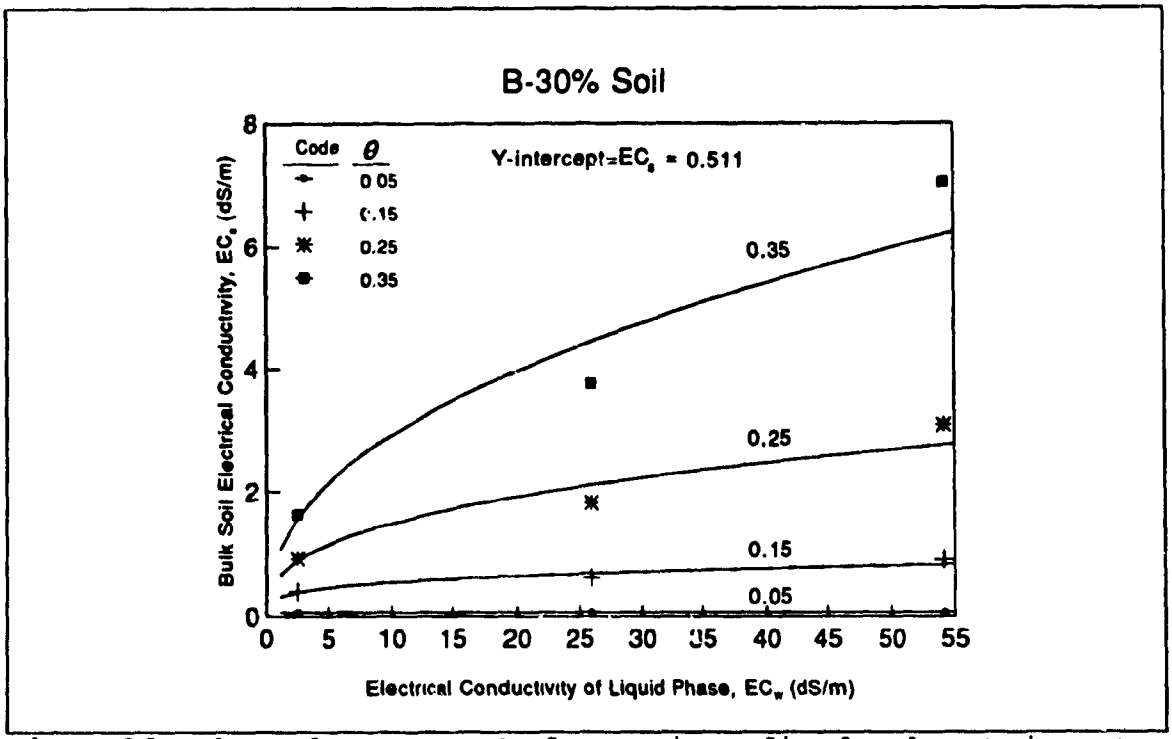

Fig. C26: Plot of EC_a vs. EC_w for various fixed volumetric water contents as interpolated from Fig. C25 for B-30% soil showing the extrapolated value of EC_s.

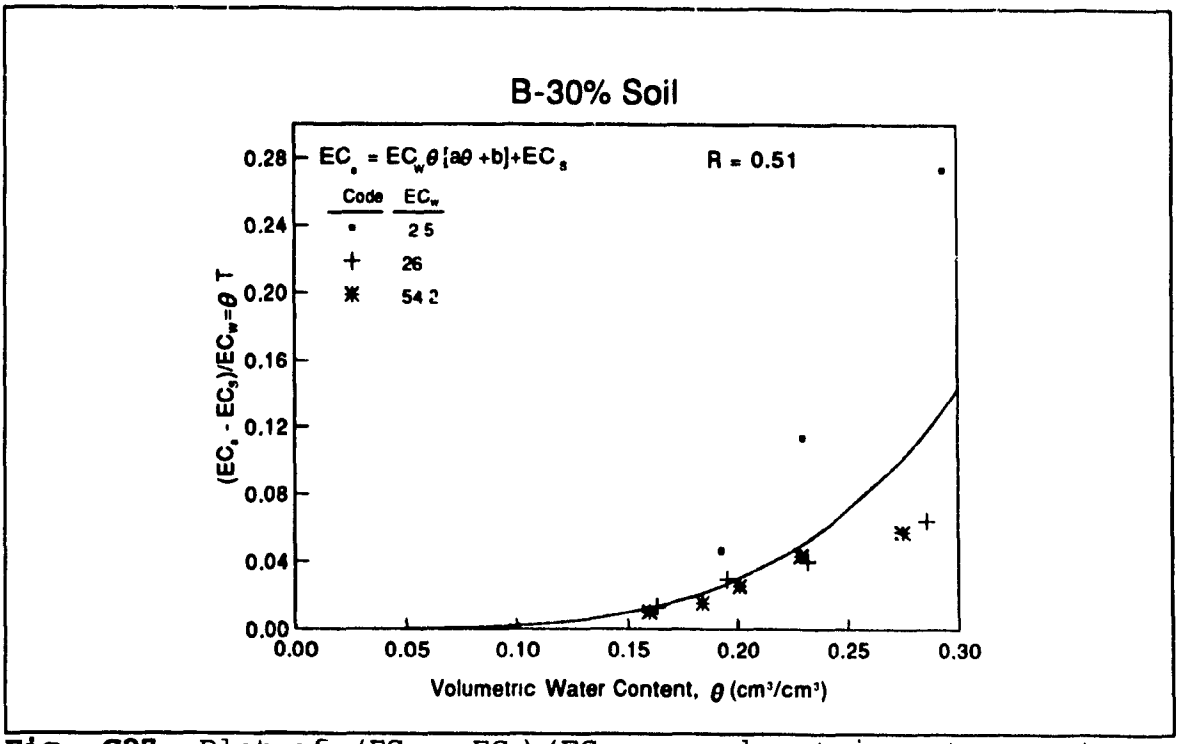

Fig. C27: Plot of $(EC_a - EC_s)/EC_w$ vs. volumetric water content, θ, for data of fig. C25 and C26.

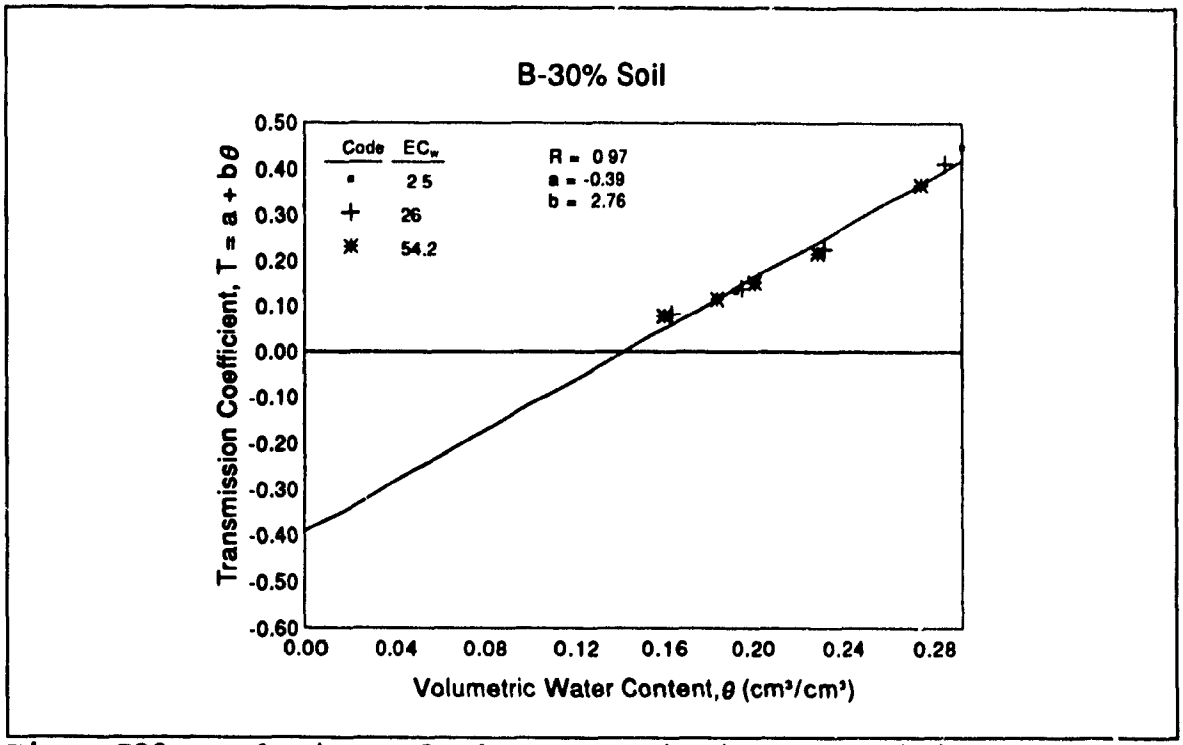

Fig. C28: Relation of the transmission coefficient, T, and volumetric water content for B-30% soil.

Surface Conductivity, EC_s, and Transmission Coefficient, T, for N-30% Soil

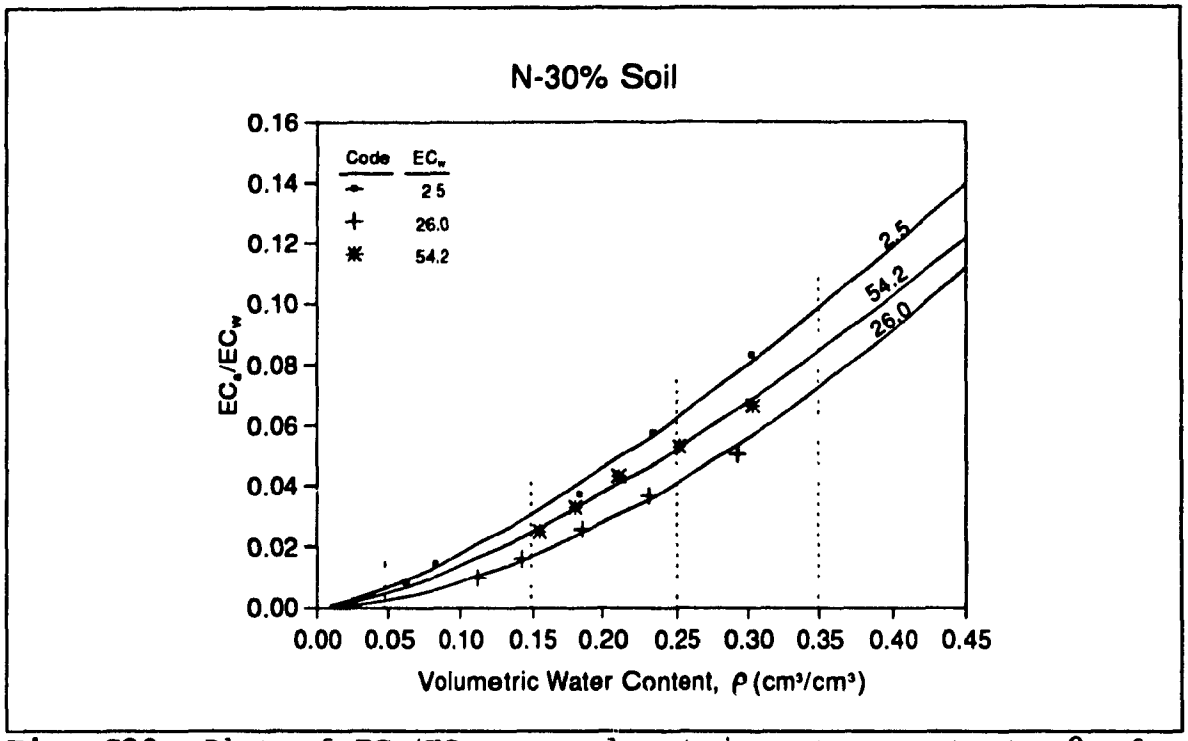

Fig. C29: Plot of EC_a/EC_w vs. volumetric water content, θ, for N-30% soil.

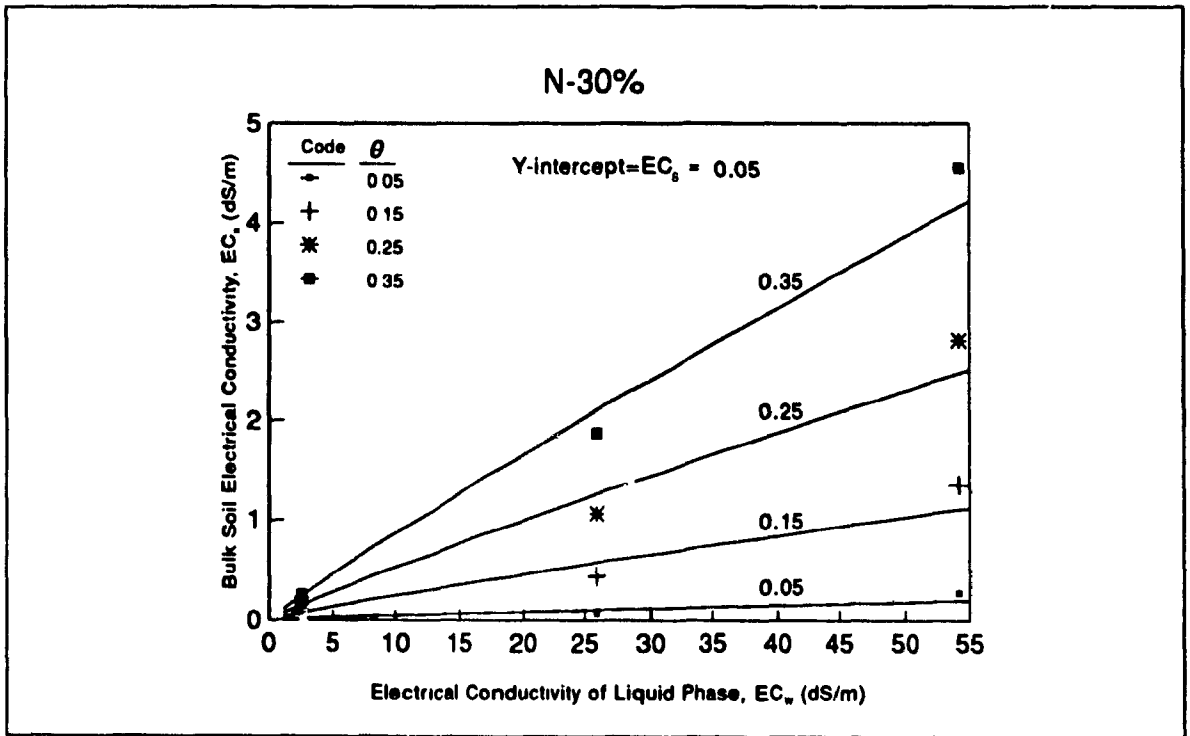

Fig. C30: Plot of EC_a vs. EC_w for various fixed volumetric water contents as interpolated from Fig. C29 for N-30% soil showing the extrapolated value of EC_s.

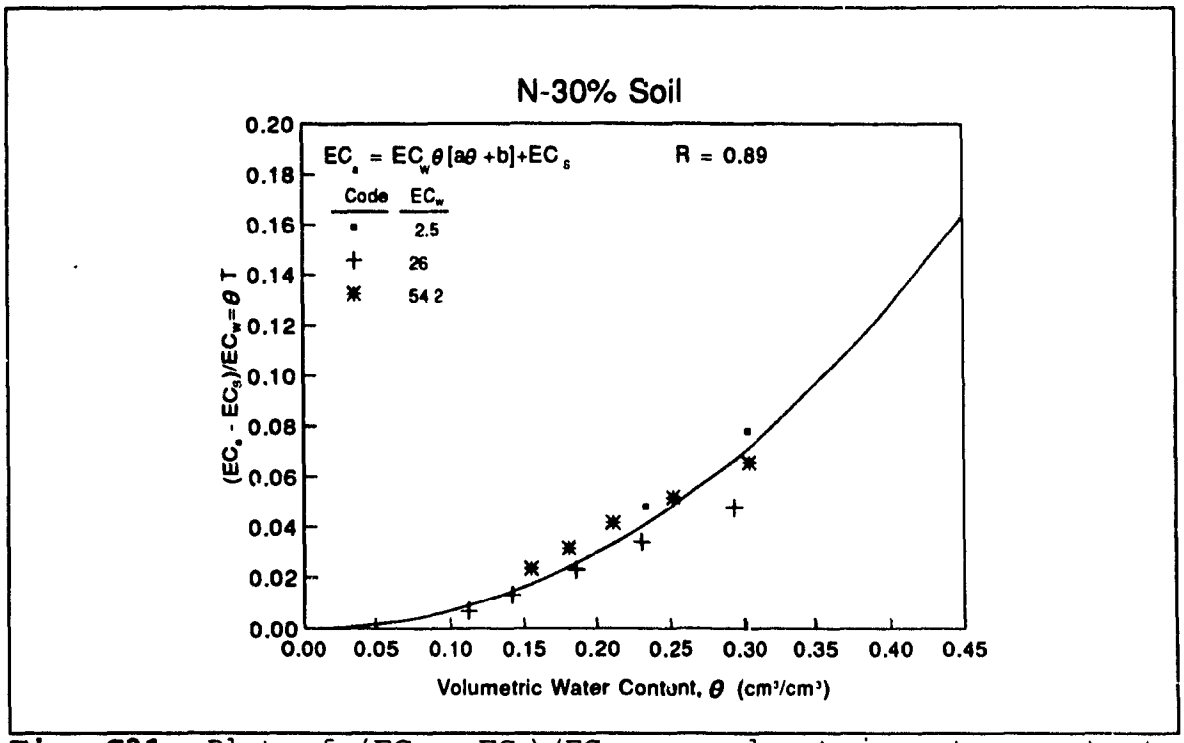

Fig. C31: Plot of $(EC_a - EC_S)/EC_W$ vs. volumetric water content, θ, for data of fig. C29 and C30.

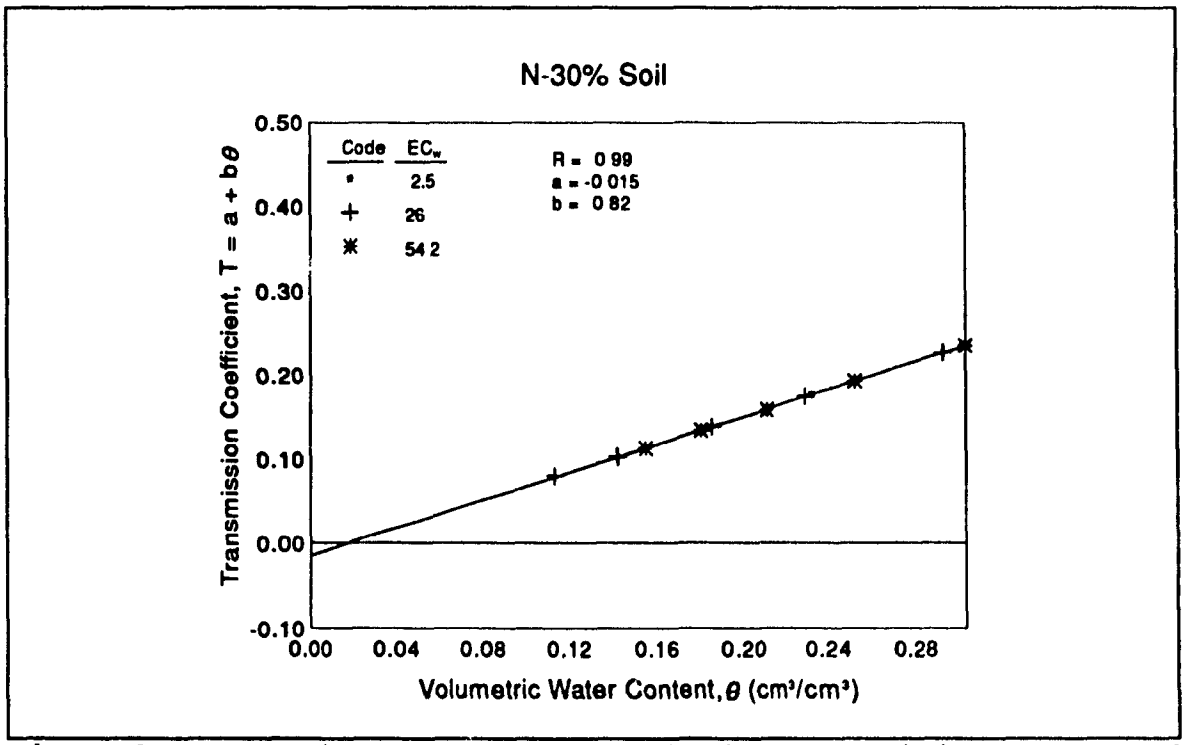

Fig. C32: Relation of the transmission coefficient, T, and volumetric water content for N-30% soil.

APPENDIX D

SAS OUTPUT

(STATISTICAL ANALYSIS RESULTS)

SAS PROGRAM AND OUTPUT FILES
for moisture content

A- HYDRITE GROUP

```
Data moisture content ;
infile 'a:\moist\hyd.prn';
input material $ Grvmoist theta;
title 'variance analysis for Hydrite materials';
proc glm;
classes material;
model theta=material Grvmoist ;
contrast' H-16% vs H-30%'material 1 -1 0;
contrast' H-16% vs H-8% 'material 1 0 -1;
contrast' H-30% vs H-8% 'material 0 1 -1;
run;
```

variance analysis for Hydrite materials

General Linear Models Procedure
Class Level Information

Class	Levels	Values
MATERIAL	3	16% 30% 8%

Number of observations in data set = 96

variance analysis for Hydrite materials

General Linear Models Procedure

Dependent Variable: THETA

Source	DF	Sum of Squares	Mean Square	F Value	Pr > F
Model	3	0.60489198	0.20163066	262.17	0.0001
Error	92	0.07075676	0.00076910		
Corrected Total	95	0.67564874			

R-Square	C.V.	Root MSE	THETA Mean
0.895276	11.46220	0.027733	0.24194792

variance analysis for Hydrite materials

General Linear Models Procedure

Dependent Variable: THETA

Source	DF	Type I SS	Mean Square	F Value	Pr > F
MATERIAL	2	0.11500166	0.05750083	74.76	0.0001
GRVMOIST	1	0.48989032	0.48989032	636.97	0.0001

Source	DF	Type III SS	Mean Square	F Value	Pr > F
MATERIAL	2	0.03624189	0.01812094	23.56	0.0001
GRVMOIST	1	0.48989032	0.48989032	636.97	0.0001

Contrast	DF	Contrast SS	Mean Square	F Value	Pr > F
H-16% vs H-30%	1	0.03606418	0.03606418	46.89	0.0001
H-16% vs H-8%	1	0.00607600	0.00607600	7.90	0.0060
H-30% vs H-8%	1	0.01226789	0.01226789	15.95	0.0001

B- BENTONITE GROUP

```
Data moisture content obtained by TDR;
infile 'a:\moist\ben.prn';
input material $ Grvmoist theta;
title 'variance analysis for Bentonite materials';
proc glm;
classes material;
model theta=material Grvmoist;
contrast' B-16% vs B-30%'material 1 -1 0;
contrast' B-16% vs B-8% 'material 1 0 -1;
contrast' B-30% vs B-8% 'material 0 1 -1;
run;
```

variance analysis for Bentonite materials

General Linear Models Procedure

Class Level Information

Class	Levels	Values
MATERIAL	3	16% 30% 8%

Number of observations in data set = 93

variance analysis for Bentonite materials

General Linear Models Procedure

Dependent Variable: THETA

Source	DF	Sum of Squares	Mean Square	F Value	Pr > F
Model	3	0.45074076	0.15024692	195.97	0.0001
Error	89	0.06823375	0.00076667		
Corrected Total	92	0.51897452			

R-Square	C.V.	Root MSE	THETA Mean
0.868522	9.966951	0.027689	0.27780645

variance analysis for Bentonite materials

General Linear Models Procedure

Dependent Variable: THETA

source	DF	Type I SS	Mean Square	F Value	Pr > F
MATERIAL	2	0.03652132	0.01826066	23.82	0.0001
GRVMOIST	1	0.41421944	0.41421944	540.28	0.0001

Source	DF	Type III SS	Mean Square	F Value	Pr > F
MATERIAL	2	0.11860307	0.05930154	77.35	0.0001
GRVMOIST	1	0.41421944	0.41421944	540.28	0.0001

Contrast	DF	Contrast SS	Mean Square	F Value	Pr > F
B-16% vs B-30%	1	0.08748358	0.08748358	114.11	0.0001
B-16% vs B-8%	1	0.00683104	0.00683104	8.91	0.0037
B-30% vs B-8%	1	0.10154546	0.10154546	132.45	0.0001

C- STE. ROSALIE (NATURAL) GROUP

```
Data moisture content obtained by TDR;
infile 'a:\moist\nat.prn';
input material $ Grvmoist theta;
title 'variance analysis for Ste. Rosalie materials';
proc glm;
classes material;
model theta=material Grvmoist ;
contrast' N-16% vs N-30%'material 1 -1 0;
contrast' N-16% vs N-8% 'material 1 0 -1;
contrast' N-30% vs N-8% 'material 0 1 -1;
run;
```

variance analysis for Ste. Rosalie materials

General Linear Models Procedure

Class Level Information

Class	Levels	Values
MATERIAL	3	16% 30% 8%

Number of observations in data set = 99

variance analysis for Ste. Rosalie materials

General Linear Models Procedure

Dependent Variable: THETA

Source	DF	Sum of Squares	Mean Square	F Value	Pr > F
Model	3	0.67969287	0.22656429	132.21	0.0001
Error	95	0.16279879	0.00171367		
Corrected Total	98	0.84249166			

R-Square	C.V.	Root MSE	THETA Mean
0.806765	13.81372	0.041397	0.29967677

variance analysis for Ste. Rosalie materials

General Linear Models Procedure

Dependent Variable: THETA

Source	DF	Type I SS	Mean Square	F Value	Pr > F
MATERIAL	2	0.01451954	0.00725977	4.24	0.0173
GRVMOIST	1	0.66517333	0.66517333	388.16	0.0001

Source	DF	Type III SS	Mean Square	F Value	Pr > F
MATERIAL	2	0.04898294	0.02449147	14.29	0.0001
GRVMOIST	1	0.66517333	0.66517333	388.16	0.0001

Contrast	DF	Contrast SS	Mean Square	F Value	Pr > F
N-16% vs N-30%	1	0.03616149	0.03616149	21.10	0.0001
N-16% vs N-8%	1	0.00018641	0.00018641	0.11	0.7423
N-30% vs N-8%	1	0.04029767	0.04029767	23.52	0.0001

D- TEST OF HETEROGENEITY OF SLOPES

```
DATA MOISTURE CONTENT;
INFILE 'A:\HBNANA.PRN';
INPUT CT $ CC MOISTURE THETA;
PROC GLM;
CLASSES CT;
MODEL THETA=CT MOISTURE CC CT*CC CC*MOISTURE ;
ESTIMATE 'CC:CTH' CC 1 CC*CT 1 0 0;
ESTIMATE 'CC:CTB' CC 1 CC*CT 0 1 0;
ESTIMATE 'CC:CTN' CC 1 CC*CT 0 0 1;
RUN;
QUIT;
```

General Linear Models Procedure
Class Level Information

Class	Levels	Values
CT	3	B H N

Number of observations in data set = 288

General Linear Models Procedure

Dependent Variable: THETA

Source	DF	Sum of Squares	Mean Square	F Value	Pr > F
Model	7	1.85802548	0.26543221	215.91	0.0001
Error	280	0.34421776	0.00122935		
Corrected Total	287	2.20224325			

R-Square	C.V.	Root MSE	THETA Mean
0.843697	12.82580	0.035062	0.27337153

General Linear Models Procedure

Dependent Variable: THETA

Source	DF	Type I SS	Mean Square	F Value	Pr > F
CT	2	0.16512833	0.08256417	67.16	0.0001
MOISTURE	1	1.41952233	1.41952233	1154.69	0.0001
CC	1	0.22728886	0.22728886	184.89	0.0001
CC*CT	2	0.03320816	0.01660408	13.51	0.0001
MOISTURE*CC	1	0.01287780	0.01287780	10.48	0.0014

Source	DF	Type III SS	Mean Square	F Value	Pr > F
CT	2	0.00623902	0.00311951	2.54	0.0809
MOISTURE	1	0.52953246	0.52953246	430.74	0.0001
CC	1	0.01538526	0.01538526	12.51	0.0005
CC*CT	2	0.01536878	0.00768439	6.25	0.0022

General Linear Models Procedure

Dependent Variable: THETA

Source	DF	Type III SS	Mean Square	F Value	Pr > F
MOISTURE*CC	1	0.01287780	0.01287780	10.48	0.0014

Parameter	Estimate	T for H0: Parameter=0	Pr > |T|	Std Error of Estimate
CC:CTH	-0.00295150	-2.77	0.0059	0.00106443
CC:CTB	-0.00087775	-1.25	0.2115	0.00070085
CC:CTN	-0.00443711	-4.05	0.0001	0.00109543

SAS PROGRAM AND OUTPUT FILES
for EC_a-TDR

A- HYDRITE GROUP

```
Data ECa obtained by TDR;
infile 'a:\ec\hyd.prn';
input material $ Grvmoist ECa;
title 'variance analysis for Hydrite materials';
proc glm;
classes material;
model ECa=material Grvmoist;
contrast' H-16% vs H-30%'material 1 -1 0;
contrast' H-16% vs H-8% 'material 1 0 -1;
contrast' H-30% vs H-8% 'material 0 1 -1;
run;
```

General Linear Models Procedure
Class Level Information

Class	Levels	Values
MATERIAL	3	16% 30% 8%

Number of observations in data set = 96

General Linear Models Procedure

Dependent Variable: ECA

Source	DF	Sum of Squares	Mean Square	F Value	Pr > F
Model	3	5.70516323	1.90172108	87.81	0.0001
Error	92	1.99251860	0.02165781		
Corrected Total	95	7.69768183			

R-Square	C.V.	Root MSE	ECA Mean
0.741153	29.80827	0.147166	0.49370833

General Linear Models Procedure

Dependent Variable: ECA

Source	DF	Type I SS	Mean Square	F Value	Pr > F
MATERIAL	2	1.60082724	0.80041362	36.96	0.0001
MOISTURE	1	4.10433600	4.10433600	189.51	0.0001

Source	DF	Type III SS	Mean Square	F Value	Pr > F
MATERIAL	2	0.29305741	0.14652870	6.77	0.0018
MOISTURE	1	4.10433600	4.10433600	189.51	0.0001

General Linear Models Procedure

Dependent Variable: ECA

Contrast	DF	Contrast SS	Mean Square	F Value	Pr > F
H-16% vs H-30%	1	0.20239989	0.20239989	9.35	0.0029
H-16% vs H-8%	1	0.00493718	0.00493718	0.23	0.6342
H-30% vs H-8%	1	0.24063280	0.24063280	11.11	0.0012

B- BENTONITE GROUP

```
Data ECa obtained by TDR;
infile 'a:\ec\ben.prn';
input material $ Grvmoist ECa;
title 'variance analysis for Bentonite materials';
proc glm;
classes material;
model ECa=material Grvmoist ;
contrast' B-16% vs B-30%'material 1 -1 0;
contrast' B-16% vs B-8% 'material 1 0 -1;
contrast' B-30% vs B-8% 'material 0 1 -1;
run;
```

variance analysis for Bentonite materials

General Linear Models Procedure
Class Level Information

Class	Levels	Values
MATERIAL	3	16% 30% 8%

Number of observations in data set = 99

variance analysis for Bentonite materials

General Linear Models Procedure

Dependent Variable: ECA

Source	DF	Sum of Squares	Mean Square	F Value	Pr > F
Model	3	9.57268502	3.19089501	158.25	0.0001
Error	95	1.91551748	0.02016334		
Corrected Total	98	11.48820251			

R-Square	C.V.	Root MSE	ECA Mean
0.833262	20.08655	0.141998	0.70692929

variance analysis for Bentonite materials

General Linear Models Procedure

Dependent Variable: ECA

Source	DF	Type I SS	Mean Square	F Value	Pr > F
MATERIAL	2	2.24449123	1.12224562	55.66	0.0001
GRVMOIST	1	7.32819379	7.32819379	363.44	0.0001

Source	DF	Type III SS	Mean Square	F Value	Pr > F
MATERIAL	2	0.51373180	0.25686590	12.74	0.0001
GRVMOIST	1	7.32819379	7.32819379	363.44	0.0001

Contrast	DF	Contrast SS	Mean Square	F Value	Pr > F
B-16% vs B-30%	1	0.49892827	0.49892827	24.74	0.0001
B-16% vs B-8%	1	0.01503876	0.01503876	0.75	0.3900
B-30% vs B-8%	1	0.24086310	0.24086310	11.95	0.0008

C- STE. ROSALIE (NATURAL) GROUP

```
Data ECa obtained by TDR;
infile 'a:\ec\nat.prn';
input material $ Grvmoist ECa;
title 'variance analysis for Natural (Ste. Rosalie) materials';
proc glm;
classes material;
model ECa=material Grvmoist ;
contrast' N-16% vs N-30%'material 1 -1 0;
contrast' N-16% vs N-8% 'material 1 0 -1;
contrast' N-30% vs N-8% 'material 0 1 -1;
run;
```

variance analysis for Natural (Ste. Rosalie) materials

General Linear Models Procedure
Class Level Information

Class	Levels	Values
MATERIAL	3	16% 30% 8%

Number of observations in data set = 99

variance analysis for Natural (Ste. Rosalie) materials

General Linear Models Procedure

Dependent Variable: ECA

Source	DF	Sum of Squares	Mean Square	F Value	Pr > F
Model	3	10.79800316	3.59933439	149.97	0.0001
Error	95	2.28003813	0.02400040		

Corrected Total	98	13.07804129	

R-Square	C.V.	Root MSE	ECA Mean
0.825659	23.39084	0.154921	0.66231313

variance analysis for Natural (Ste. Rosalie) materials

General Linear Models Procedure

Dependent Variable: ECA

Source	DF	Type I SS	Mean Square	F Value	Pr > F
MATERIAL	2	1.00175699	0.50087849	20.87	0.0001
GRVMOIST	1	9.79624617	9.79624617	408.17	0.0001

Source	DF	Type III SS	Mean Square	F Value	Pr > F
MATERIAL	2	0.04075991	0.02037996	0.85	0.4310
GRVMOIST	1	9.79624617	9.79624617	408.17	0.0001

Contrast	DF	Contrast SS	Mean Square	F Value	Pr > F
N-16% vs N-30%	1	0.01955804	0.01955804	0.81	0.3690
N-16% vs N-8%	1	0.00404500	0.00404500	0.17	0.6823
N-30% vs N-8%	1	0.03940775	0.03940775	1.64	0.2032

D- TEST OF HETEROGENEITY OF SLOPES

```
DATA ECa;
INFILE 'A:\EC\HBN.PRN';
INPUT CT $ CC MOISTURE ECa;
TITLE'TEST OF HETEROGENEITY';
PROC GLM;
CLASSES CT;
MODEL ECa=CT MOISTURE CC CT*CC CC*MOISTURE ;
ESTIMATE 'CC:CTH' CC 1 CC*CT 1 0 0;
ESTIMATE 'CC:CTB' CC 1 CC*CT 0 1 0;
ESTIMATE 'CC:CTN' CC 1 CC*CT 0 0 1;
RUN;
QUIT;
```

TEST OF HETEROGENEITY

General Linear Models Procedure
Class Level Information

Class	Levels	Values
CT	3	B H N

Number of observations in data set = 297

TEST OF HETEROGENEITY

General Linear Models Procedure

Dependent Variable: ECA

Source	DF	Sum of Squares	Mean Square	F Value	Pr > F
Model	7	27.94023183	3.99146169	166.24	0.0001
Error	289	6.93887041	0.02400993		
Corrected Total	296	34.87910224			

R-Square	C.V.	Root MSE	ECA Mean
0.801059	24.98565	0.154951	0.62016162

TEST OF HETEROGENEITY

General Linear Models Procedure

Dependent Variable: ECA

Source	DF	Type I SS	Mean Square	F Value	Pr > F
CT	2	2.56662826	1.28331413	53.45	0.0001
MOISTURE	1	24.79294888	24.79294888	1032.61	0.0001
CC	1	0.22718713	0.22718713	9.46	0.0023
CC*CT	2	0.34537319	0.17268660	7.19	0.0009
MOISTURE*CC	1	0.00809436	0.00809436	0.34	0.5619

Source	DF	Type III SS	Mean Square	F Value	Pr > F
CT	2	0.01397576	0.00698788	0.29	0.7477
MOISTURE	1	6.12072612	6.12072612	254.92	0.0001
CC	1	0.01951632	0.01951632	0.81	0.3680
CC*CT	2	0.22851551	0.11425776	4.76	0.0093
MOISTURE*CC	1	0.00809436	0.00809436	0.34	0.5619

Parameter	Estimate	T for H0: Parameter=0	Pr > |T|	Std Error of Estimate
CC:CTH	-0.00747071	-1.69	0.0913	0.00440913
CC:CTB	0.00293676	0.95	0.3451	0.00310556
CC:CTN	-0.00447393	-0.95	0.3442	0.00472201